

A Thesis entitled

An Investigation of the Problems in a Channelled
Electron Image Intensifier

by

Dimitri G. Theodorou

Presented for the Degree of Doctor of Philosophy
in the University of London

August, 1963

Department of Physics
Imperial College.

ABSTRACT.

The efficiency and advantages of the photoemissive effect for detecting optical images of very low light intensity are compared with those of the common photographic effect. A brief review of image devices using the photoemissive effect is given and the potential advantages of a system using channelled electron multiplication are enumerated. Possible electrode structures suitable for such a system and the theoretical performance of such a tube are next considered.

A detailed investigation on suitable secondary emitting surfaces for use in the channel electron intensifier is undertaken and experiments are described where the coefficient of secondary electron emission is measured for different surfaces under various operating conditions.

The techniques of construction of suitable dynodes are next given and the development of the optimum parameters in the design of the tube is described. The methods of preparing the secondary emitting surfaces are then outlined. A method is also developed for processing the photocathode in an external chamber and subsequently introducing it to the main intensifier body through a rectangular section tubing.

The results of the measurements on the performance of several tubes are given. A fourteen-stage tube using KCl as a secondary emitter has been constructed, giving electron

gain of 8×10^5 and blue light gain of over 10^6 . Measurements on the resolution of the tube indicate that a nett gain of 2.1 is obtained by the use of "dynamic viewing".

In Chapter VII the stability of the electron gain and photocathode sensitivity of the tube are investigated. It is found that the electron gain remains reasonably stable but that the photocathode sensitivity deteriorates during operation of the tube. In the following chapter an investigation of the bombardment of the secondary emitter on the photocathode sensitivity is undertaken and a theory is proposed to account for the rate of deterioration of the photocathode sensitivity with the time of electron bombardment of the KCl surface.

Finally suggestions are made for the further development of the channelled electron intensifier and its possible use as a colour image intensifier.

CONTENTS

	<u>Page</u>
Chapter I. REVIEW OF METHODS OF IMAGE INTENSIFICATION	8
1. Introduction	8
2. The ideal image detector	9
3. Practical detectors - photographic emulsions and photoemissive surfaces	10
4. Photoelectronic image intensifiers	12
(i) Single stage image intensifiers	13
(ii) Electronographic tubes - Lallemand's Electronic Camera - Two chamber, single stage image recording tube - Electron transmitting mica window image tube	15
(iii) Multi-stage image intensifiers - Cascade intensifier - Transmission secondary emission intensifier - Channelled electron image intensifier	19
Chapter II. ELECTRODE STRUCTURE AND THEORETICAL PARAMETERS OF CHANNELLED TUBE	27
1. Electrode structure	27
(i) Modified Venetian blind structure	29
(ii) Symmetrical cylindrical structure	29
(iii) Asymmetrical cylindrical structure	31
(iv) Other possible structures	33
2. Minimum detectable light flux and contrast difference	34
3. Gain	38
4. Resolution	40
(i) Static viewing	42
(ii) Dynamic viewing	42
5. Cell size and dynode area	44

Chapter III.	INVESTIGATION OF SECONDARY EMITTING MATERIALS	46
1.	Conditions imposed on secondary emitter	46
2.	Design of tubes for the measurement of the secondary emission coefficient.	47
(i)	Tube with electron gun	47
(a)	Systematic errors of tube	51
(ii)	Triode tube	55
3.	Experimental results	61
(i)	Potassium chloride - KCl	61
(ii)	Magnesium oxide - MgO	66
(iii)	Barium fluoride - BaF ₂	73
(iv)	Antimony-caesium - Sb:Cs	75
4.	Conclusion	76
Chapter IV.	DESIGN AND CONSTRUCTION OF MULTI-STAGE IMAGE INTENSIFIERS	78
1.	Construction of dynodes	78
2.	Separation of dynodes	87
3.	Coupling of photocathode plate with first dynode	90
4.	Coupling of last dynode with phosphor screen	92
5.	Design of channel intensifier	95
6.	Preparation of secondary emitting surfaces	103
(i)	MgO surface	103
(ii)	Sb-Cs surface	105
(iii)	KCl surface	108
7.	Assembly of tubes	115
Chapter V.	INTRODUCTION OF PREFORMED PHOTOCATHODES INTO IMAGE INTENSIFIER TUBES	117
1.	Principle of method	117
2.	Processing of photocathode	121
3.	Results	122

Chapter VI.	PERFORMANCE OF CHANNELLED IMAGE INTENSIFIERS	124
1.	Criteria for assessment of the performance of the tube	124
2.	Mounting and connections of the tube	124
3.	Measurement of electron gain	127
4.	Measurement of light gain	128
5.	Measurement of resolution	129
6.	Experimental results	129
	(i) Gain measurements	129
	(ii) Resolution - static and dynamic	135
	(iii) Contrast	141
	(iv) Background	142
Chapter VII.	STABILITY OF CHARACTERISTICS OF IMAGE INTENSIFIERS	143
1.	Shelf life of photocathode	143
2.	Operational life of photocathode and secondary emitter	144
Chapter VIII.	INVESTIGATION OF THE BOMBARDMENT OF THE SECONDARY EMITTER ON PHOTOCATHODE SENSITIVITY	154
1.	Experimental work	154
	(i) Introduction and method of measurement	154
	(ii) Experimental results	155
	(a) Potassium chloride - KCl	155
	(b) Barium fluoride - BaF ₂	170
2.	Proposed theory to account for rate of deterioration of photocathode sensitivity	173

Chapter IX. PROPOSED IMPROVEMENTS IN THE CHANNELLED ELECTRON INTENSIFIER	187
1. General considerations	187
2. A colour image intensifier	190
Chapter X. CONCLUSIONS	193
Summary of collaboration with colleagues	196
Acknowledgements	197
References	198

CHAPTER I. Review of Methods of Image Intensification.

1. Introduction.

It is required in many fields of science at present to detect and record images of very low light intensity. In modern observational astronomy, for example, there is a pressing need for a device capable of increasing the efficiency of recording of the light photons collected by optical telescopes, above that achieved by direct photography. For small and medium sized telescopes, this is even more important since such instruments are limited by their size. A device, capable in addition of recording more information from an image than possible by direct photography, would also be of great value in the work with large telescopes for improving the detection of faint objects against the night-sky background.

Other requirements occur where it is desirable to be able to detect individual photons when a very small number of them is available to be recorded in a particular experimental observation. For example, in the investigation of particle tracks in "scintillation chambers" or the recording of a flash of Cerenkov radiation emitted from a fast particle in a transparent dense medium, the total number of photons produced is too small to be recorded directly on a photo-

graphic plate, and an "intermediate detector" is required to enable as many as possible of these photons to be registered as distinct data on the photographic plate.

In various fields of spectroscopy, both conventional and astronomical, there are situations in which the amount and the nature of the light available is a serious limitation to experimental observation. The same applies in the accuracy of observation of X-ray patterns, particularly so in medical radiology where X-ray examinations are required to be made with the minimum radiation dosage to the patient. Finally such devices would also be exceptionally useful in extending the range of nocturnal human vision.

2. The ideal image detector.

The detection of an optical image is essentially a counting process and in an ideal detector every photon incident on it should produce an individual, identical and identifiable record such as one developed grain in a photographic emulsion. Further, every recorded event should be defined with the same statistical weight without any spurious events being introduced by the detector.

Practical image detectors fall short of these requirements to varying degrees, and in order to compare their performance it is convenient to introduce the concept of "equivalent quantum efficiency".¹ This may be defined as the quantum

efficiency that an otherwise ideal detector must have to yield the same amount of information as the practical detector from the same photon signal. The equivalent quantum efficiency is not generally constant for a given detector but may depend upon the intensity and wavelength of the incident light, as well as upon the duration of the observation.

3. Practical detectors - photographic emulsions and photoemissive surfaces.

The most common detector, used extensively for the recording of optical images, is the photographic emulsion. The quantum efficiency of this emulsion is, however, relatively low and varies widely with the intensity of illumination. The peak quantum efficiency for a fast blue-sensitive emulsion under normal conditions of use is generally taken as 0.1%^{2,3} although Felgett⁴ states that under special conditions, where the emulsion is only exposed to very low densities of 0.25 above fog, the efficiency may rise to 1.1%. At this exposure density, however, the information storage capacity of the plate is too low for most applications. For very low light intensities, and it is these levels that present the real problems in modern observation, reciprocity failure occurs and the quantum efficiency falls rapidly as the level of illumination is reduced until below a certain threshold level

the emulsion becomes completely insensitive.

The photoemissive effect, in common with the photoconductive and photovoltaic effects, has a quantum sensitivity two orders of magnitude greater than that of the photographic effect. Peak monochromatic quantum efficiencies of 35% have been reported⁵ for tri-alkali (Sb-Na-K-Cs) photocathodes, but for the antimony-caesium photocathodes most commonly used at present, the mean efficiency over the visible spectrum is normally taken as 10%. In fact, for any given spectral region in the range of 1000 - 14,000 Å, a photocathode can always be selected to give a higher quantum efficiency than the best photographic emulsion available. Another very important advantage of the photoelectric effect is that the quantum sensitivity of a photocathode is strictly linear over all illumination densities. Using a photocathode, it is also practicable to convert the electron image to an electrical signal, which can be transmitted over a distance, if necessary, by cable and radio link. This is especially useful for observations made in satellites where it would be very difficult to retrieve any photographic plates.

Provided, therefore, that the electron image from a photocathode surface can be recorded without any loss of information and that the imaging device introduces as few spurious events as possible, the photoelectric technique ..

should be about one hundred times as efficient as the photographic method of recording. In the next section are discussed possible methods of recording electron images produced by optical images in such a way as to make full use of all the above advantages.

4. Photoelectronic image intensifiers.

Photoelectronic image detectors may be divided into the following three classes:

- (i) Those in which the light from an optical image is converted into free electrons, which may then be given energy and multiplied to produce an intensified image.
- (ii) Those in which the electrons excited by the photons of an optical image travel within a solid where they may be multiplied and given energy to produce a fluorescent image.
- (iii) Those in which an optical image is converted into a charge image on a two-dimensional array of minute, parallel capacitors. The charge image is then scanned by a beam of electrons to produce a television picture signal which can then be reconverted back to the image.

Only devices from class (i) will be discussed in this thesis. These devices are generally known as image intensifiers.

(i) Single-stage image intensifier..

This tube consists essentially of a photocathode and a fluorescent screen. Photoelectrons liberated from an optical image on the semi-transparent plate are accelerated and focused to form an electron image on the phosphor screen. The light output from the screen is then collected by a lens and the image photographed. The light gain of the tube will depend on the quantum sensitivity of the photocathode, the overall accelerating voltage and the efficiency of the phosphor. Mandel⁶ has shown that for an Sb-Cs photocathode of 80 $\mu\text{A/lumen}$ sensitivity, a high efficiency (20%) zinc sulphide silver activated phosphor backed by an aluminium film and an accelerating voltage of 20 kV, the expected gain in speed over direct photography for a 5,400°K light source is approximately 90 for unity magnification. In practice, however, this gain cannot be realized due to the very low transfer efficiency (not greater than 10%) of the optical system used to photograph the image on the phosphor screen. Thus the overall gain of such a system is not likely to be greater than 5 - 9 times and therefore of no great practical use.

A solution to the problem of the poor transfer efficiency of the optical system was successfully developed by McGee et al.⁷ In this method the phosphor screen is deposited on

a thin mica window sealed on to one end of the tube. A photographic emulsion is then pressed against the mica window of the tube, thus virtually taking a contact print of the phosphor image. In this way, almost all the light emitted by the phosphor is collected and provided the mica window is sufficiently thin, good resolution can be obtained. Photographic blue light gains between 50 and 100 have been realized⁸ in such tubes using mica windows 12 - 15 microns thick. The effective output resolution was 30 line-pairs mm^{-1} with good geometrical resolution and background illumination, allowing very faint images to be photographed by long exposures.

In recent years developments in the field of fibre-optics^{9,10} have also enabled the possibility of replacing the phosphor end window of a single stage intensifier tube by a vacuum-tight bundle of fibres with the phosphor deposited on the inner surface. The information can then be recorded directly by placing the photographic film in intimate contact with the outer surface of the fibre bundle. Fused plates of 5 micron fibres and numerical aperture, NA, greater than 1 (NA = 1.2) have been used¹¹ with transfer efficiencies in the case of settled phosphors of 70% and capable of a resolution of 50 line pairs mm^{-1} , but there appears to be some doubt as to whether this can be achieved in practice. This method can be further

extended to coupling directly together several such single stage intensifiers to give a high overall light gain. In this case the photocathode end window would also have to be replaced by another fibre fused plate. The effective resolution of a number of coupled stages n , each with resolving power R , would then be given by $R/\sqrt{2n}$.¹¹

(ii) Electronographic tubes: Lallemand's Electronic Camera

- Two chamber, single-stage image-recording tube -

Electron-transmitting mica window image tube.

In the electronographic system of recording optical images, the photoelectrons of a single stage tube are accelerated and focused directly on to an electronsensitive emulsion. In this way the coupling losses between the phosphor screen and the photographic plate are eliminated as well as taking advantage of the superiority of the electronsensitive emulsion over the normal photographic one. The electronographic emulsion, for example, is a very efficient means of recording electrons with energy of a few keV. A 10 - 20 keV electron will, in fact, produce several developable grains so that every photoelectron will be directly recorded. In addition it is possible to record an image containing a great deal of information on an electronographic emulsion because of its very small grain size. The recorded density on an

electronographic emulsion is also strictly linear, whereas the relation of density to exposure of a photographic plate is very nonlinear. Finally the low inherent fog level of the electronsensitive emulsion allows for better discrimination of very low densities.

It is seen, therefore, from all the features discussed so far, that image devices employing an electronographic technique would be particularly useful in astronomy for detecting very faint objects against the sky background, this being the factor which limits the range of very large telescopes in photographing such objects.

The first successful tube designed for this purpose was by Lallemand and his co-workers.^{12,13,14} In Lallemand's Electronic Camera the photoelectrons from the photocathode are accelerated and electrostatically focused on to an electronsensitive emulsion exposed in the same vacuum chamber. The early tubes of this type suffered severely from very rapid "poisoning" of the photocathode by gases evolved from the emulsion. By refrigerating the photocathode and the emulsion and using "getters", the deterioration in sensitivity in later tubes was very considerably reduced. At present the tube can be operated for over 12 hours with negligible deterioration of the photocathode. Recently a titanium ion pump¹⁵ was also incorporated in the tube to remove any

residual gases. With this pump, and cooling continuously, exposures up to several hours were achieved without any objectionable background. Gains in exposure time of up to 100 compared to direct photography have been reported^{16,17} with a resolution in the image of 70 line pairs per mm at the centre of the field. More recent measurements¹⁸ indicate that the gain is more of the order of 10 times in the blue region of the spectrum.

In an attempt to overcome the considerable practical difficulties associated with the Lallemand Electronic Camera and the disadvantage of replacing the photocathode whenever the electronographic emulsions are changed, various workers^{19, 20,21,22} have interposed a thin membrane, impervious to the vapour molecules but relatively transparent to electrons, between the photocathode and the emulsion. Both compartments formed by the thin dividing diaphragm can then be separately pumped, the electronsensitive emulsion being introduced through a vacuum lock and brought into close proximity (20 microns) to the thin membrane. The membrane is made extremely thin as it is not called upon to withstand atmospheric pressure, so that the electrons pass through it with the minimum of scattering or loss of energy. Membranes made from aluminium foils 0.1 micron thick were investigated, but the photocathodes in these tubes had a half-life of only a few weeks²⁰ due to

small pinholes in the barrier-membrane through which molecules penetrated to poison the photocathode. Considerably greater success²³ was obtained by replacing the aluminium foils with more impervious aluminium oxide films, 0.14 microns thick. These were found to preserve the photocathode over periods in excess of one month, without any change in sensitivity. The background of these tubes was also very much reduced over the earlier type by the application of a semi-conductor coating between the anode and cathode. During operation the tubes are pumped continuously by cryogenic pumps and under these conditions gains in speed of the order of 50 over direct photography have been obtained with a resolution of 50 line-pairs per mm.

Both of the systems discussed so far require continuous or semi-continuous pumping. In practice it would be more convenient if the electronographic technique could be realized in a completely sealed-off vacuum tube. Such tubes have been constructed by McGee, Wheeler and Khogali^{24,25,26} by further developing the thin mica window intensifier with a phosphor output described in the previous section. The operating voltage in this case is increased by lengthening the tube and the mica end window is made sufficiently thin to allow the electrons to be projected right through it with sufficient residual velocity to be recorded on a nuclear

stripping emulsion in contact with it. At the same time, however, the mica window is still strong enough to withstand atmospheric pressure. Tubes of this type have been constructed, operating at 40 keV, in which 75 per cent or more of the electrons incident on a 4.5 micron thick mica window are transmitted. Under these conditions single photoelectrons can be detected. The tubes have a resolution of 80 line-pairs per mm. and exposure density gains of 5 have been obtained over direct photography.²⁷ It should also be noted that a greater amount of information is recorded per unit area of emulsion over the normal fast light-sensitive conditions due to the fine grain of the electronographic emulsion. Recent improvements²⁷ in reducing the background of the tube have permitted exposure times of up to 5 hours to be taken on Ilford G.5 emulsion before reaching a background comparable to that of chemical fog of ordinary photographic emulsion.

(iii) Multi-stage image intensifiers: Cascade intensifier -

Transmission secondary emission intensifier - channelled electron image intensifier.

In devices of this kind the image photoelectrons are not only accelerated but the individual photoelectrons are also multiplied in number by a large factor to produce an intensified image on a phosphor screen. If the multiplication

factor is large enough and the energy of the incident electrons on the phosphor screen is high enough, then the descendants of a single photoelectron can produce enough photons from the output phosphor to enable it to be recorded as a spot on a photographic plate.

The most direct method of achieving this is by coupling several single stage image tubes together in the same vacuum chamber. In the cascade image intensifier, originally proposed in a patent originating in the Philips Laboratories²⁸ in 1928, the phosphor of the first stage and the photocathode of the second stage are prepared on opposite sides of a thin transparent membrane of glass or mica. A particularly efficient combination giving a high stage gain of the order of 70 is obtained using a silver-activated zinc sulphide phosphor and an antimony-caesium photocathode, the output of the phosphor matching the peak of the spectral response quite closely. The resolution of the tube is set by the electron-optics, the thickness of the phosphor screen, the size of the phosphor particles and the membrane thickness.

Tubes with up to five intensifying sandwiches have been reported.²⁹⁻³⁵ For instance, cascade tubes with two sandwiches, i.e. three stages, and magnetic field focusing designed by McGee and his co-workers³⁴ have given light gains of 1×10^5 with an adequate background at operating

voltages of 45 keV and a resolution of the order of 20 line-pairs per mm.

The great advantage of the cascade tube over other multi-stage intensifiers is in the high electron gain obtainable per stage. The mean percentage deviation from this gain is therefore small and the variation in brightness of output scintillations produced by individual photoelectrons will therefore also be small. If Poissonian statistics are assumed, a tube with a stage gain of 70, for example would show a mean deviation of 12% at the first stage and probably less than 15% at the end of three stages in the brightness of the output scintillations, since this value is determined primarily by the gain of the first stage.

Another method of multiplying the photoelectrons may be accomplished by using the phenomenon of secondary electron emission. There are two possible alternatives: in the first, multiplication is achieved by using the transmitted secondary electrons from thin films as in the transmission secondary emission image intensifier, while in the second, the reflected secondary electrons are used to obtain the necessary multiplication, e.g. channelled image intensifier.

In the transmission secondary emission (T.S.E.) image intensifier, electrons liberated by the photocathode are accelerated and focused on to a thin secondary emitting film. The secondary electrons emitted from the other side of the

film are again accelerated and focused on to a further film. After several such steps, when a sufficiently high electron gain has been obtained, the electrons are projected on to a phosphor screen to give an intensified image.

The main difficulty in this tube is in the preparation of the thin self-supporting secondary emitting films. This principle was suggested as far back as 1934 by Orvin³⁶ but the first practical dynodes to be constructed were by Sternglass^{37,38} in 1953. The films were supported on an open area nickel mesh and consisted of a secondary emitting layer, 500 Å thick, of potassium chloride on a 150 Å layer of aluminium. The aluminium layer served as a conductive backing and maintained the KCl film at the correct potential.

The first really satisfactory tube of this type reported was by Wilcock et al.^{39,40} A 500 Å layer of KCl was also used as the secondary emitter; this layer, together with a 200 Å film of aluminium, was supported in this case by a thin film 450 Å thick of aluminium oxide. Gains of 5 - 6 per stage at 4.5 keV primary energy were obtained from such dynodes. The performance of T.S.E. tubes has steadily been improved; the latest tubes made by 20th Century Electronics,⁴¹ employing five dynodes, give a blue light gain of 10^5 and a resolution of 30 line-pairs per mm. The background at room temperature corresponds to less than 100 electrons $\text{cm}^{-2} \text{sec}^{-1}$. Similar

tubes made by Westinghouse Electric Corporation^{42,43,44} have a slightly better performance, blue light gain of 10^6 and resolution better than 30 line pairs per mm being quoted.

Owing to the relatively low gain per stage, the statistics of the tube are fairly poor. Results obtained by Emberson, Todkill and Wilcock⁴⁵ appear to show that the brightness distribution of output scintillations for single photoelectrons is exponential, giving an even wider variation than if the multiplication process were Poissonian, as is usually assumed. There is a large possibility that the photoelectrons may be lost in the first dynode without any subsequent intensification. Recent measurements⁴⁶ have indicated that up to 60% of the primary photoelectrons are lost on the first stage. A small number of primary electrons also penetrate the dynodes causing a loss of contrast in the final image.

Life tests on this type of tube have shown that fatigue of the secondary electron gain occurs together with a deterioration in the photocathode sensitivity. This is probably due to the dissociation of the KCl under electron bombardment. The results reported by various workers on these two effects vary. Thus Anderson⁴⁷ of Westinghouse quotes a drop of 50% in the secondary emissive yield after bombardment with a total charge density of $72 \text{ micro-coulomb cm}^{-2}$, while in contrast

Wilcock et al⁴⁵ have found that the current gain drops to 15% of its initial value and the photocathode to 30% after a charge density output of 45 millicoulombs cm^{-2} . Recently, however, revised data on the T.S.E. tubes at Westinghouse⁴⁴ have shown that a decrease in electron gain of only 10% now occurred after a bombarding charge density output of 10 millicoulombs cm^{-2} . The photocathode sensitivity after the same interval was found to decrease by 35 - 40% of its initial value.

The fatigue of the secondary emission yield of KCl under electron bombardment, together with the associated decay characteristics of the photocathode sensitivity, have been extensively examined by the author, the results being given in Chapters III, VII and VIII.

The second type of image intensifier using secondary electron emission for multiplying the primary photoelectrons is the channelled image intensifier. The principle of this intensifier was originally proposed by McGee⁴⁸ in 1953, and is essentially a development of the ordinary photomultiplier. The image is divided into a large number of picture points and the photoelectrons from each picture point on the photocathode are made to enter a minute separate photomultiplier. The multiplied output electrons from the multipliers are then accelerated and combined on to a phosphor screen to give the

intensified image. Since each individual multiplier cell integrates all the photoelectrons incident in it from the image, the smallest detail in the intensified image is governed by the diameter of the channels. On the other hand, the resolution is independent of the number of stages of the array of photomultiplier cells - dynodes - so that large gains can be obtained without any further loss in resolution.

The main difficulty with this type of tube is to align the cells from one dynode to another and prevent straying of electrons from one channel to another. At the same time the channels must be of sufficiently small cross-section to obtain a useful resolution, and the dynode structure robust enough to enable the intensification of a large number of picture points to give an adequate image area.

Since secondary emission from a surface occurs at primary energies of a few hundred volts, the voltage requirement per stage of the channelled tube is an order of magnitude lower than that of the multi-stage intensifiers already discussed. Focusing of the tube is purely electrostatic and an inherent property of the dynode structure. No magnetic fields are therefore required, and the E.H.T. supply does not need to be accurately stabilized. The ancillary equipment to operate this tube is hence very simple and can be made very light and compact. This renders the channelled intensifier potentially

ideally suitable for use in earth satellites where power consumption and weight must be kept to a minimum and strong magnetic fields are undesirable. Other applications in which this tube can be used are in X-ray fluoroscopy and fibre scintillation chamber experiments.

It is seen from this brief review of practical image intensifiers available at present, that the usefulness of the intensifier depends largely upon the application for which it is required. For applications where high resolution is not of primary importance, the channelled image intensifier is potentially the most suitable and simplest high-gain intensifier. The experimental contributions to the development of this tube for which the author was partly and wholly responsible are treated in the remainder of the thesis.

CHAPTER II. Electrode Structure and Theoretical Parameters of Channelled Tube.

1. Electrode Structure.

The initial problem associated with the development of the channelled image intensifier is in the choice of a suitable multiplying electrode structure. Such a structure must conform to the following basic requirements.

1. Electrons from the photocathode, or secondary electrons from any stage, must strike the secondary emitting surface of the following dynode.
2. A high percentage of the secondaries produced at each dynode must be extracted to the next.
3. Straying of electrons into neighbouring channels must be kept to an absolute minimum.
4. The dynodes must be of such geometrical structure that they can be miniaturized sufficiently to give reasonable image definition and at the same time be robust, relatively simple to fabricate and easy to align on assembly.

On the commencement of work on the project by the author, a preliminary investigation of various possible dynode systems had already been carried out by Flinn and Evans.^{49,50} Three structures were considered (Fig. 1): (a) an "egg-box" type based on the Venetian blind photomultiplier, (b) an arrangement in which each dynode consisted of an array of

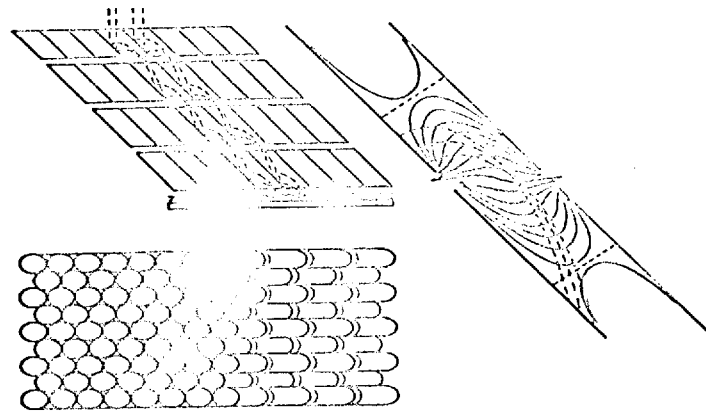
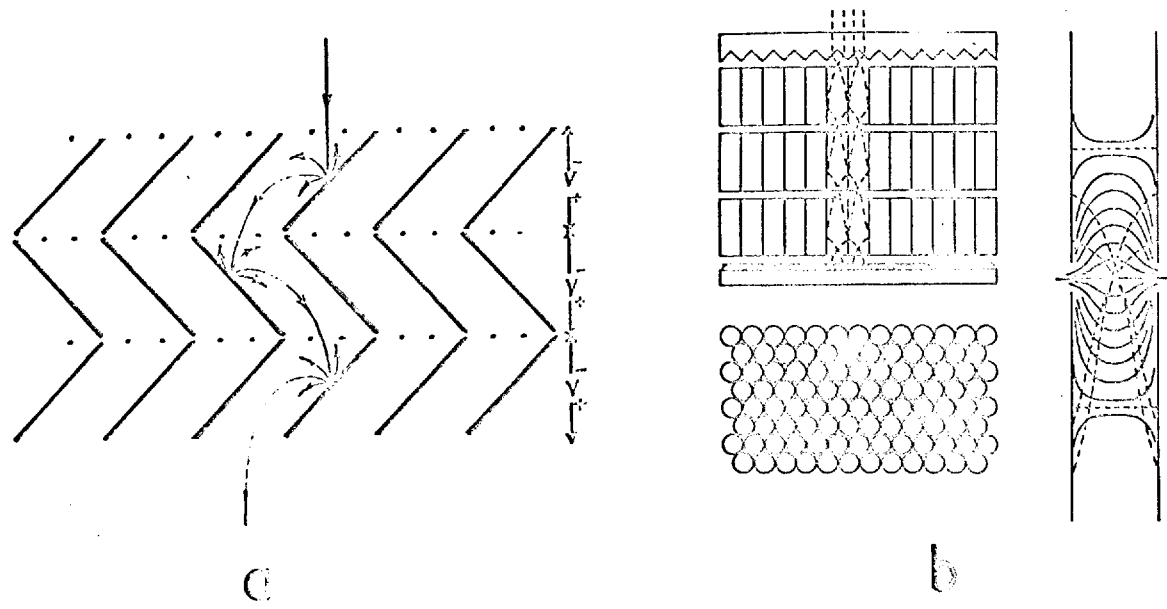


FIG. I.

short right cylinders, placed side by side and (c) a structure similar to (b) but in which the ends of the cylinders were cut at an angle to their axis. The electron trajectories of large-scale single-channel models were investigated and the following is a brief summary of the results obtained.

(i) Modified Venetian blind structure.

This structure is illustrated in Fig. 1a. The primary electrons in the large one-cell model were provided by a high velocity electron gun, firing into the open end of the egg-box structure. The points of impact of the secondary and tertiary electrons were observed by coating the glass electrodes with thin layers of stannous oxide and willemite phosphor, which also served as the secondary emitter. The results obtained were fairly satisfactory. The electrons were found to stay well focused and their points of impact on the cell walls were substantially independent of the relative stage voltages and angle of incidence of the primaries. Unfortunately a disadvantage with such dynodes is that they would be very difficult to make in small dimensions with sufficient accuracy and to assemble in exact alignment.

(ii) Symmetrical cylindrical structure.

A single channel of two such stages may be regarded as a two-tube electrostatic lens (Fig. 1b) with the electron

object, or source, lying on the wall of the first tube. In order that the maximum number of secondary electrons can be extracted from the first tube and accelerated to strike the opposite wall of the second, the secondary electrons must be liberated in the region of the penetrating extracting field. The length to diameter ratio ($\frac{L}{d}$) of the cylinder is therefore an important factor in the efficiency of operation of such a system. Two types of large scale models were built. In the first, the primary electrons were supplied by a photocathode formed on the wall of the first electrode, while in the second the first electrode was slit along one side and the primary electrons allowed to enter the system through this slit from an electron gun in a side arm. The remaining electrodes in both cases were made of glass and coated with Nesa and willemite. The electron trajectories of the secondary electrons were investigated for cylinders of different lengths and for various points of incidence of the primaries. Results were confusing: after some early experiments that were promising, it was found later that it was not possible to obtain focusing of the secondary electrons from the cylinder walls to the appropriate point on the next stage. Further it was also impossible to reproduce any stable progression down the tubes. It thus appeared that an electrode structure of this type was unsuitable for use in

the channelled intensifier. The least unsatisfactory results were obtained in tubes where the length to diameter ratio of the cylinders was two and a quarter to one.

(iii) Asymmetrical cylindrical electrodes.

In a dynode of this form (Fig. 1c) each cell consists of a short cylinder with its ends cut at an angle instead of normally to the longitudinal axis. The effect of this asymmetry is to introduce a lateral component into the field between adjacent dynodes, so that the electrons now impinge always on the same side of the walls of successive tubes. As with the right angled cylindrical electrodes, the length to diameter ratio is very important since if the ratio is made too great the extracting field will be weakened and gain would again decrease. There would also be an increase in the tendency of electrons to stray into neighbouring channels. The angle of the ends of the cylinder is equally important. For too obtuse angles the electrons would not be deflected sufficiently strongly and would tend to skip a stage as well as to stray into adjoining channels. For angles that were too acute, the electron trajectories would be very strongly controlled, but the fields from one dynode would penetrate too far into the succeeding dynode and prevent secondaries from escaping.

Large scale models were again built similar in design to the two types already described in connection with the previous electrode form. The results obtained from both designs of tubes were found to be in close agreement. The electron trajectories obtained were very satisfactory, a stable progression of the secondaries occurring over several stages with the electrons impinging on the cell walls at a series of equidistantly spaced spots. The optimum values, to an accuracy of 5%, required for the parameters were found to be 2:1 for the length to diameter ratio and 55° for the angle between the end faces and the longitudinal axis. The extraction efficiency of the secondary electrons under these conditions was determined to be 60%.

As a result of these investigations it was decided to use this type of cell structure in the dynodes of the channelled intensifier. When the author commenced work on this project the proposed technique for making these dynodes was to bunch together a number of cylindrical tubes in a hexagonal close packed configuration and braze them. The resulting block of tubes would then be cut into slices at 55° to the axis, and the dynodes reassembled in the tube in exactly the same orientation to one another as they had originally, thus assuring easy and accurate alignment. Details of the construction of such dynodes are given in Chapter IV.1.

This cell structure also lends itself to a simple and relatively efficient input system for coupling a plane photocathode with the first dynode. Provided the separation between the photocathode plate and the first dynode is small enough, the slow photoelectrons can be accelerated directly into the channel immediately below without fear of any lateral spread occurring.

(iv) Other possible electrode structures.

The cell structures previously discussed are not the only possible configurations. Burns and his co-workers^{52, 53} have developed dynodes consisting of a metal mesh, the bars of which have a trapezoidal cross-section. Thus the mesh apertures are cones of square cross-section. Here again extraction of the secondaries occurs only at the lower half of the dynode so that the electron trajectories have to be arranged so that electrons can impinge at the appropriate areas of the dynodes. The main difficulty with the electron optics of this structure is in the introduction of the photoelectrons into the first stage.

Another very simple electrode structure is being currently developed by Goodrich and his colleagues.^{54,55,56} In this instance the cells are single long glass tubes coated on the inside with a semiconducting metallic oxide, and have an

accelerating potential applied between the ends of the tube. Secondary electrons created within the channel have a sufficient transverse velocity to enable them to travel from side to side of the tube, acquiring enough energy from the longitudinal field during each transit to liberate several secondaries on impact with the tube wall. A cascading action is thus instigated producing the electron gain. Such an electrode structure was also originally investigated by the author, but with very little success due to the great difficulty of producing, with the facilities available, a uniform high resistance layer inside a large number of channels of sufficiently small diameter.

2. Minimum detectable light flux and contrast difference.

The limit of the threshold of image detection is set by the quantum nature of the light. When the number of photons arriving per second at a detector is very small, the associated statistical fluctuations in this number become comparable with the number itself thus setting the lower limit of detectability.

If we now consider an illumination of I_0 lumen ft^{-2} falling on an extended scene, the maximum illumination I_i of the image plate for areas of perfect white and magnification much smaller than 1 is then given by:

$$I_i = \frac{I_o T}{4F^2} \dots\dots\dots 2.1$$

where F is the reciprocal of the relative aperture of the lens and T is the transmission efficiency for the light used. For a photocathode area, $A \text{ ft}^2$, of the channelled tube with a total of n channels or picture points, the number of photoelectrons, N , leaving the photocathode per picture point corresponding to peak white areas in time t is

$$N = \frac{I_o T A P \eta t}{4F^2 n} \dots\dots\dots 2.2$$

where P is the number of photons per second per lumen ($P = 1.4 \times 10^{16}$ photons per second per lumen for "white" light) and η is the quantum efficiency of the photocathode. If every photoelectron leaving the photocathode were recorded at the output stage as an individual event, the mean statistical deviation in the number of electrons recorded in any period would then be \sqrt{N} . The assumption that every primary photoelectron is recorded, however, is not strictly true and another factor ϵ has to be incorporated taking into account (a) the theoretical transfer loss of photoelectrons to the first stage due to cell wall thickness and the dead area due to the packing of the cells, and (b) the probability that secondary electrons emitted by the photoelectron

at the first stage are not extracted to the second. (c) The loss in signal-to-noise ratio during multiplication.

So far it has also been assumed that the noise or random fluctuations observed at the output are solely due to the quantum nature of light, additional fluctuations will also be introduced due to noise generated inside the detecting device. This may be taken into account by including a term $n_t t$ to express the mean deviation of these additional fluctuations. The total mean deviation at the output of the tube is then

$$\delta = \sqrt{\epsilon N + \epsilon N_t} \quad \text{where } N_t = n_t t \quad \dots\dots 2.3$$

and the peak white signal/r.m.s. ratio is

$$S = \frac{\epsilon N}{\sqrt{\epsilon N + \epsilon N_t}}$$

Substituting for N in equation 2.2,

$$S = \left\{ \frac{\epsilon \left(\frac{I_o T A P_{\eta} t}{4 F^2 n} \right)^2}{\frac{I_o T A P_{\eta} t}{4 F^2 n} + n_t t} \right\}^{\frac{1}{2}} \quad \dots\dots 2.4$$

Similarly the contrast difference between two adjacent picture points of brightness B and B + ΔB is limited to the detectability between the mean difference of the recorded impression of the two picture points. It is usual to assume a "coefficient of certainty" k by which the minimum brightness step can be detected with reasonable certainty. Thus the

minimum contrast difference C is

$$C = \left(\frac{\Delta B}{B} \right)_{\min} = k \frac{\sqrt{2\delta}}{\epsilon N}$$

Substituting again for N from equation 2.2,

$$C = \left(\frac{\Delta B}{B} \right)_{\min} = k \left\{ \frac{\frac{I_o T A P \eta t}{2 F_n^2} + 2 n_t t}{\epsilon \left(\frac{I_o T A P \eta t}{4 F_n^2} \right)^2} \right\}^{\frac{1}{2}} \quad \dots\dots 2.5$$

Generally k is taken as 5,^{1,57} a value ensuring almost complete certainty of detection. This is rather pessimistic, however, since in images exhibiting a recognizable pattern as opposed to random distribution a value of k of 2 or 3 gives adequate detection.

The two most important possible sources of noise, or spurious emission, generated in the intensifier, are field emission and thermionic emission. With careful experimental techniques and the exclusion of caesium from the dynode structure, it is possible to greatly reduce any field emission taking place at normal operating voltages so that the major contribution to the noise is then due to the thermionic emission of the photocathode. This is a random process and depends largely on the nature and the temperature of the photocathode. An average value for an Sb-Cs

photocathode of 10% peak quantum efficiency is generally taken as $100 \text{ electrons cm}^{-2} \text{ sec}^{-1}$. If we now assume a value of 10 for the peak white signal/r.m.s. noise ratio, thus obtaining a fairly intelligible picture, we can determine the required illumination from equation 2.4. Considering a channelled intensifier giving a picture comparable to a 200 line television picture with 0.5 mm diameter channels, then $n = (200)^2$ and $A = (10)^2 \text{ cm}^2 = \frac{1}{9} \text{ sq.ft}$; taking also realizable values for the remaining parameters involved such as $F = 1$, $T = 0.8$, $\eta = 0.2$, $\epsilon = 0.5$, $t = 1/10 \text{ sec}$, $P = 1.3 \times 10^{16} \text{ photons/sec}$, $n_t = 3000 \text{ electrons ft}^{-2} \text{ sec}^{-1}$, then $I_0 \sim 2 \times 10^{-6} \text{ lumen ft}^{-2}$.

This is about two orders of magnitude less than the ambient illumination on a clear star-lit night, and although the spectral response of the cathode would not be perfectly matched with the spectrum of the incident light, the sensitivity is ample to give a satisfactory image by starlight alone.

3. Gain.

The limit of useful gain on an intensifier is generally specified by the application for which it is intended. For observations of weak spectral lines, for example, where a continuous steady flux of radiation is arriving at the

detector, the useful limit of the gain of the intensifier is reached when each primary photoelectron makes a significant contribution to the total integrated information on the photographic plate. In the case of the investigation of particle tracks in scintillation chambers, however, the whole of the available light may comprise a few thousand, or even a few hundred photons. Under these circumstances, it is necessary to record with sufficient definition every primary photoelectron.

The potential gain of the channelled intensifier, similar to that of an ordinary photomultiplier, can be very high and within reason may be increased to any desired value, since the inherent resolution of the tube is independent of the number of multiplying stages. Considering, for example, a 15 stage tube with a mean gain of 3 per stage, the overall electron gain would be of the order of 10^7 . Assuming a 10 kV accelerating potential is applied between the last dynode and the phosphor, for every electron striking the aluminium-backed ZnS:Ag phosphor 500 photons would be liberated in the forward direction.⁵⁸ For a picture point 0.5 mm square, the photon density per primary photoelectron would then be 2×10^{12} photons cm^{-2} . This level of photon density is readily detectable by the photopic eye and is three orders of magnitude above that required to expose a

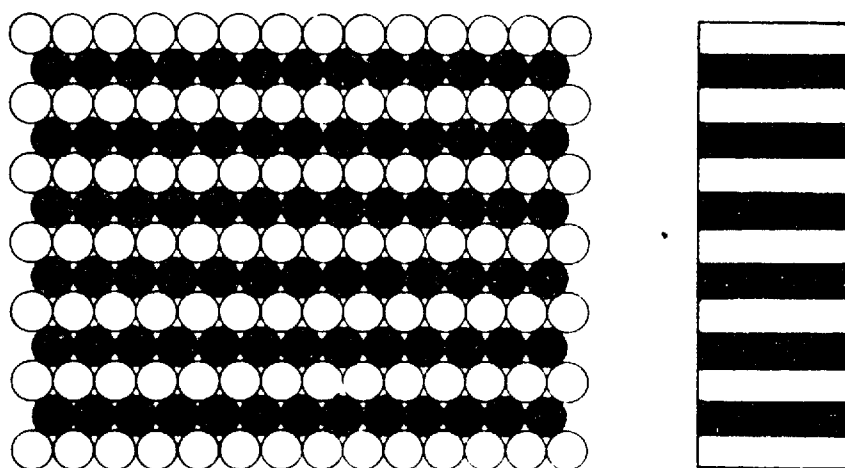
fast photographic emulsion (10^9 photon cm^{-2}). Allowing for optical coupling losses, a photographic record would still be readily obtainable.

4. Resolution.

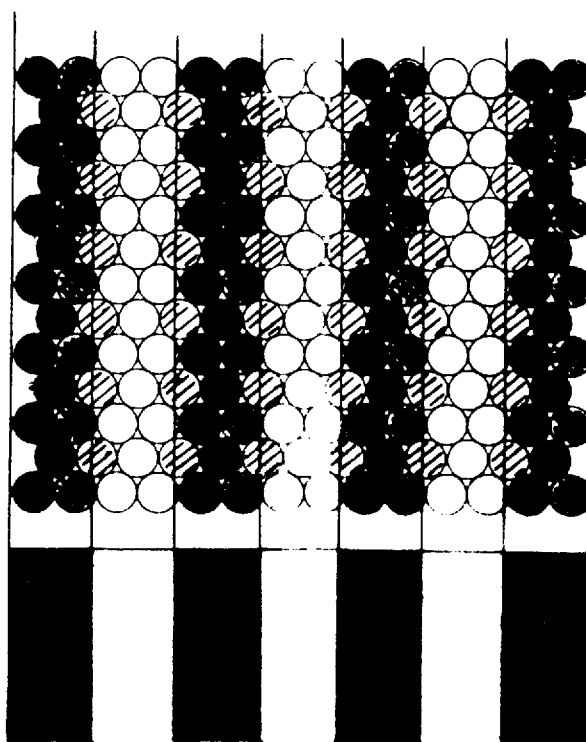
(i) Static viewing.

In the channelled image intensifier, each individual multiplying channel integrates all the photoelectrons incident on its aperture. Thus the smallest detail visible in the intensified image is governed by the diameter of the channels. Since the cell structure adopted is a short cylinder with its ends cut at an angle of 55° to the axis, the cross-section of the cell at its end faces is elliptical with a ratio of 1.22:1 between the major and the minor axes. The projected picture points on the phosphor screen are therefore also elliptical, but for reasons of simplicity circular picture elements will only be considered, since results obtained on the resolution along the major axis can be directly converted to the correct cell shape by taking into account the ratio between the major and minor axes.

For a dynode of circular elements arranged in a hexagonal close-packed array, the maximum resolution is obtained for a pattern of parallel black and white bars of equal width



a



b

Fig 2 .

(Foucault pattern) when the bars are accurately aligned with rows of cells in the dynode (Fig. 2a). For cells of d mm in diameter the resolution is then $\frac{1}{1.74d}$ line pairs per mm, since the centres of adjacent rows are separated by $0.87 d$ mm. Such a resolution can only be obtained, however, if the test pattern is exactly of the right spacing and arranged in one of the three possible angular distributions relative to the dynode. If, for instance, the pattern is moved laterally by half a diameter, the pattern will totally disappear since electrons from each illuminated bar on the photocathode are now divided equally between the two neighbouring rows of cells. Patterns slightly worse than the limit will also not be perfectly resolved as they would tend to "beat" with the dynode structure giving a Moire fringe effect (Fig. 29e) thus greatly reducing the resolution. In the general case of random alignment between dynode and test pattern, good resolution is obtained down to $\frac{1}{4d}$ line-pairs mm^{-1} (Fig. 2b) although patterns down to $\frac{1}{3d}$ line-pairs can still be resolved with difficulty.

(ii) Dynamic viewing.

A notable improvement in the resolution for a given channel diameter is obtained when the tube is moved in the plane of the image with random direction and amplitude.

This results not only in improved definition, but also in a blurring out of the structure of the cell packing, producing thereby a much more acceptable output image. Similar results were obtained by Kapany et al⁵⁹ on work on the resolution of images transferred through hexagonal close-packed fibre bundles. In both cases the interpretation of dynamic scanning can be thought of in terms of a single cell or fibre which is made to scan uniformly an image area. Since each cell integrates the flux falling upon its entrance aperture, if all the area is equally scanned, then the spectrum of the integrated transmitted image would be the product of the spectrum of the incident image and the frequency response or resolving power of the scanning cell. Kapany⁵⁹ has derived a theoretical analysis of this effect giving an expected improvement in resolution by a factor 2.12 over static viewing. Both experimental results by Kapany and those obtained by the author (Chapter VI.6.ii, Figs. 28 and 29) agree closely with the above factor.

Another great advantage obtained by dynamic viewing is that since the spatial frequency response is now continuous, the "beating" effect previously mentioned is no longer observed (Fig. 29f). It is seen, therefore, that the advantages offered by such a method of viewing, notably improvement in resolution, picture quality and freedom from "beating"

effects, would off-set the inconvenience of the extra apparatus necessary to provide the scanning motion.

5. Cell size and dynode area.

Since the information content of an image is dependent on the total number of picture points, the diameter of the channels in a dynode and its area are directly interdependent. A lower limit to the cell size is imposed by the interdynode spacing, for as the diameter of a channel is decreased the separation between the dynodes must also be proportionately reduced, while at the same time the inter-stage voltage must remain the same to obtain the necessary secondary emission yield. The field strength between the dynodes is thus inversely proportional to the cell size and consequently field emission becomes increasingly important. In addition, the finite wall thickness of the tubes also becomes important as the diameter is reduced. The thinnest wall tubing readily available at present has a thickness of 0.0015 in, although this can be further reduced by etching the completed dynode. The smallest channels made at present have a diameter of 0.5 mm and a 0.002 inch wall thickness. The cross-sectional area occupied by the wall is about 36% and this limits accordingly the efficiency of extraction of the photoelectrons from the photocathode.

It is seen, therefore, from the previous considerations, as well as from practical experience, that with the present method of constructing the dynodes, cell sizes below 0.2 mm diameter would not be practicable. On the other hand, the area of the dynode can be readily increased over that used at present. For a dynode of 0.5 mm diameter channels an area of 10 - 12 cms square is quite feasible. With dynamic viewing this would correspond to a 400-line square television picture, adequate for most observational purposes for which this tube is intended.

CHAPTER III. Investigation of Secondary Emitting Materials.

1. Conditions imposed on secondary emitter.

Before proceeding with the work undertaken on the secondary emitting surfaces, the conditions required from an emitter intended for the intensifier tube should first be considered. These are as follows:

- (1) The emitter must have a high secondary emission yield at low primary energy. Since only 60% of the secondaries give rise to subsequent intensification and the inter-dynode voltage is of the order of a few hundred volts, to obtain a reasonable gain, preferably over 3 per stage, the secondary emission coefficient δ of the material must be greater than 5 for 500 eV primary energies.
- (2) The secondary electron yield should remain stable under prolonged electron bombardment. If the surface dissociates giving off a gas under the bombardment, this may attack the photocathode in close proximity resulting in a decrease in its photosensitivity.
- (3) The geometry of the dynodes is such that the emitter cannot be evaporated after the dynodes have been assembled and aligned. Unless the channels themselves are made from a material like the Ag-Mg alloys which can be activated to yield a secondary emitting surface, evaporation of the

emitter has to take place prior to assembly in a demountable belljar. A further condition thus imposed is that the material must remain stable on exposure to the atmosphere.

(4) In the case where the emitter is an insulator, the surface must be thin enough to allow adequate conduction to the substrate so as to maintain the correct electric fields necessary for the electron optics of the channels.

Consideration of the above factors led to the detailed examination of the following secondary emitting materials: KCl , BaF_2 , MgO , SbCs_3 . The tubes employed for the investigation of these materials were of two different designs, tubes with an electron gun and "triodes".

2. Design of tubes for the measurement of the secondary emission coefficient.

(i) Tube with an electron gun.

The design of this tube with only slight modifications has been used extensively by most research workers for the accurate determination of the secondary emission yield. A particular variant of such a tube, as used in this instance, is given in Fig.3a,b. The tungsten filament 1 is the source of primary electrons. The electron beam is controlled by a standard C.P.S. Emitron electron gun arrangement 2 focused and deflected by the external magnetic coil 3. A magnetic



FIG. 3a.

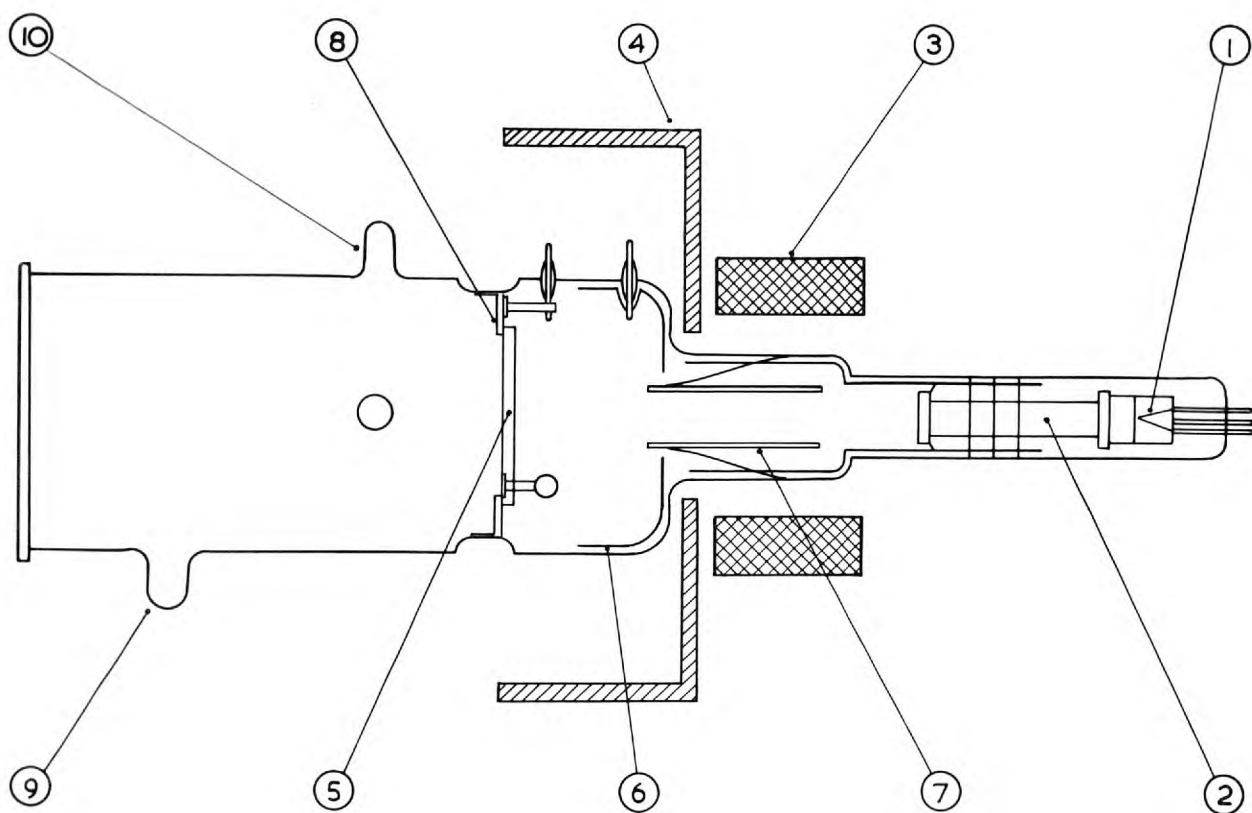


FIG. 3b.

shield 4 is placed in position to prevent any stray fields from affecting the slow secondaries emitted from the target 5. The secondary electrons are collected on the hemispherical collector 6 formed by coating the inner walls of the envelope with a conducting material of Aquadag or platinum paint. The purpose of the cylindrical shield 7, kept at anode gun potential and protruding slightly into the collector area, is to prevent any primary electrons from reaching the collector directly.

The target 5 is a circular pyrex plate kept in position on the stainless steel annulus 8 by means of a magnetic spring arrangement and capable of being turned over to expose the surface first to the evaporating side of the tube and then to the electron gun side.

The substances to be investigated are in magnetically retractable evaporators and introduced to the tube from the side-arm 9.

The target plate 5 is initially coated with a highly reflecting film of aluminium by evaporation. The purpose of this is twofold, first to provide a conducting backing for the insulating secondary emitting films and second to act as a highly reflecting layer, to facilitate the measurement of the thickness of the film by increasing the modulation of the multiple beam interference fringes, which result from the

thickness of the films. These fringes give a very easy and accurate control of film thickness of the dielectric material, the same method being used later for the evaporation of KCl and BaF_2 on to the dynodes in a demountable assembly (Chapter IV.6.iii).

Measurements of the secondary emission ratio are carried out either after the tube has been sealed off the pump or in situ. In the latter case the target plate is pivoted on an axis and can be rotated externally by means of a small horseshoe magnet. With this method, the variation of δ with increasing film thickness can be investigated as well as the effect of gases and moisture on the various secondary emitters. The effect of Cs on δ can also be studied, Cs being admitted from the side-arm 10.

During measurement of δ the target plate, together with the anode gun cylinder, is kept at earth potential while the collector potential (V_c) is alternated from + 200 V to - 200 V. The primary bombardment energy is varied by keeping the filament at progressively higher negative potentials up to - 1.0 kV. For a further increase in primary energy in order to keep the electron beam accurately focused, the target plate voltage is increased positive to earth while maintaining the same collector voltages relative to the target plate.

If i_p is the electric current flowing to the target plate when $V_c = -200$ V, $(-i_t)$ the current leaving the plate at $V_c = +200$ and i_c the collector current at $V_c = 200$ V, the secondary emission yield is given by

$$= \frac{i_c}{i_p} = \frac{i_c}{i_c - (-i_t)} \quad \dots\dots\dots 3.1$$

(a) Systematic errors of tube.

From consideration of the geometry of the electrodes the following spurious currents are possible:

1. "Direct" current - a part of the primary beam being collected directly by the collector.
2. "Back" current - the fraction of the secondary electrons collected by the gun anode instead of the collector.
3. "Secondary" primary current - the electron beam from the cathode hitting the sides of the gun anode and liberating slow secondaries which can then proceed to the target and collector.
4. Backscattered primaries - during the cycle when the collector voltage is negative to the target plate, reflected primaries with energy greater than the collector voltages can arrive at the collector and liberate secondaries. These secondaries, or tertiary electrons, as they are called, can then travel back to the target plate, and appear as part of the primary beam.

If we now consider each of these effects individually bearing in mind the actual electrode voltages used during measurement of δ , we can determine the relative contribution of each to the total error.

(1) "Direct" current.

Care was taken during the design of the tube to have the anode cylinder protruding slightly in the collecting hemisphere and thus physically preventing the primary electrons from hitting the collector in the vicinity of the aperture. Accurate focusing of the electron beam was possible by means of the external magnetic coil. This was confirmed by a visual check of the electron spot due to fluorescing of the target under bombardment. It can thus be assumed that for primary energies greater than 100 eV the error due to such an effect can be neglected.

(2) "Back" current.

With the present electrode geometry and operating voltages this current appears to be the most important contributor to the total error. To keep it to a minimum at the low primary range (200 - 1000 eV) the target plate and anode gun potential are kept at earth. For greater primary energies the target voltage is positive to the gun anode, thus restricting the

leakage to the fast secondaries only.

(3) "Secondary" primary currents.

The electron gun geometry together with the strong focusing action from the coils prevents the electron beam from spreading. If any collisions with the gun anode should occur, however, they would be confined most likely to the end of the cylinder nearest the gun where the extracting field for secondaries, if any, is very weak.

(4) Backscattered primaries.

This is another important source of error, particularly so in the measurement of δ by a triode to be discussed in the next section.

The coefficient of elastic scattering η is large for very low primary energies,^{60,61,62} e.g. for $V_p = 10$ eV, $\eta = 40\%$, but decreases with increasing energy of primary electrons ($V_p = 100$ eV, $\eta < 10\%$) up to a region of several keV when it starts to increase again.

For low primary energies less than 40 eV insulators show a much larger value for η than metals.^{60,63,64} This difference may be explained by the difference in the energy level structure of the two materials. In the case of metals, low energy electrons can make inelastic collisions involving any amount of energy transfer to the electrons in the valence

levels, whereas in insulators such collisions are only possible if the energy transferred is sufficient to raise the valence electron across the forbidden gap. As a result low energy electrons in insulators can diffuse over large distances allowing many to escape from the surface.

For the region of primary energies used in the tube with electron gun η is low. The coefficient of secondary emission of the collector is also low; in some tubes the collector consisted of a coating of Aquadag giving a very low δ while for a platinum film coating $\delta_{\max} = 1.8$ for $V_p = 700$ eV.⁶⁵ The secondaries from the collector are attracted to the target and anode-gun cylinder so that for 1 reflected primary leaving the target, about 1 secondary arrives, reducing the error in measuring I_p . For energies greater than 1 keV primary, only the gun cylinder is at earth potential. There is thus a preferential capture of secondaries by the cylinder and the error in I_p becomes correspondingly greater.

(5) Conclusions.

All the leakage currents discussed so far are very small and in some cases cancel each other out. For the region of primary energies 200 V - 1 keV, accuracy in δ is better than 2%, and for the region above 1 keV primary energy, accuracy is better than 4%.

(ii) Triode.

This type of tube was primarily designed to examine the effect of electron bombardment of various secondary emitting surfaces on the sensitivity of a photocathode. The full details and results of such measurements are given in Chapter VIII. In this section we will consider the tube as used in measuring all the secondary emitting surfaces.

Fig 4a,b gives a picture and the cross-section of the tube. The photocathode 1 is processed in an external chamber (Chapter V) and introduced to the tube from the rectangular side arm 2. With this method caesium is effectively prevented from contaminating the secondary emitting layers.

With the tube sealed off the pump, the photocathode is tapped into place on the photocathode shelf 3. When in position, half of the area of the photocathode is protected from contamination by lying flat against a thin metal foil. The other half faces the secondary emitting surface previously evaporated on the stainless steel disc 4. Between the photocathode and the target surface is a wire mesh 5 of low geometrical shadow ratio - 9%. The mesh is kept taught by means of two stainless steel annuli 6, which in turn are spaced away from the photocathode shelf and target plate by the glass cylindrical spacers 7 and mica washers 8. The distance between photocathode and grid is 2.0 mm while that



FIG. 4a.

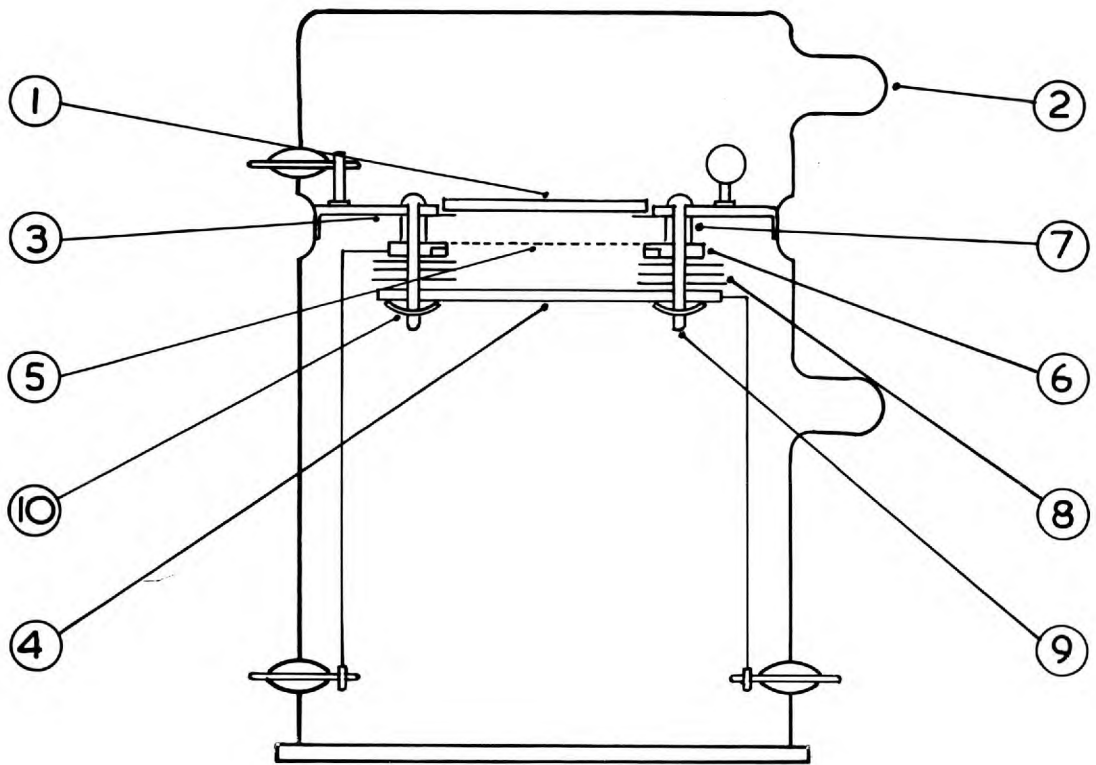


FIG. 4b.

between the grid and the target plate is 1.5 mm. The whole unit is kept together by four ceramic rods 9 domed over at one end and clamped by steel "spire" nuts 10 at the other.

The photocathode acts as the source of primary electrons, while at the same time its surface is exposed to any particles liberated from the target surface during bombardment. The potential difference V_g between the mesh and the cathode is kept higher than the potential V_a between target and cathode so that the secondary electrons are collected by the mesh. By altering the mesh potential positive or negative relative to the target potential, the mesh can also act as an electrical shutter for any positive ions liberated from the target. If we denote the primary current emitted by the photocathode by i_c , a fraction s of this current will be intercepted by the grid before reaching the target surface. The current arriving at the surface is therefore $(1 - s)i_c$ and if δ is the secondary emission coefficient of the surface, the secondary current collected by the grid will be $\delta(1-s)i_c$.

The total grid current ($-i_g$) = $si_c + \delta(1 - s)i_c$, the negative sign indicating the arrival of electrons at the grid, and the total target current

$$\begin{aligned} i_a &= \delta(1 - s)i_c - (1 - s)i_c \\ &= i_c(1 - s)(\delta - 1). \end{aligned}$$

Hence the secondary emission coefficient

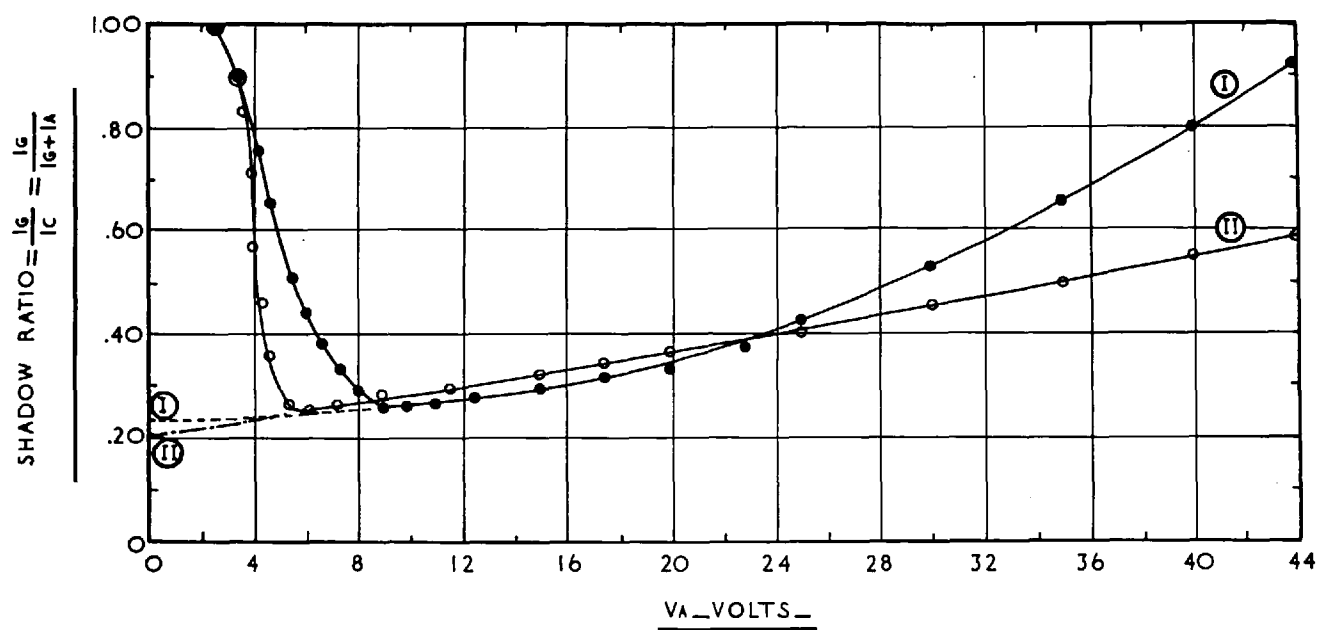
$$\delta = \frac{(-i_g) - si_c}{i_c(1 - s)} = 1 + \frac{i_a}{i_c(1 - s)} \quad \dots\dots 3.2$$

The main disadvantage of this method lies in the uncertainty in the determination of the fraction of the primary electrons intercepted by the mesh. A second difficulty is that smaller values of δ will be found with this type of tube as compared to the tube with an electron gun due to some of the secondaries making several passes to the mesh before capture and returning back to the target plate. Thirdly, the angle of incidence of the primary electrons is not well defined because some of them are deflected by the wires of the mesh.

Several methods for the determination of s are quoted in the literature,⁶⁶⁻⁷³ the method employed in this instance being a slight variant of that originated by Tonk⁶⁶ and Van der Pol.⁶⁷

If the initial velocities of the electrons are neglected the ratio of the primary current i_c to mesh and target is a function of the quotient $\frac{V_g}{V_a}$. If i_g and i_c are therefore measured for low values of V_g and V_a where δ is small, s will be equal to $\frac{i_g}{i_c}$ and would remain the same for higher values of V_a provided $\frac{V_g}{V_a}$ is kept constant. If a graph of $\frac{i_g}{i_c}$ is plotted for progressively lower values of V_a , s can be obtained by extrapolating the curve to $V_a = 0$. A typical

DETERMINATION OF SHADOW RATIO OF MESH OF TRIODE



I. — KCL AREA.

II. — STAINLESS STEEL AREA.

$$\frac{V_a}{V_g} = \text{CONST.} = 0.7$$

FIG. 5.

graph is given in Fig. 5. This method, however, only partly eliminates the effect due to secondary emission for although at these low plate voltages the true secondary emission is small, the fraction η of electrons undergoing elastic reflection is considerable. It was already pointed out that in this region η is very much greater for insulators than for metals, e.g. at $V_p = 10$ eV, η for metals = 10%, while for insulators, e.g. NaCl, $\eta = 40\%$. An indication of the error in measuring the shadow ratio can therefore be obtained if the measurements could be repeated with the primary electrons striking the metal target first and then the target coated with the secondary emitter. Fig. 5 gives the result of two such measurements. Only half the area of the stainless steel target of a triode was coated with a KCl film of 1000 \AA thickness. For large values, the curves showing the variation of V_a with $\frac{i_g}{i_c}$ for the KCl region is greater than that for the stainless steel due to higher secondary emission coefficient of the former. For low values of V_a , extrapolation of the two curves for $V_a = 0$ gives a difference of only 4% between the shadow ratio as measured above the KCl and metal areas, thus indicating that the contribution of the reflected primaries to s is not as high as originally feared. All the curves examined so far show a minimum in the region $V_a = 4 - 10$ V, followed by a sudden increase in the proportion of

primaries captured by the mesh. This can be attributed to space charge effects in the vicinity of the photocathode due to the very low extracting fields resulting in direct capture of most of the photoelectrons by the mesh. This argument is further substantiated by the fact that whereas until the minimum was reached the photocathode current remained constant for a given light input, in this region the photocathode current dropped rapidly.

Since this series of tubes was used to obtain measurements for the comparison of δ for various secondary emitters where the actual value of δ was not of great importance, no further corrections in the determination of the shadow ratio were made. For more accurate measurements a correction has to be applied for the reflected primaries, the initial energy of the primary electrons and the differences in contact potential.

Measurements of the secondary emission of the various materials were carried out by one or other of the two types of tubes and in some cases both.

3. Experimental results.

(i) Potassium chloride - KCl.

The ease in preparation of the surface together with the high gain obtainable from it led to this substance being the first to be examined. The KCl was evaporated on to the

target plate of the electron gun tube to a thickness of 1000 \AA . According to Nakhodin and Romanovsky⁷⁴ the optimum yield at moderate bombarding voltages is obtained from a layer of such a thickness, while at the same time the films are thin enough to allow conduction of electrons from the backing metallic layer across the film, minimizing any charging effects.

The results obtained for δ on reflection for KCl giving a maximum δ of over 10 for 1 keV primary energy are reproduced in Fig. 6. These results are in very good agreement with those obtained by Pelzel⁷⁵ and Gomoyunova⁷⁶ for KCl and NaCl films using elaborate single pulse techniques. It should be noted too that the yield on reflection is considerably higher than that obtained for transmission from thin films of the transmission secondary emission tubes^{39,40} where the maximum gain is 5 - 7.

Although the secondary emission yields obtained are adequate for the purpose of the channelled image intensifier, such surfaces suffer from two main drawbacks. Firstly, under prolonged electron bombardment the KCl dissociates, free chlorine atoms are liberated and "colour centres" generated which act as electron traps reducing the electron yield (Chapter VIII.2). The chlorine so produced tends to attack

SECONDARY EMISSION YIELD OF KCL FILM

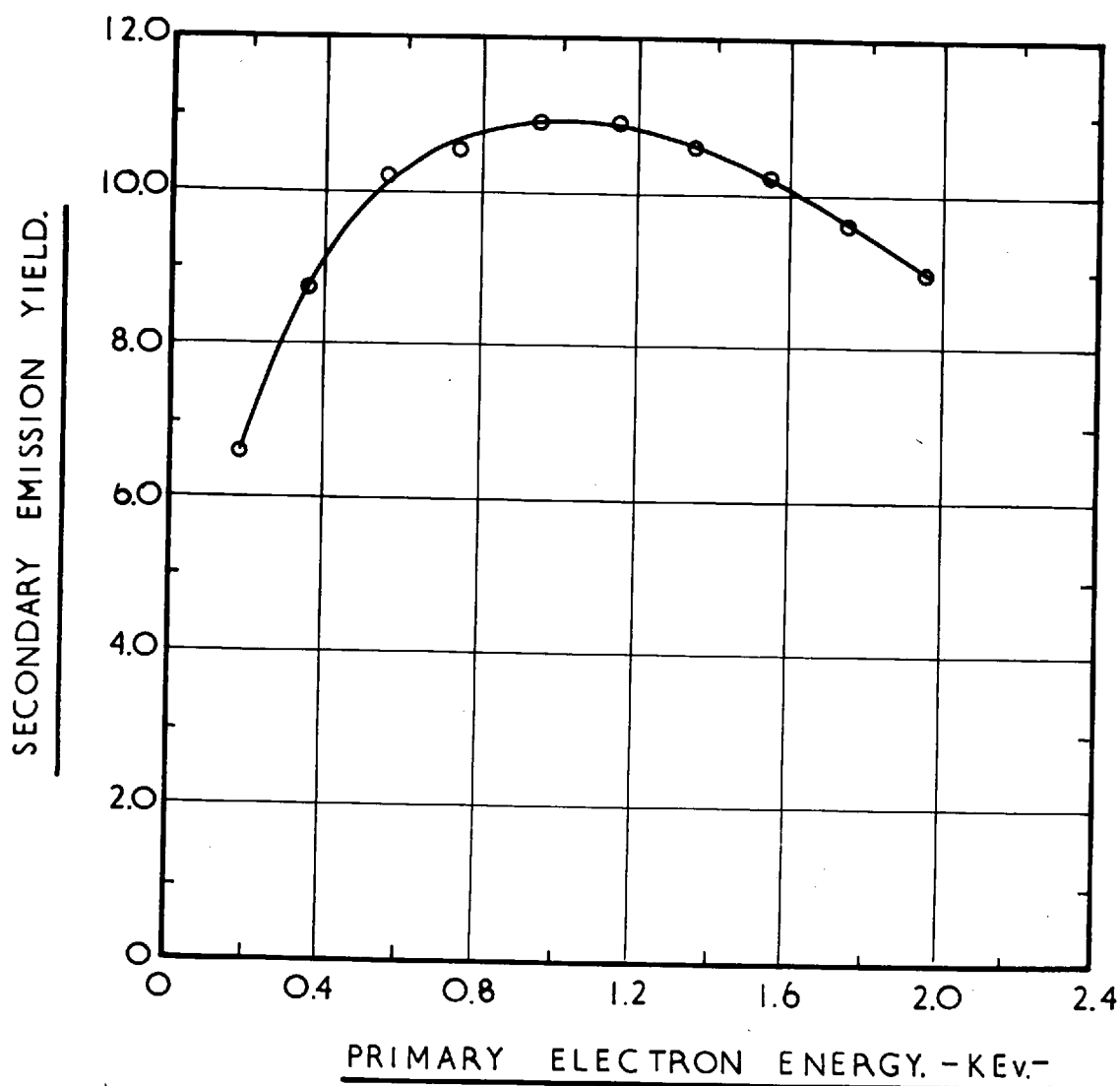
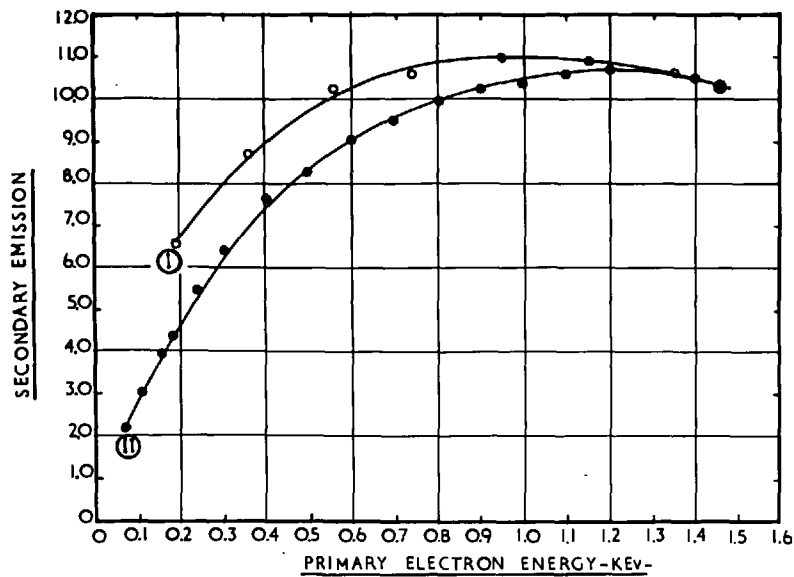


FIG.6.

the photocathode, resulting in a loss in sensitivity. This process was fully examined by means of triodes (Chapter VIII. 1). Figures for the fatigue of δ of KCl with electron bombardment quoted by different workers vary.^{44,45,47,77,78,79} With the electron gun a typical set of results is shown in Fig. 8. A rapid fall in gain initially occurs followed by a gradual leveling out of the decay to a steady value 45% lower than the original yield. The charge density at this point is 12 millicoulombs cm^{-2} . A further increase even up to 12 coulombs cm^{-2} gives no further decrease in the secondary emission. After the experiment the bombarding area was found to be clearly defined having a deep purple colouration thus confirming the generation of the colour centres.

One practical disadvantage of KCl as a secondary emitting surface is its extreme susceptibility to attack by atmospheric moisture. After a few minute exposure to damp air, the normally clear film becomes milky in appearance and the secondary emission yield falls drastically. Subsequent baking of the film does not restore the original yield. If pre-evaporated films are used, assembly of tube components must take place in a very dry atmosphere maintained inside a glove-box.



§ AS MEASURED BY: I TUBE WITH ELECTRON GUN
II TRIODE

FIG. 7.

FATIGUE OF SECONDARY EMISSION OF KCL FILM
UNDER ELECTRON BOMBARDMENT

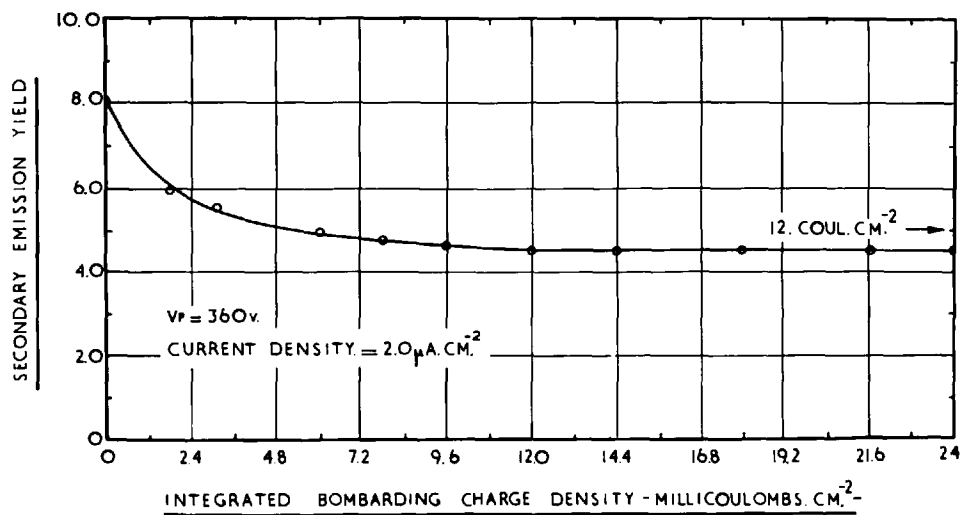


FIG. 8.

The secondary emission of KCl was also measured by triode tubes; in this case the KCl was evaporated on to the target plate in a demountable bell-jar. Dry air was admitted to the apparatus and the components assembled in the glove-box. During the sealing on of the end window by AgCl, a copious flow of cool, dry argon was directed over the target surface to minimize contamination. Comparing the results obtained for δ (Fig. 7) with the previous set of results, it can be seen that for primary energies below 1 keV the yield is lower, indicating that even with the elaborate precautions taken above a slight contamination of the upper layers of the KCl surface did take place. For higher primary energies where the secondary emission process occurs at progressively greater depth, the two curves coincide.

(ii) Magnesium Oxide - MgO.

This secondary emitter has been widely investigated by several workers.^{77,80-89} Unfortunately there is little agreement between the various results as well as in the method of preparation of the surface.

The MgO film can be prepared in two ways. Starting from an alloy of silver with about 2% magnesium and baking for a suitable time in an oxidizing atmosphere, the magnesium in the silver becomes mobile, diffuses to the surface, and is

subsequently oxidized. The silver in the alloy does not contribute to the secondary emission, but serves as a host to the magnesium. By using an oxidizing atmosphere of water vapour Rappaport⁸⁶ obtained yields of 7 at 800 V primary while Shepheard et al,⁸⁷ oxidizing in O_2 or CO_2 , showed maximum yields of 12 at 500 eV primary energy. Another possible alloy giving approximately the same results is that of copper-aluminium magnesium (Cu - 9%, Al - 6%, Mg - 1%).⁸² Unfortunately the mechanical properties of all these alloys prevent them from being drawn into fine walled tubing such as are used in the construction of the dynodes of the channelled intensifier. Attention was therefore turned to the second method of preparation of the films by evaporating the magnesium on to a metal substrate and subsequently oxidizing it. Such films have been studied by Whetton and Lapovsky⁸³ who report a maximum yield of 18 at 1200 eV primary energy, falling to 10 at 300 eV, for a MgO layer of 800 \AA thickness. The magnesium was oxidized at $550^\circ C$ at a pressure of 50 - 100 mm Hg. Other workers have successfully used a wide range of oxidizing conditions, with baking temperature varying considerably, but all in excess of $500^\circ C$.

In the case of the intensifier tube, the use of a silver chloride seal limits the upper temperature to which the tube can be baked to $400^\circ C$. It was therefore necessary to

investigate whether adequate oxidation of the magnesium would occur at a lower temperature. The tube used was of the usual electron gun type with a pivoted target plate operated externally with a magnet, allowing measurements to be taken with the tube pumped continuously. The end window was also sealed by glass-blowing to permit higher baking temperatures. After evacuation and a preliminary bake, the target plate was cleaned by maintaining a discharge by R.F. excitation in hydrogen. The magnesium was evaporated at a pressure of $4 - 8 \times 10^{-7}$ mm Hg to an optical transmission of 3%. This corresponded to a thickness of 250 - 300 Å. The film was kept so thin so as to minimize charging of the surface, the effects of which were observed by Whetten and Laponsky⁸³ on film thicknesses down to 600 Å. Dry O₂ to 5 mm pressure was admitted and the tube then baked to 400°C for 40 mins; on cooling it was found that only a very superficial layer of the Mg had become oxidized, indicating that for the intensifier tube the dynodes have to be oxidized prior to assembly. Further oxidation of the magnesium was carried out at 480°C for 30 mins. This proved to be adequate, the resulting film being clear and transparent. The results of the measurement on δ with primary energy are shown in Fig. 9 giving a maximum yield of 7.5 at 950 V primary energy.

SECONDARY EMISSION YIELD OF MgO FILM

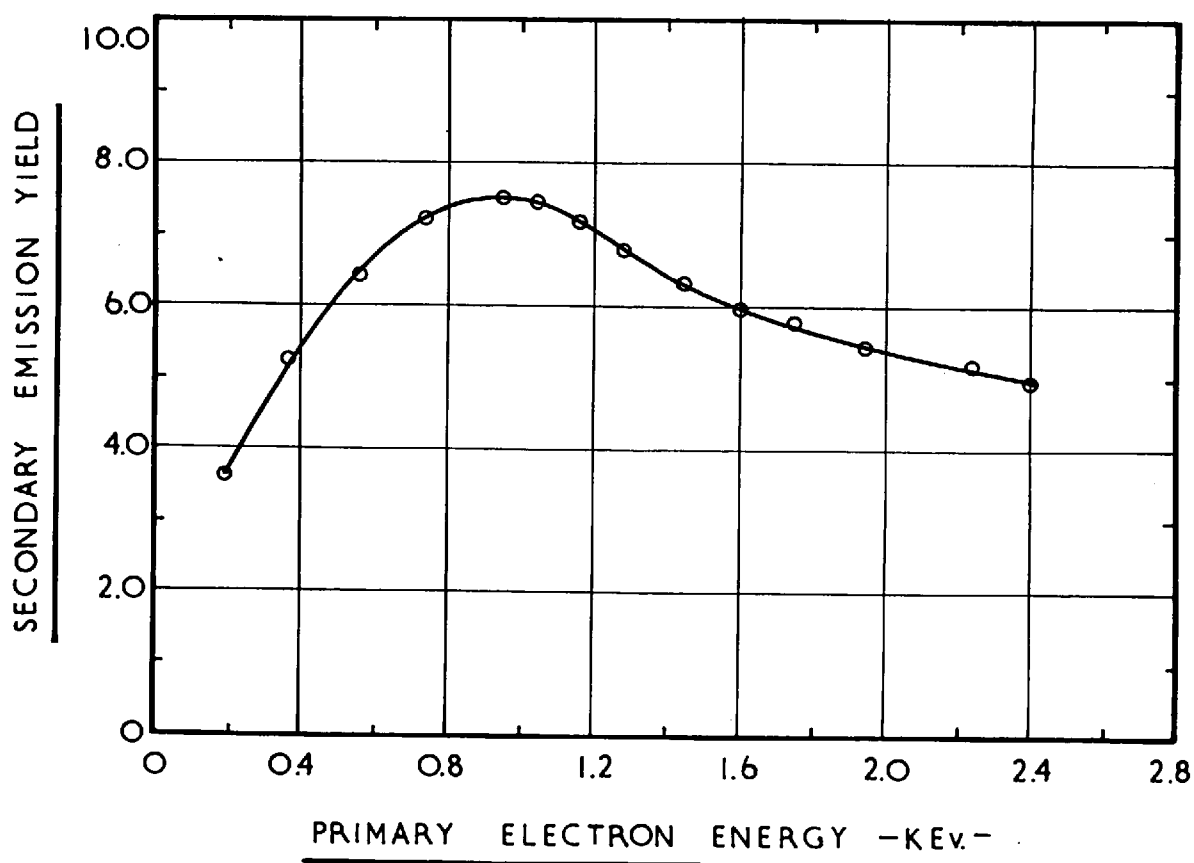


FIG. 9.

Exposure to dry air for 15 mins had no measureable effect on the yield, but an exposure of 15 mins to air saturated with water vapour at room temperature reduced the maximum yield to 6.6 (Fig. 10).

The film was again let down to ordinary atmospheric air for 24 hours, but no further decrease in the yield was observed. Attempts were then made to discover if it was possible to restore the initial yield by baking the film in vacuum at 320°C . On cooling no change in δ was observed. A re-oxidation in 5 mm of dry O_2 resulted in further decrease in the yield (Fig. 11).

Since small traces of caesium from the activation of the photocathode will be present in the intensifier, the effect of caesium on the MgO surface was also investigated. With the tube baking at 140°C , caesium was allowed to distil in from a side arm, the amount entering being monitored by checking the electrical leak between the collector and anode cylinder. When a sufficiently large amount of caesium had been admitted the baking was stopped and the secondary emission yield measured. δ was found to increase from its previous maximum of 5.5 to 7.2. The caesium side arm was then sealed off and the tube baked again at 180°C for 30 mins. On cooling a further increase in the maximum yield from 7.2 to 8.2 was observed. A third bake at 180°C for

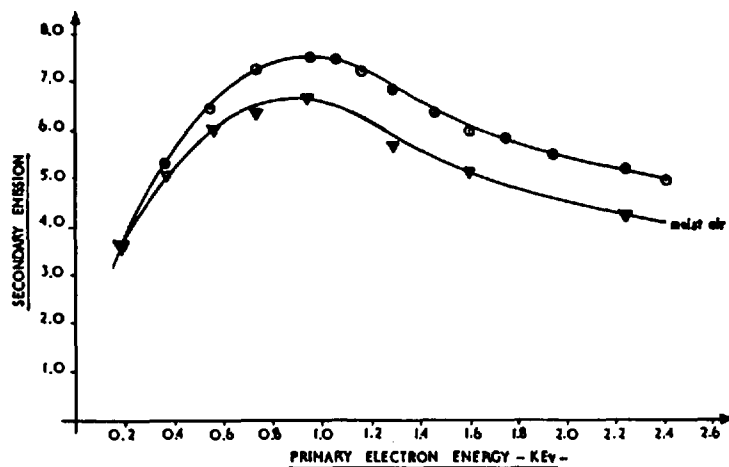


FIG. 10.

SECONDARY EMISSION YIELD OF H_2O FILM BEFORE & AFTER REOXIDATION

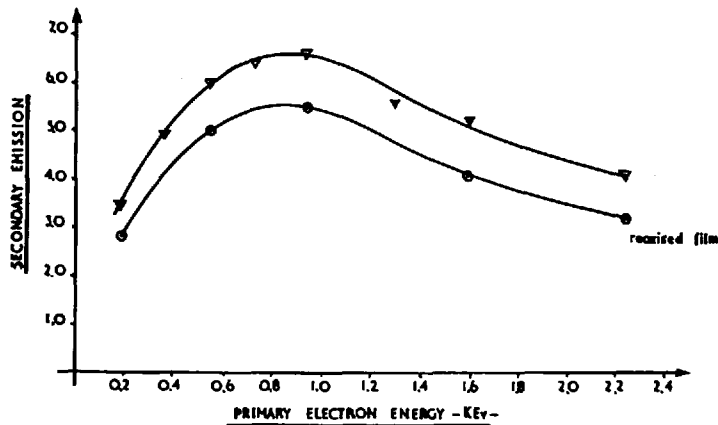


FIG. 11.

SECONDARY EMISSION OF H_2O FILM BEFORE & AFTER CESIATION & BAKING

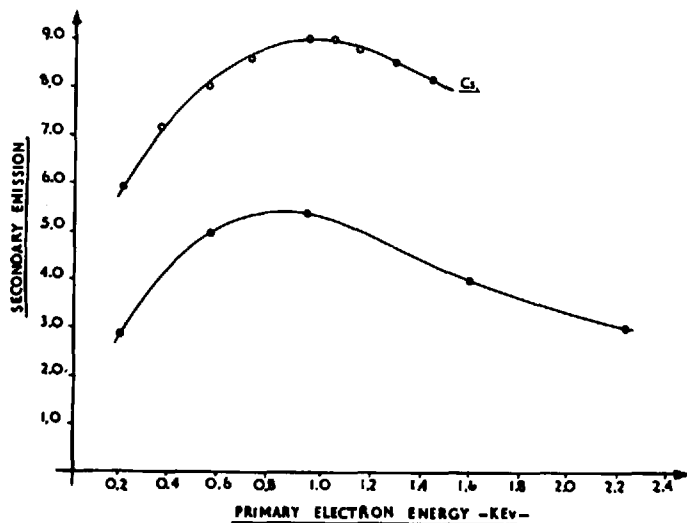


FIG. 12.

45 mins increased the maximum even further to 9.0. At this stage the electrical leak between collector and gun anode even at baking temperature had disappeared completely. A subsequent bake under the same conditions gave no further increase in the yield. The final curve is reproduced in Fig. 12, giving higher values of δ than originally obtained from the uncontaminated surface. It appears, therefore, that in the optimum condition a monoatomic layer of caesium remains very tightly bound to the surface by electrostatic forces and as a result lowers the work function of the surface. This argument is further substantiated by the fact that the surface became slightly photosensitive giving a response of $0.2 \mu\text{A/lumen}$ for 2820°K tungsten radiation.

The figures obtained for the secondary emission yield of the uncontaminated MgO are lower than those given by some other workers, but agree well with those obtained by Arntz and Van Vliet⁸⁴ and Johnston and McKay.⁸⁰ The low secondary emission is probably due to the thinness of the films used in all cases.

The effect on the yield for different oxidizing atmospheres was also investigated but the results proved disappointing. A surface oxidized in CO_2 at 420°C for 20 mm gave a yield of 5 at 950 eV and 3.9 at 560 eV. The CO_2 was generated by heating pure CaCO_3 in a side arm. It was

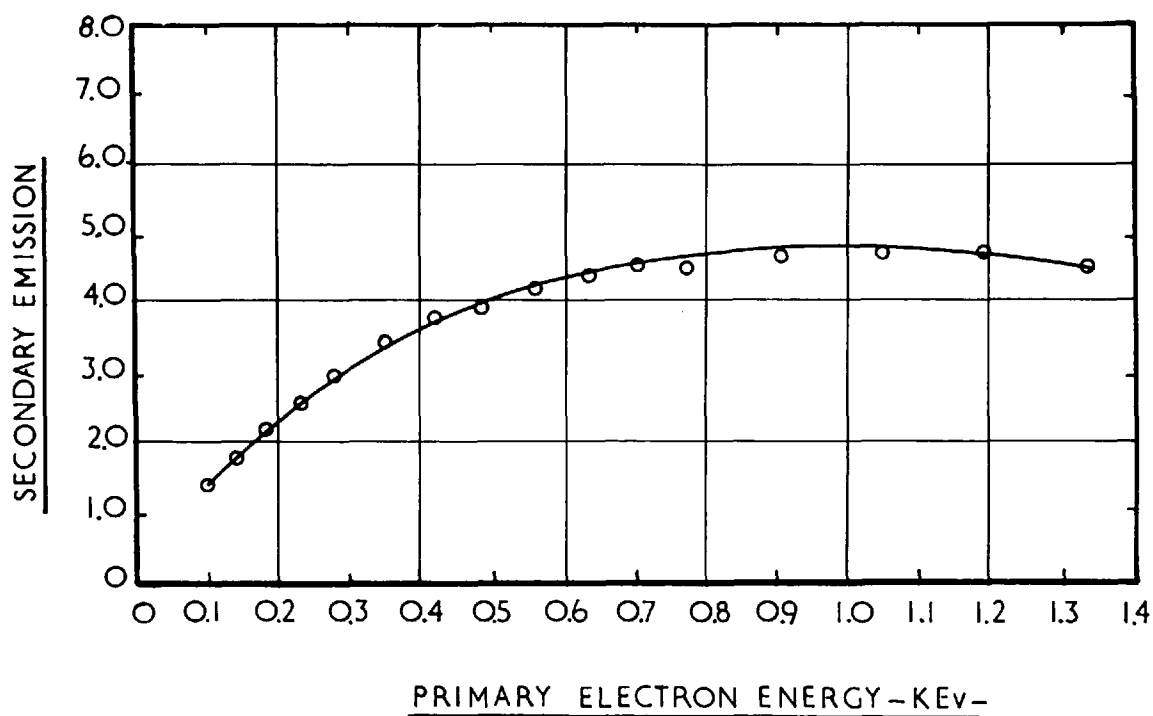
learnt later⁹⁰ that small traces of CO are also evolved in the reaction. The CO is very difficult to eliminate and is known to have deleterious effects on the oxide surface, which probably explains the low yields obtained.

(iii) Barium Fluoride - BaF₂.

This material was investigated in an attempt to find a secondary electron emitter which was more stable than KCl under electron bombardment. It was therefore decided first to examine the BaF₂ in a triode, so that its effect on the photocathode sensitivity could be studied simultaneously. Unfortunately in respect of chemical stability the emitter proved to be no better than KCl (Chapter VIII) and as a result further measurements of the secondary emission by the electron gun tube were not undertaken.

The BaF₂ was evaporated on to the target plate in a demountable bell-jar and the assembly of the components was carried out in both the glove-box and in the open under ordinary atmospheric conditions. Since BaF₂ is 200 times less soluble than KCl, it was felt that the BaF₂ films would be less susceptible to attack by atmospheric moisture. This was verified by obtaining identical secondary emission yields (Fig. 13) for both methods of assembly. The yield $\delta_{\max} = 4.8$ at 1.0 keV primary is disappointingly low, but

SECONDARY EMISSION YIELD OF
BaF₂ FILM.



SECONDARY EMISSION YIELD FOR BOTH UNCONTAMINATED & CONTAMINATED FILMS BY EXPOSURE TO ATMOSPHERIC MOISTURE.

FIG. 13.

agrees well with that obtained by Bruining and de Boer.⁷⁷
It is however less than that obtained by Sternglass.³⁸

Antimony-caesium.

This surface is the most commonly used secondary emitter in industry for the manufacture of photomultipliers. No measurements of its secondary emission yield were undertaken since this is well known⁹¹ and there is no difficulty in the preparation of the surface. The values given for maximum δ range from 6.5 to 10 at 500 - 700 eV primary energies. The yield is fairly stable under prolonged electron bombardment and as the photocathode is also of antimony-caesium, there is no danger of disintegration products from the emitter affecting the photocathode. The use of this surface in the image intensifier, however, raises several other problems. The pre-evaporated layers of antimony which have to be employed are susceptible to attack by heating during the silver chloride sealing process, particularly so as the volume of the intensifier is very small. During the processing of the surface it must also be ensured that the caesium diffuses uniformly throughout the dynode structure. Further, although the overall voltage on the tube is relatively low, the electric field gradients between the dynodes are very great and the presence of caesium in the tube

reduces the work function and therefore, under these conditions of high field gradient, increases the danger of field emission and breakdown between the dynodes and between the last dynode and phosphor screen. On the other hand, it must be pointed out that if antimony-caesium is used as the secondary emitter, the photocathode plate could be dispensed with and the first dynode used as the photocathode. This is particularly useful in improving the contrast of the image as it was found that most of the loss occurs between photocathode plate and the first dynode rather than between the dynodes (Chapter IV.3).

4. Conclusions.

None of the secondary emitters investigated is completely suitable for use in an image intensifier. The antimony-caesium surface has properties which approach closest to those of an ideal secondary emitter as outlined in the beginning of this chapter, but it is feared that the flooding of the electrode structure with caesium would cause serious insulating difficulties, as well as increasing the field emission.

BaF_2 is the only emitter not noticeably attacked by atmospheric moisture. This would greatly facilitate assembly of the dynodes, but it appears to have, however, a low secondary emission yield and dissociates under electron

bombardment.

MgO is stable under electron bombardment and has a high secondary emission yield. For very thin films the yield apparently drops but is still adequate; the films have to be thin as the thicker surfaces are particularly susceptible to field enhanced emission. Such a field would upset the electron optics configuration in the dynode channels and also limit the frequency response of the instrument. The preparation of the surface necessitates prolonged oxidation of the dynodes at high temperature. This makes the dynodes difficult to reclaim for use in further tubes - a very desirable property, at least in the early stages of the work. For KCl all that is necessary in this case is to rinse the electrodes in distilled water. The KCl surface is exceptionally easy to prepare and gives consistently high yields. The only precaution necessary is to protect the evaporated films from attack by atmospheric moisture. The fatigue of its secondary emission due to electron bombardment with subsequent attack on the photocathode is the only drawback. In spite of this, it was felt that for the early stages of the work KCl would be the most suitable material to use to establish the feasibility of the principle of the channelled image intensifier; when this was ascertained a further review of the problem could then be made.

CHAPTER IV. Design and Construction of Multi-stage Image Intensifiers.

1. Construction of Dynodes.

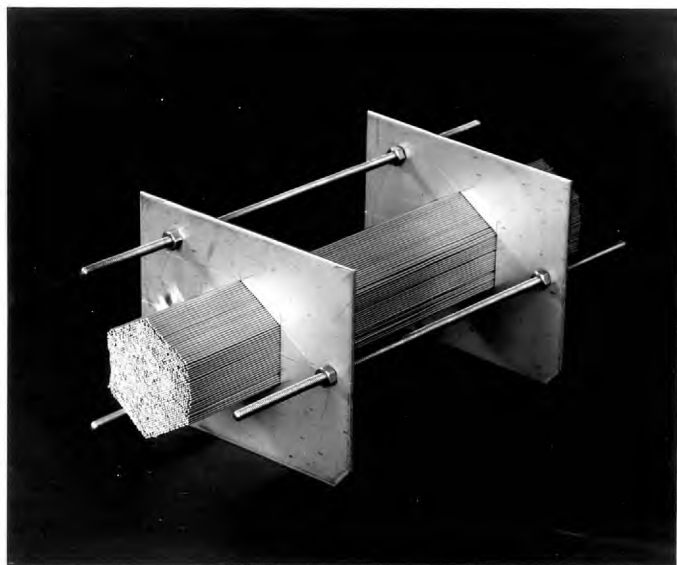
The basic principle of the construction of the dynodes is similar to that proposed by McGee and used by Flinn^{49,50} of this Department. Briefly it consists of brazing a stack of a closely packed hexagonal array of thin walled metal tubing together to form a solid block. Slices are then cut from this block at the requisite angle to give the dynodes.

Initially the dynodes used were of the same design as those employed by Flinn. Later several modifications in the method of manufacture were developed and the dynode area increased. The fabrication of the dynodes to be described is that of the latest type.

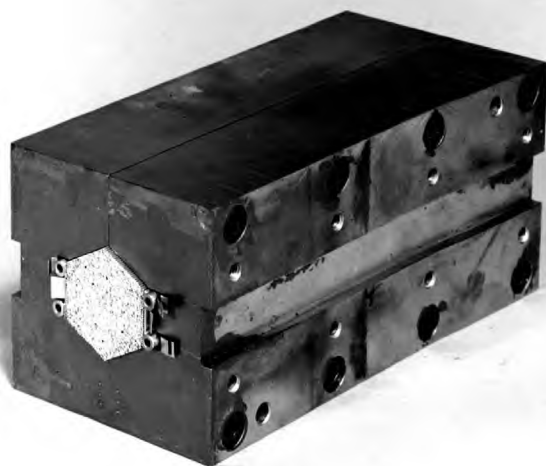
The tubing was obtained commercially and is known as "cathode tubing". It was made from O-type nickel of composition 99.5% nickel and the remainder consisting chiefly of carbon with small controlled additions of manganese, silicon and magnesium. It was purchased in six-inch lengths with 0.5 and 1.0 mm O.D. and with the thinnest wall available - 0.002 in. The ends of the tubes were cleaned from all burr and then plugged with "gun cement" (a mixture of aluminium oxide and potassium silicate solution) to prevent the brazing

alloy from blocking up the tubes. To facilitate stacking of the tubes, especially those with diameter of 0.5 mm or less, a hexagonal area was chosen for the dynodes. Such an area is of course ideally suited for close packing. Since the number of channels in each row differs by only one whole unit from the neighbouring ones, in the early rectangular area dynodes each alternative row of channels had to have a wire of half the diameter of the channels inserted at both ends.

The tubes were stacked in a subsidiary jig (Fig. 14a) consisting of two aluminium rectangular plates with an accurately cut-out hexagonal area at the centre of each. The plates were separated and their cut-out areas aligned by three threaded rods. Next the assembled tubes were carefully slid into position in a mild steel brazing jig. At this stage four mild steel tubes with internal diameter just below $3/32$ " wall thickness were also introduced at the corners of two opposite flats of the hexagon. The purpose of these tubes was to act as support for the dynodes as well as to ensure accurate alignment of the channels. The whole unit (Fig. 14b) was then thoroughly cleaned by degreasing in acetone and vacuum stoving to 1000°C . This step is of great importance since the molten brazing alloys will only adhere to chemically clean metal surfaces. All foreign



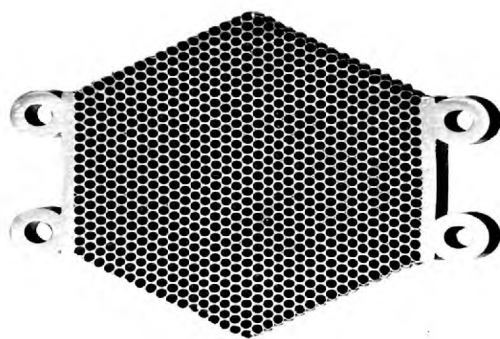
a.



b.



c.



d.

materials which might contain sulphur, e.g. oil, grease, marking pencils or cutting lubricants, were also removed before any heating took place as the nickel is subject to their attack resulting in embrittlement.

The brazing alloy to be used was carefully chosen to conform to the following conditions.

1. Actual fusion between the brazing alloy and the thin walled nickel tubing should not occur.
2. The same alloy should be suitable for brazing nickel and mild steel.
3. It should have a low vapour pressure up to the baking temperature (350°) of the intensifier.
4. The dynodes after brazing, prior to assembly, should be vacuum stoved to as high a temperature as possible (up to 1000°C). It is therefore essential that the melting point of the brazing alloy should be higher than the temperature at which the vacuum heat treatment is carried out.

In recent years^{92,93} the palladium-silver-copper range has been developed especially for use in vacuum work. These alloys have a lower vapour pressure than the silver-copper eutectics most commonly used until then, and they also have excellent flowing and wetting properties. This greatly facilitates the filling of the large gaps between the

channels. A selection from the range available commercially (Fig. 15) may enable the dynodes to be assembled in steps. Thus the total dynode area can be increased by brazing the "block" unit with an alloy melting around 1100°C , slicing the dynodes and then rebrazing several of them together side by side, at a lower temperature.

The palladium-containing alloy found to be most applicable for the initial braze is SCP5 (Ag 95% - Pd 5%). This is the only alloy in the range not containing any copper in its composition, enabling the dynodes to be subsequently etched if required without fear of the filler material being attacked.

Brazing was carried out in a vacuum stove. The brazing jig was stood up on one end and the alloy (m.p. 1010°C) placed at the top. The temperature was raised to 1040°C for half an hour and the process repeated until a sufficient quantity, about 150 gms, had been administered.

In the beginning considerable trouble was experienced due to burring of the dynodes during the slicing process. To minimize this the channels in the block were filled with a suitable liquid Perspex solution which was then allowed to set hard. Attempts to plug the tubing with molten aluminium in the vacuum furnace proved unsuccessful as the aluminium was found to attack the thin nickel walls considerably.

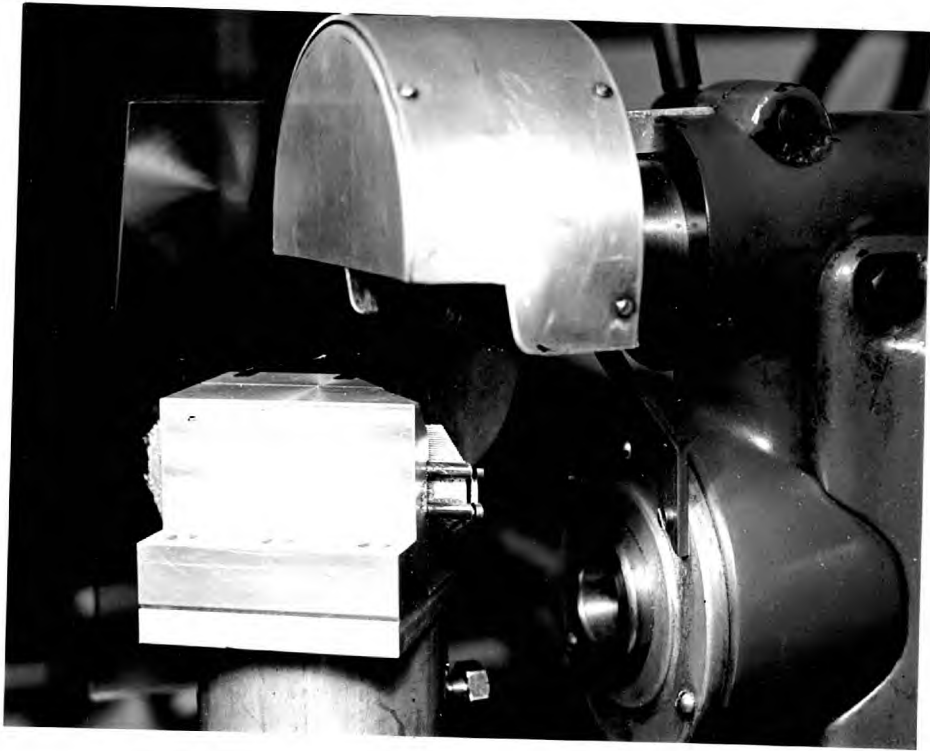
Alloy (% Composition)	Liquidus (°C.)	Solidus (°C.)	Brazing Temp. (°C.)
SPM1 (Ag 75, Pd 20, Mn 5) (Baker 2601)	1,120	1,000	1,120
SPM2 (Ag 64, Pd 33, Mn 3) (Baker 2602)	1,200	1,180	1,220
NMPI (Ni 48, Mn 31, Pd 21) (Baker 318)	1,120	1,120	1,125
SCPI (Ag 68.4, Cu 26.6, Pd 5) (Baker 722)	810	807	815
SCP2 (Ag 58.5, Cu 31.5, Pd 10) (Baker 723)	852	824	860
SCP3 (Ag 65, Cu 20, Pd 15) (Baker 724)	900	850	905
SCP4 (Ag 54, Pd 25, Cu 21) (Baker 725)	950	901	955
SCP5 (Ag 95, Pd 5) (Baker 718)	1,010	970	1,015
SCP6 (Cu 82, Pd 18) (Baker 719)	1,090	1,080	1,095
SCP7 (Ag 52, Cu 28, Pd 20) (Baker 748)	898	879	905
PNI (Pd 60, Ni 40) (Baker 288)	1,237	1,237	1,250

Fig. 15.

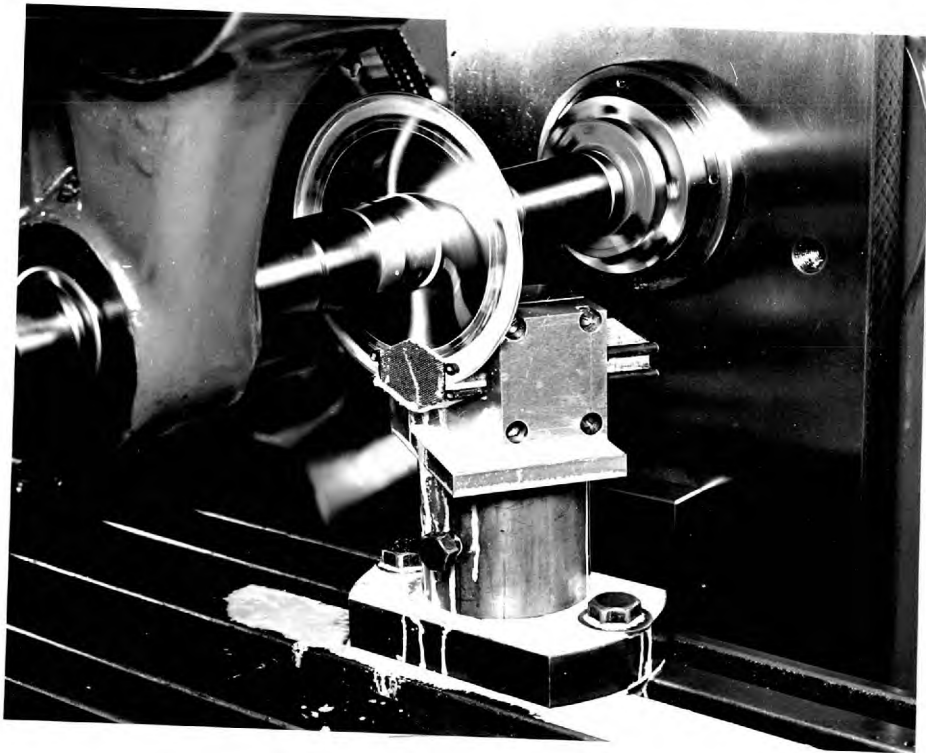
The Perspex filling in the dynodes was dissolved away by immersing them overnight in acetone. Some burr was still present, however, but this was confined to the surface only and was easily removed with a wire brush and a jet of compressed air.

Slicing of the block (Fig. 14c) to the appropriate thickness and angle was performed by a high-speed cut-off wheel operating at a peripheral speed of 14,000 ft. per minute. The motor used for this purpose was pneumatic, powered by dried cylinder nitrogen at 100 lbs/sq.in, and containing a fine oil mist for lubrication (Fig. 16a). Initially several problems were encountered with this motor. The torque available was insufficient and rapid wear developed in the front bearings. Subsequently it was replaced by one specially designed to withstand side thrust to the end bearings and with twice the torque of the previous model. The motor was rigidly mounted at the head stock of a disused milling machine and the dynode block held by a small machine vice clamped to the bed of the miller. Accurately controlled movements of the workpiece in all directions were consequently obtained.

The cutting wheels employed were of rubber bonded aluminium oxide with a diameter of 4 - 5" and thicknesses ranging from 0.020 to 0.030". Burring of the dynodes was kept to a



a.



b.

FIG. 16.

minimum by the use of soft grade wheels of very fine grit size: 320 grit was found very suitable and 280 grit almost as good. During the cutting process the wheels were kept cool by a continuous jet of very dilute soluble oil. In addition more uniform slices were obtained by allowing the cutting wheels to traverse the block several times, each at a progressively greater depth.

It was found recently that far better results were obtained by using ordinary slitting saws 0.015" thick with fine teeth, operating from a conventional milling machine (Fig. 16b). In addition to greatly reducing burring, the cuts were more accurate, and the slicing could be carried out in a semi-automatic process.

When all the techniques were sufficiently mastered, the cut slices were uniform in thickness across their surface to within 0.001". The dynodes were next stuck on to a flat metal plate by means of double sided Scotch sticking tape and the last irregularities in their surface removed by a surface grinder machine. The final product (Fig. 14c) had a thickness accurate to within 0.0005".

Accurate alignment of the dynodes was achieved by stacking them in the order in which they were cut and threading several fine drills through the channels. The alignment of the multiplying section being ensured, the external supporting holes

were reamed to $3/32$ " diameter to take $3/32$ " diameter steatite ceramic rocks during the final assembly. The nickel wire leads of the dynodes were then spot-welded in position in shallow grooves cut with the slicing wheel around the edges of the dynodes. At the other end of the leads small Inconel tags were fixed. These tags were drilled to be a tight push fit over the 1 mm diameter tungsten pins sealed through the envelope walls.

Finally the completed dynodes were cleaned thoroughly, degreased in acetone and vacuum stoved to 950°C .

2. Separation of dynodes.

It was assumed originally that in the multiplier assembly the dynodes should be kept as close as possible to each other, to avoid straying of electrons into neighbouring channels. The separation used in the early intensifier tubes was 0.004 ". The dynodes were kept separate and insulated from each other by two mica-spacers. These spacers were punched out from 0.002 " thick mica sheets. To prevent gassing of the mica in vacuum the spacers were rinsed in acetone, soaked in methyl alcohol for 30 mins and finally baked in air to 650°C for 2 hours.

Attempts were made also to evaporate a thick coating of insulating MgF_2 on to the base of the dynodes to enable them

to be stacked directly on top of and in contact with each other. The MgF_2 was evaporated from a molybdenum boat in a demountable pumping system. The dynodes were kept at 275°C by the radiant energy from a coiled tungsten wire heater above them to allow thick and resilient coatings of the MgF_2 to be applied. Coatings 10 microns thick were successfully laid down but on testing the dynodes for insulation, breakdown invariably occurred above 250 V and the process eventually was discontinued.

It was soon discovered, however, that a strong focusing of the secondary electrons occurred from one channel to the next so that their separation could be increased without fear of electrons from one channel straying into neighbouring ones. Various intensifiers were built with the dynode spacing increased in steps of 0.002" (1 mica washer). The image was checked for cross-talk by projecting on to the photocathode a very sharply focused spot of light with diameter less than one channel. Since it was difficult to ensure that the spot of light was directly above the channel, it was aligned with a row and the tube then moved slowly horizontally so that the spot traversed along the row. The image on the phosphor screen was examined. When the spot of light on the photocathode was in such a position that the photoelectrons emitted entered only one channel, one picture point appeared

on the screen. Moving the spot, however, such that the photoelectrons now entered two channels, two picture points were illuminated at the phosphor screen. The optimum condition for the spacing for 1 mm channels was found to be 0.008 - 0.010", and a further increase in the separation resulted in a slight amount of cross-talk.

The discovery of the focusing properties of the electrons is exceptionally advantageous since a lower limit to the channel size is imposed by the interdynode spacing. As the channel size is decreased, the spacing between the dynodes is reduced in proportion. A certain minimum interstage voltage is required for a reasonable secondary emission yield, so that the field strength between the dynodes is inversely proportional to the cell size. Consequently field emission would become increasingly important and ultimately impose a lower limit on the diameter of the cells. Thus for a maximum separation of 0.010" for 1 mm channels, one might assume that the separation has to be reduced to 0.0025" for 0.25 mm channels. Since the earliest intensifiers with 1 mm diameter channels had such a separation and operated satisfactorily, it can be assumed that the lower limit in channel diameter is below 0.25 mm diameter.

3. Coupling of photocathode plate with first dynode.

In order to ensure the minimum loss of information in the input signal, the efficiency of extraction of the photoelectrons from the photocathode to the first dynode must be kept as high as possible. It is therefore important to keep the photocathode plate close to the first dynode. This was done by arranging the photocathode plate to be located in a rectangular aperture cut in the photocathode shelf and resting on a 1 mm ledge of thin (0.005") stainless steel foil spot-welded on the underside of the shelf. The dynode structure was fixed to the photocathode plate by extending the ceramic rods, used for the support and alignment of the dynodes, through 3/32" holes drilled at an angle of 55° in the photocathode plate and the entire assembly firmly clamped together by small "spire" nuts. The separation of the photocathode and dynodes was thus the thickness of the stainless steel ledge and the two mica spacers inserted for insulation. The photocathode plate was made from soda glass, of such size as to be a snug fit in the photocathode shelf recess, and held in position there by a spring loaded magnetic catch. Electrical contact between the shelf and the plate was ensured by platinum paste around the edges of the plate. In the intensifiers where the secondary emitting surface was

antimony-caesium, it was possible to examine the effectiveness of the coupling of the photocathode and first dynode by comparing the quality of the image when the photocathode plate was in position and when it was removed and the first dynode used as a photocathode instead. It was found that the contrast in the image was improved in the latter case. It is unlikely that this was due to straying of the photoelectrons into neighbouring channels since the separation between the photocathode and the first dynode is only a few thousands of an inch. The loss in contrast is therefore probably due to light from the image being transmitted through the semi-transparent photocathode, reflected back from the surface of the first dynode, and arriving slightly out of register on to the photocathode surface.

In the early tubes the first dynode also gave consistently lower electron gain than the remainder; in some cases the gain was less than half that of the other stages. This is partly because of the fairly large dead area of the dynode due to the packing array of the channels and their finite wall thickness. In addition the field configuration inside these cells is considerably different from that in the other stages owing to the presence of the plane photocathode surface. The field of the following dynode did not penetrate so far into the cells so that the percentage of secondaries

extracted was reduced. In later tubes the electron gain of the first stage was improved by making the dynode thinner than the rest.

In these tubes the effective life of the photocathode was also doubled by incorporating a spare photocathode in the photocathode shelf. The length of the rectangular aperture in the shelf was widened to twice its width and the metal foil extended over the whole of this new area while still maintaining the ledge around the dynode perimeter (Fig. 17). The photocathode plate was of the new dimensions and when in position half its area was protected from contamination by the KCl by lying flat against the metal foil. When the photocathode sensitivity in the first half had dropped to an impractical value, the magnetic catch retaining the photocathode was released and the plate turned end to end bringing the new half over the dynodes. This method of lengthening the photocathode life proved very effective; measurements of the sensitivity taken on the shielded half of the photocathode showed no change even though the sensitivity in the other half had decreased by 70%.

4. Coupling of the last dynode with the phosphor screen.

The electrons, after being multiplied in the dynode structure, were accelerated over a short distance before

striking the phosphor screen. The screens used in the intensifier were aluminium backed ZnS:Ag phosphors settled in the normal manner. the aluminium backing was either floated on directly onto the phosphor or alternatively, in some cases, evaporated on to an organic film on the surface of the phosphor and the organic film subsequently baked away. The focusing property of the secondary electrons previously mentioned (p. 88) was apparent in this instance also, the final image appearing on the screen as a series of sharply defined picture points. This was a great advantage as it enabled the phosphor and dynodes to be further separated, allowing higher accelerating potentials to be applied. For, providing there is no overlap of the picture points, there is no loss in image information. The gap was increased in steps from 1 to 15 mm and the optimum separation for tubes with 1 mm channels was found to be 13 mm.

Even with the larger gaps, however, the electric field gradients were quite steep (approximately 1 kV per mm). To prevent tracking across the gap the phosphor unit was mounted separately on the end-window of the tube (Fig. 17). The screen was settled on a Pyrex glass plate previously drop-sealed into a Pyrex cylinder. Electrical contact from the surface of the plate to the inner walls of the cylinder was made through the seal by tags of platinum paste painted on the

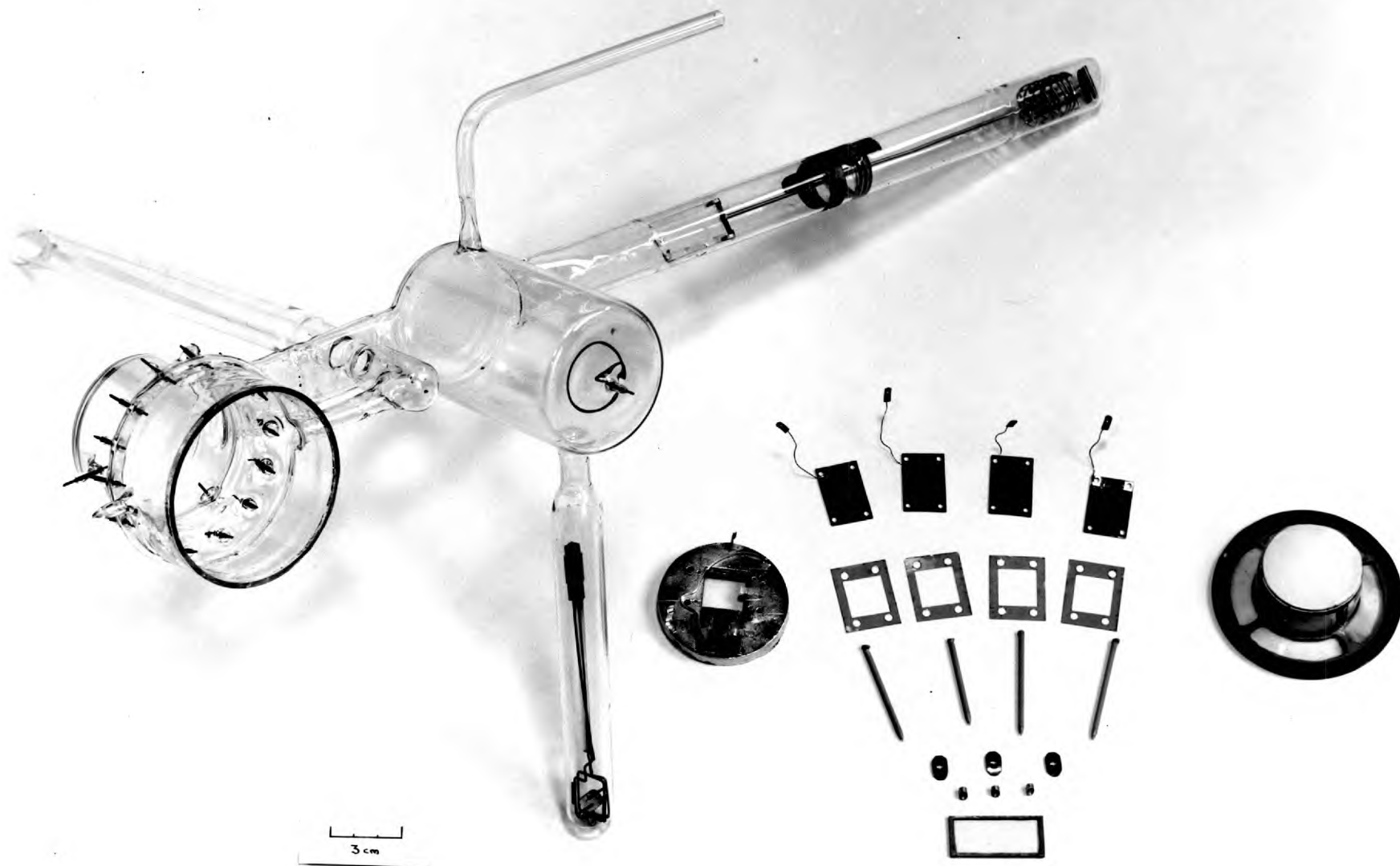


FIG.17.

sides of the phosphor plate prior to the drop-sealing process. The inner walls of the cylinder were coated with platinum paint, the purpose of which was to extend the contact of the screen to the end window and also to prevent the scattered light from the phosphor reflecting on the walls of the tube and feeding back to the photocathode. The end of the cylinder and a corresponding ring on the end window were painted with liquid bright platinum and between these the silver chloride seal was made. The platinum provided the final link of the contact, from the cylinder walls across the two silver chloride seals to the outside of the tube. Electrical connection to the screen was admittedly complicated, but this method enabled the minimum amount of conducting area in the tube at high potential to face the electrode structure.

5. Design of Channel Intensifier.

The various steps in the development of the dynode structure and phosphor unit have already been separately discussed. The general layout of these components together with the improvements in envelope design can now be considered. Since the ultimate practical intensifier is envisaged as a flat unit of large dynode area, and a little longer than the electrode assembly itself, the envelope design was

developed to conform as closely as possible to these requirements.

The first models of the intensifier have been described in detail by Flinn⁵⁰ so a brief outline of their design will only be given. Originally the electrode structure and phosphor screen were kept a long way away (7") from the end window and caesium was allowed to circulate freely throughout the tube. In later intensifiers the caesium was confined to a processing compartment between the photocathode shelf and the front window (Fig. 18). After it was established that by flushing the tube with dry argon the secondary emitting surface could be adequately protected from contamination during the silver chloride sealing process, the overall dimensions of the tube were reduced considerably bringing the phosphor screen nearer to the end window (Fig. 19). These tubes, however, still suffered from several disadvantages. The antimony was evaporated from an evaporator in a side arm of the processing compartment, a very short distance away from the photocathode plate, and it was only possible to monitor the thickness deposited at the extreme end of the plate. Even though great care was taken to design evaporators to give a uniform film thickness over large angles of evaporation, the resulting photocathodes varied greatly in sensitivity across their surface. Further small amounts of

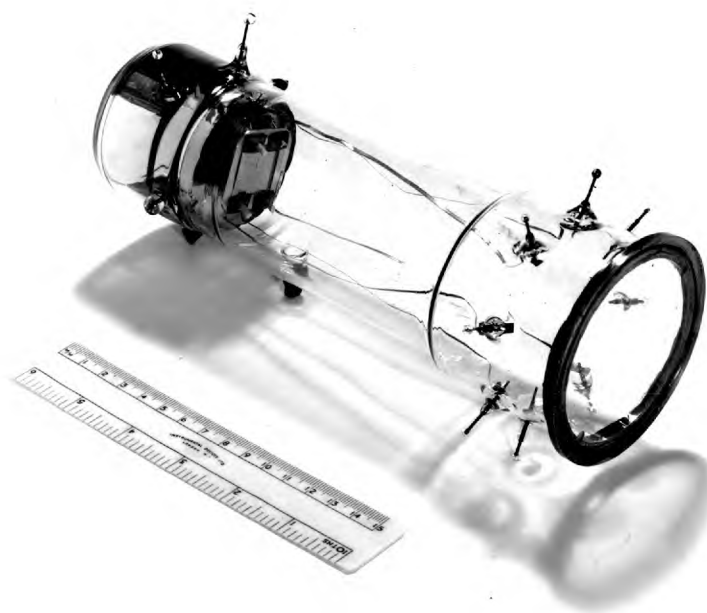


FIG. 18.



FIG. 19.

caesium still penetrated into the electrode and screen structure and some field emission still occurred at high inter-stage voltages.

To eliminate all these difficulties a technique was developed (Chapter V) of processing the photocathode in a separate chamber and introducing it to the main intensifier body through a rectangular cross-section glass tubing. The intensifier was subsequently sealed off the pump at the rectangular tubing and the main pumping stem. With this method caesium was completely kept out of the intensifier body. The overall length of the envelope was also reduced a step further by shortening the distance between the front window and the photocathode. Fig. 20a,b gives the cross-section and photograph of such a tube. The envelope (1) is made of Pyrex glass, electrical contact to the dynodes being made by tungsten pins (2) sealed through the glass around the circumference of the tube. Three other tungsten pins (3), two of them blind, act as supports for the photocathode shelf (4) and external contact to it. The shelf is the base of the dynode structure (5) and is located accurately in position in the tube by three inconel springs clipping over the tungsten pins. The tooled down portion of the glass envelope (6) and the springy stainless steel skirt around the circumference of the photocathode shelf were originally developed



FIG. 20a.

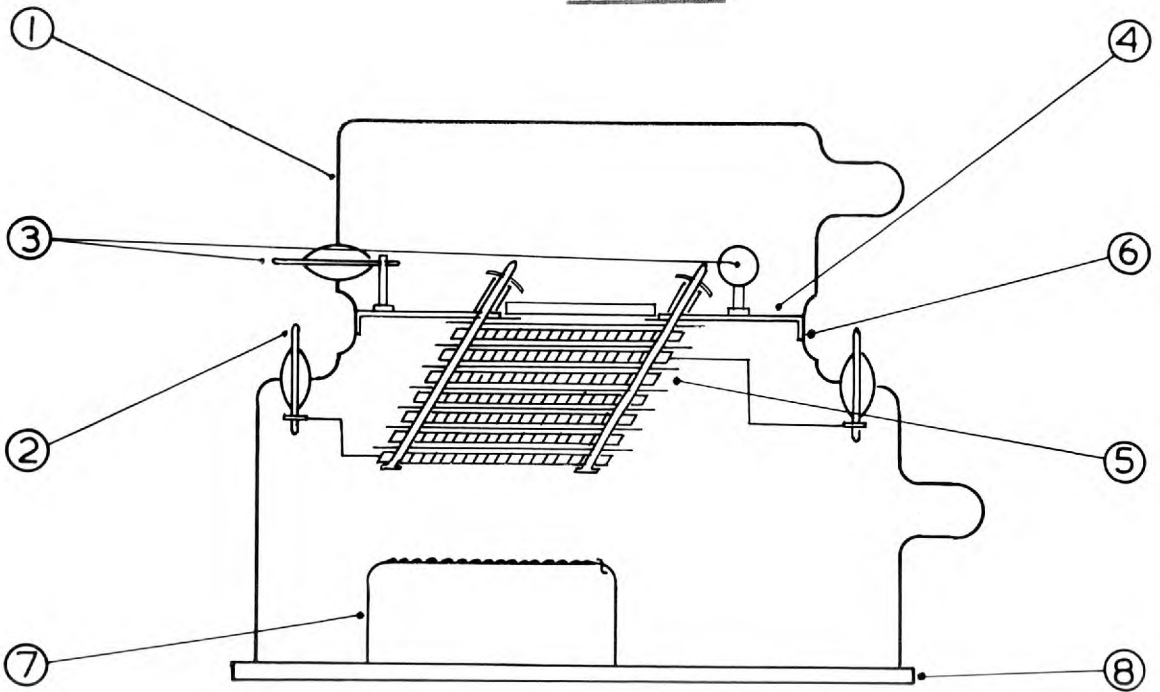


FIG. 20b.

to prevent the passage of caesium to the electrode structure, but were retained in this design since the tight fit of the skirt on the tooled down portion increased the rigidity of support of the photocathode shelf and dynode structure. The correct length for the phosphor cylinder (7) to give the required gap between the screen and dynodes was accurately determined for each tube, and the cylinder then sealed on to the end window (8) prior to assembly. During the final silver chloride seal a baffle on the heater ring prevented the inner seal from melting and dislodging the phosphor unit.

To minimize field emission due to the large field gradients present in the tube, care was taken to ensure that all the surfaces of the components were smooth and free from sharp projections. The photocathode shelf was first vacuum stoved to 1000°C and then the various inconel clips spot-welded onto it. Next it was electropolished for 5 mins at a current density of 5 amps per sq.in. in a solution of 56% glycerine, 37% ortho-phosphoric acid and 7% water, and finally vacuum stoved again at 500°C just prior to assembly. All the sharp corners of the inconel tags locating over the tungsten pins were carefully filed away, and the dynode leads kept as short and as separated as possible.

The design of the tubes using Sb-Cs as a secondary emitting material was slightly different. Since it was now

possible to dispense with the photocathode plate and use the first dynode as the photocathode instead, the dimensions of the envelope could be further reduced by settling the phosphor screen directly onto the end window and carrying out the final silver chloride seal at the photocathode end. In these tubes the activation of the Sb-Cs surfaces was carried out in the tube envelope, so that even greater care had to be taken in the design and preparation of the various components to minimize the increased danger of field emission due to the presence of caesium in the tube. A cross-section and photograph of this type of tube is given in Fig. 21a,b. Contact to the phosphor screen (1) is now made through a platinum tape seal (2) close to the end of the tube. The phosphor screen has an aluminium backing floated on to it, since such backings are considerably more free of pinholes than directly evaporated backings, thus protecting the phosphor from attack by caesium vapour during the processing of the Sb-Cs surface. The dynode structure (3) is supported on a stainless steel shelf (4) clipping over three tungsten pins (5) along the circumference of the wall of the tube. Two of these pins are blind while the other provides electrical contact to the last dynode of the electrode structure, lying flat against the stainless steel shelf. The Inconel springs, clipping over the tungsten pins, are arranged on the underside of the shelf. The heads



FIG. 21a.

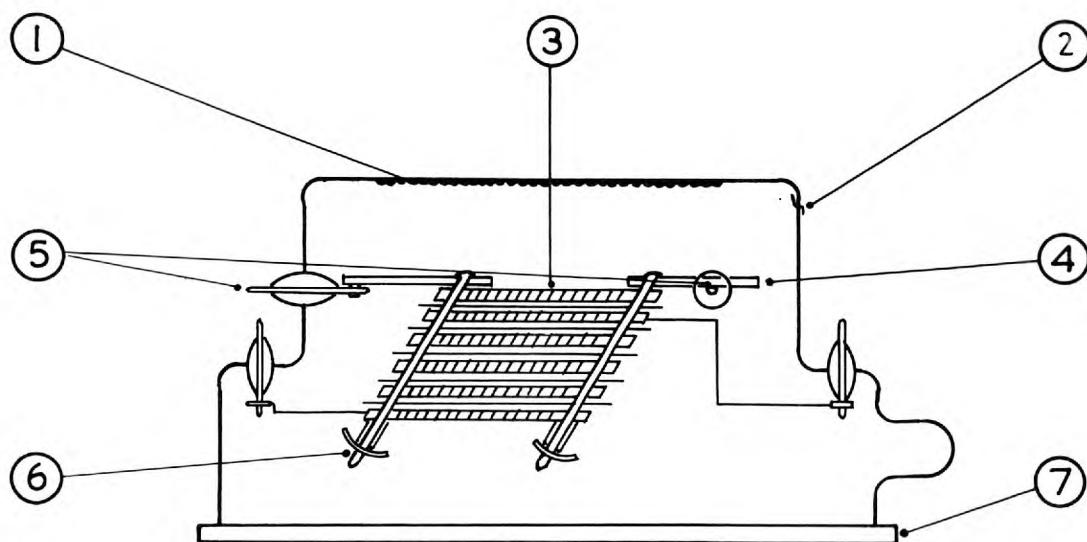


FIG. 21b.

of the four ceramic rods (6) used for stacking and aligning the dynodes are ground flat with the surface of the shelf, so that when in position a smooth surface is presented to the phosphor screen, thus allowing reasonable accelerating voltages (up to 6 kV) to be applied to the screen before any field emission or breakdown occurs. Details of the stacking, alignment and electrical contact of the dynode structure are similar to the previous tubes. Before sealing the end-window (7), a wide annular ring of bright platinum is painted on the inside as this served (p.107) as a collector for the photoelectrons from the first dynode during the processing of the antimony surface.

6. Preparation of secondary emitting surfaces.

Before deposition of the secondary emitter, the dynodes were degreased and vacuum stoved. Three different surfaces were used in the intensifier; these were MgO , SbCs_3 and KCl .

(i) MgO surface.

The preliminary investigations of this emitter (Chapter III.3.ii) showed that it was necessary to oxidize the magnesium before assembly and also to protect the MgO surface from attack by atmospheric moisture.

Activation of the emitter was carried out in a thick

walled conical flask with its neck domed over and a side arm sealed on the side to contain the magnesium evaporator. The dynodes were arranged at the bottom of the flask which was tooled to a hemispherical form with the centre of curvature at the point occupied by the evaporator. The flask was sealed through a wide pumping stem on its side, to an all-glass vacuum system capable of attaining pressures of less than 5×10^{-7} mm Hg. Before evaporation of the magnesium, the dynodes were outgassed by eddy current heating and the flask baked to 320°C until a sufficiently low pressure was attained. A magnesium layer, about 400 \AA thick, was then evaporated, the thickness of the film deposited being monitored by measuring the optical transmission through the bottom of the flask. Next the evaporator side arm with the evaporator inside was sealed off, the liquid nitrogen in the cold trap replaced with liquid oxygen and dry oxygen was admitted to the system to a pressure of 5 mm Hg. Complete oxidation of the magnesium was ensured by baking the flask at 520°C for 30 mins. After the bake the remaining oxygen was pumped away and dry nitrogen at atmospheric pressure admitted instead. At this stage the flask was sealed off the pump and the dynodes were ready for assembly. Before placing in the dry box, the neck of the flask was cracked with a hot glass point, but the top was securely

kept in place until the glove box had been thoroughly flushed with dry air.

(ii) Antimony-caesium, Sb-Cs surface.

The antimony was pre-evaporated on to the dynodes in the same demountable and transportable apparatus as used for the evaporation of KCl (p.108). Care was also taken to protect the antimony surface from contamination by atmospheric moisture by assembling the tube in a dry inert atmosphere maintained inside a glove box.

The main disadvantage with pre-evaporated antimony surfaces is that the antimony starts to re-evaporate from the surface at a relatively low temperature. It is difficult, therefore, to outgas the tube sufficiently in order to maintain good vacuum in it after seal-off. A series of simple photocells were first made to determine the maximum temperature and the time at which a tube could be safely baked. The antimony film was evaporated down to 50% transmission at the end wall of the photocell, and the cell then baked at progressively higher temperatures while monitoring continuously the transmission of the film. It was found that the films were fairly stable up to 250°C, the transmission increasing by about 2% after a bake of 4 hours. As the temperature was raised above 250°C, however, the

antimony started to re-evaporate from the end window at a progressively quicker rate until at 300°C a film of 50% transmission had completely re-evaporated in 1 hour.

It was suggested by McGee⁹⁴ that films evaporated from an alloy of antimony and palladium would be more stable at the baking temperatures used for the tubes. The alloy was prepared by heating equal proportions by weight of powdered antimony and palladium to 600°C in an inert argon atmosphere. The stability of such films was also investigated in simple photocells. A slight improvement was obtained, the films now remaining stable up to 280°C. At 300°C, however, considerable evaporation from the film surface still occurred. In addition, after processing, the sensitivity of the resulting photocathodes was always found to be lower than that obtained from ordinary Sb-Cs surfaces, the maximum obtained being 17 $\mu\text{A}/\text{lumen}$. It was therefore decided that the slight improvement in the stability of these films was not enough to warrant their use in the intensifier tubes.

Since the outgassing temperature of the tubes was limited to 260°C, extra care was taken in thoroughly vacuum stoving, electro-polishing and degreasing all the components. The tube envelope was also pre-pumped before assembly of the components and baked at 320°C for several hours.

In the intensifier tube, since both the photocathode and the secondary emitter are used on reflection, there is no restriction to the thickness of the antimony films. It should be noted, however, that the amount of antimony re-evaporated during the baking of the tube should be kept to a strict minimum, as it distills throughout the tube causing severe breakdown on the admission of caesium, even at very low voltages. The optimum conditions in this respect were found to be a thickness of evaporated antimony onto the dynodes to 30% transmission with the tube being baked for four hours at 250°C and one hour at 275°C. Under these conditions the pressure in the tubes after sealing-off remained sufficiently low to be unable to detect any ionization in the residual gas after several months.

The Sb-Cs surface in the tubes was activated in the normal processing schedule. At first attempts were made to monitor both the photocathode sensitivity and the secondary emission during the processing of the surface by connecting all the dynodes to a voltage divider. When caesium was admitted at the activating temperature (150°C), however, the electrical insulation between the dynodes invariably broke down completely and it was impossible to continue the monitoring of the activation. In later tubes, therefore, a separate collector was incorporated by painting with bright

platinum a wide annular ring at the end window nearest the photocathode and monitoring the sensitivity of the first stage only.

In spite of the above precautions, the sensitivity and electron gain of all tubes with Sb-Cs surfaces was found to be very poor (p.135). It appears, therefore, that the antimony surface is contaminated during the final silver chloride seal of the end window, in spite of maintaining a continuous flow of dry argon in the tube during the sealing process. In an effort to regenerate the antimony surface before caesiation, an R.F. discharge in hydrogen was excited in some tubes, but this had little apparent effect.

(iii) KCl surface.

The main difficulty encountered with this emitter is in protecting its surface from attack by moist air. A system was therefore developed (Fig. 22) such that the KCl was evaporated onto the dynodes in a bell-jar and the bell-jar bodily moved to the glove-box while still under vacuum. This was achieved by sealing on to the dome of the bell-jar a short pumping stem terminating in a standard B.24 ground joint. A vacuum stop-cock situated between the ground joint and the evaporating chamber enabled the chamber to be isolated from the rest of the pumping system. After the ground

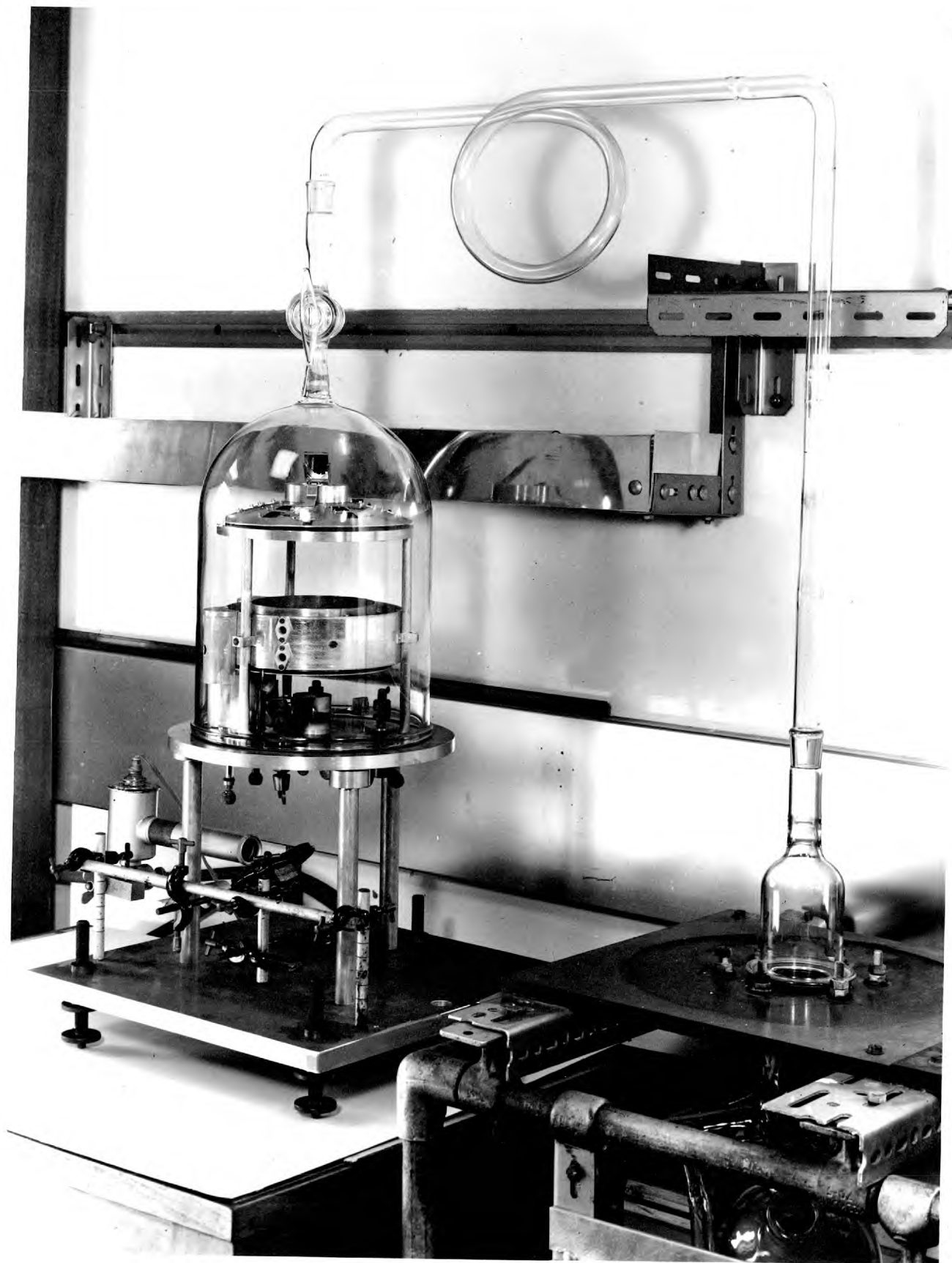
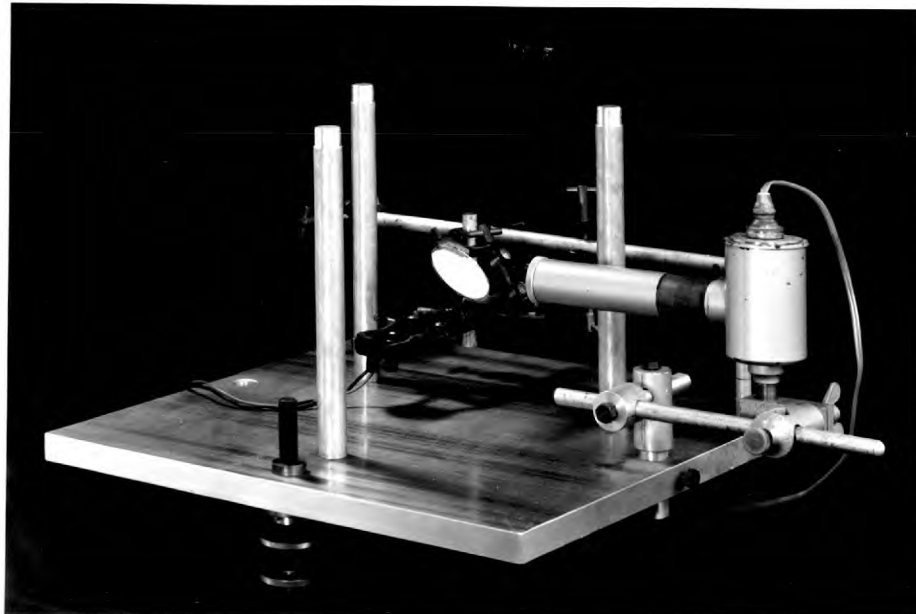


Fig. 22.

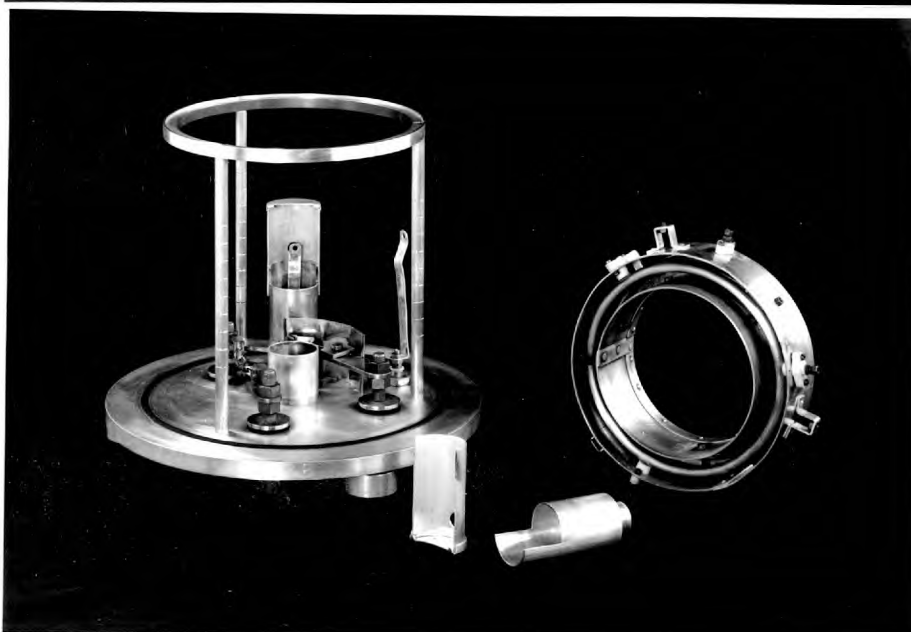
joint, the pumping line continued by a long length of large diameter glass tubing to a small bell-jar sealed with a Neoprene O-ring on to the face plate of a normal demountable pumping system.

The evaporating chamber was supported on three spacers rigidly mounted on a large Duralumin base (Fig. 23a). These spacers fitted into shallow grooves at the bottom of the base plate of the bell-jar. Through this plate, also made from Duralumin, passed three evaporator leads of thick brass rod, the vacuum seal being maintained by large Neoprene washers. Provision was also made for two highly insulated H.T. terminals for the connection of the electrodes of the ion bombardment cleaning unit (Fig. 23b). The A.C. glow discharge was operated from a high tension transformer and two insulated aluminium rings of equal diameter. The electrodes were shielded by two concentric metal bands - the inner preventing the KCl and aluminium vapour from reaching the electrodes and the outer band preventing the glow discharge from overheating the vacuum chamber. The bombardment rings were separated by a gap which at low gas pressures was less than the distance required for sustained ionization. Consequently the discharge took the path from the outer surface of the rings. This had the effect of concentrating

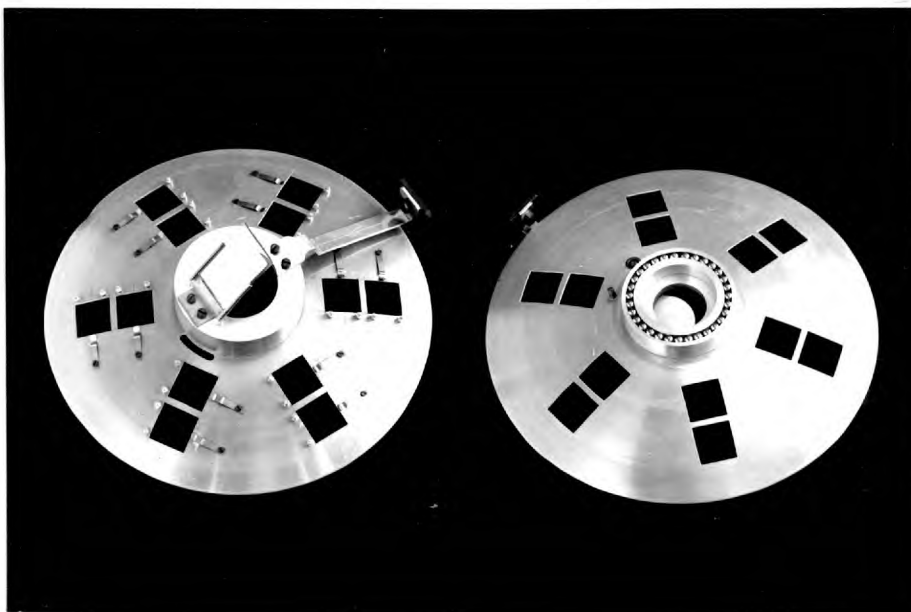
a.



b.



c.

FIG. 23.

the bombardment in the centre of the chamber.

The dynodes were mounted on top of a hemispherical aluminium plate 1.5 mm thick, with apertures equivalent to the dynode area cut through it (Fig. 23c). The dynodes were mounted over these apertures with one edge slightly raised to ensure that the KCl was evaporated on to the correct region inside the channels necessary for the secondary emission to take place (Chapter II.1.iii). The dynode plate was pivoted over another identical plate fixed on a frame above the ion bombardment unit. The apertures on these two plates were so arranged that by swivelling the dynode plate over a short arc by means of an external magnet, its apertures could be aligned with those of the bottom plate for evaporation, or alternatively made to coincide with the area between the lower apertures, thus effectively shielding the dynodes during the degassing of the evaporators. The dynode plate was mounted on a circular ball race fixed around the centre of the lower plate on which it could be rotated. With this method a very free and stable movement was obtained as well as leaving a small area in the centre free to take the test slide used for monitoring the thickness of the evaporated KCl film. A small magnetically operated shield was also incorporated over the test slide on the lower plate.

The thickness of the evaporated layer was monitored by measuring the reflection of light on the test slide. As a film of KCl is deposited on glass the interference fringes resulting from the reflection of the light at the two surfaces causes the reflection coefficient of the glass to go through a series of minima and maxima according as the layer is an odd or even number of quarter wavelengths thick. Complementary fringes with the same modulation occur for the transmitted light also. The reflected fringes were chosen for observation, however, since these give an improvement of over 25 in the ratio of the signal to "modulation noise" over that of the transmitted fringes.

Unfortunately the refractive index of the KCl film was found to match very closely that of the soda glass used for the test slide so that the resultant modulation between maximum and minimum of the reflected light was only 3%. This modulation could be greatly improved, however, on increasing the reflecting power of the surface by evaporating onto it a thin film of aluminium. The reflecting film also changes the shape of the fringes from approximately sinusoidal to ones with very sharp maxima and broad minima. The slight absorption of the light by the aluminium coating brings about phase changes in the process of reflection which are neither 0° nor 180° , so that the maxima and minima

no longer coincide with an integral number of quarter wavelengths. The effect, however, is very small, and for the purpose of this work was neglected. Consequently it was decided to improve the accuracy of the measurements by evaporating a thin coating of aluminium on the test slide to 50% transmission, the thickness being arbitrarily chosen to standardize the procedure. The result was that the modulation increased from 3% to 55% of the original reflected intensity of light.

The monitoring light beam was supplied from a 240 V pigmy bulb housed in a small projector unit. Light from the projector was deflected by a silvered mirror through a glass window, incorporated at the centre of the base-plate of the bell-jar, and focused on the test slide (Fig. 23a). The reflected light from the slide then travelled back through the end window and was collected by a selenium barrier layer cell. The pigmy bulb was run from a stabilized current supply giving a light output stable to 0.1%. The selenium cell had a peaked response at 5700 \AA and with the tungsten light source used the optimum thickness of 1000 \AA ,⁷⁴ after allowing for the angle of incidence of the KCl on the cell walls and the refractive index of KCl, was found to correspond to a point approximately midway between the first minimum and the succeeding maximum.

The complete procedure for coating the dynodes with KCl was as follows: the degassed dynodes were mounted in position on the dynode plate, the various vacuum seals connected up and the system evacuated to an indicated pressure of 4×10^{-6} mm Hg. The dynodes and the test slide were then blanked off and the KCl and aluminium evaporators degassed. Following this, air was admitted through a needle valve and the pressure was stabilized at 10 - 12 microns Hg. Both shutters were then opened and the dynodes and slide cleaned by ion bombardment for 15 minutes. With the bombardment completed the system was evacuated again to 4×10^{-6} mm Hg and keeping the dynodes still blanked off a layer of aluminium, corresponding to 50% transmission, was evaporated onto the slide. Next the dynodes were also brought into alignment with the evaporators and the KCl deposited on them. The stopcock was then closed, the pumps stopped and air was allowed in the system. Finally the pumping stem was dismantled at the ground joint and the O-ring seal, leaving the evaporating chamber with its base plate ready to be transferred to the glove box.

7. Assembly of Tubes.

All the tubes discussed so far were assembled in a dry inert atmosphere maintained inside a glove box. Due to the

limited space available in the box, assembly of the intensifiers was done in two stages. In the first stage the dynodes were mounted and aligned together on the photocathode shelf and in the second the electrode structure was fixed in the glass envelope, the dynode leads clipped over the appropriate tungsten pin and the end window, together with the phosphor screen, sealed in position with silver chloride.

Since there was no air lock on the glove box a vacuum dessicator was provided inside to store the dynode structure when ever the box was opened. During the making of the silver chloride seal, the tube was flushed with a steady supply of cool, dry argon allowing the glove box to be opened to facilitate the sealing process.

A magnetically operated ball valve was incorporated in the pumping stem of the envelope to prevent ingress of moisture generated by the coal gas during the sealing of the tube on the pump. On completion of the glassblowing the ball valve was opened and the tube evacuated.

CHAPTER V. Introduction of Preformed Photocathodes into
Image Intensifier Tubes.

1. Principle of method.

Originally the channelled intensifiers were made with the photocathode processed in an isolated chamber at the front end of the tubes. This method, however, suffered from several disadvantages.

- a. It was very difficult to prevent small amounts of caesium from penetrating into the electrode structure and giving rise to considerable field emission at interstage voltages greater than 550 V.
- b. The antimony was evaporated onto the photocathode plate from too short a distance away and it was difficult to monitor accurately the thickness deposited. The photocathodes therefore invariably had a large variation in photosensitivity across their surface.
- c. This system was impractical for the ultimate design envisaged for the intensifier - large dynode area with length a little longer than the electrode assembly - since it necessitated the photocathode being located at least its diameter away from the front window of the tube to enable it to be turned over.

To overcome these difficulties a method originated by

Folkes^{95,96} was developed where the photocathode was processed in a separate chamber and then introduced or "posted" to the intensifier through a rectangular section glass tubing. A disadvantage of this method is that the gases liberated during the sealing off of the rectangular tubing attack the photocathode destroying part or all of its sensitivity. To prevent this the surface of the photocathode was simply and very effectively protected from contamination by arranging the photocathode plate to lie with the photocathode surface flat against the front window of the intensifier during the sealing of the rectangular tubing. A second ordinary pumping stem provided on the tube enabled the gases to be pumped away before the final seal-off at a constriction on this stem.

Fig. 24 shows an intensifier tube set up on the pump. The intensifier body and the processing chamber lie on opposite sides of the main pumping stem and are sealed onto it by the rectangular tubing in parallel with two small diameter tubes. These subsidiary pumping stems are arranged to meet the main stem at different levels so as to prevent straight through access of caesium vapour from the processing chamber to the intensifier body. The entrance of the rectangular tubing to the chamber is also effectively sealed by the photocathode plate situated at the bottom of the chamber.

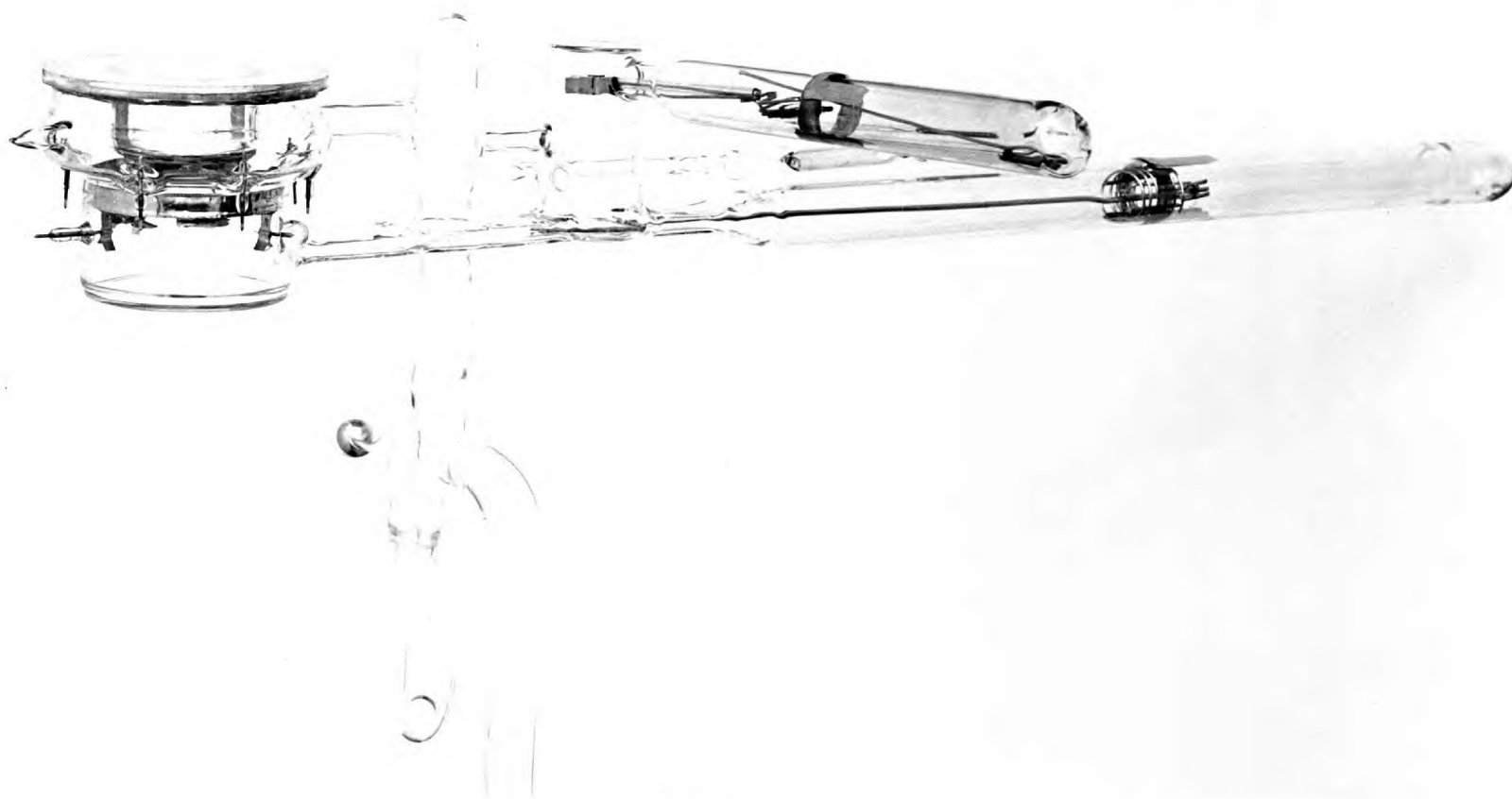


FIG.24.

The rectangular tubing is slightly extended after the processing chamber and a long length of cylindrical tubing of the same diameter as the width of the rectangular tubing is sealed onto it. The photocathode plate is lightly clipped on a rectangular frame of Inconel strips fixed at the end of a mild-steel rod. The rod is centralized in the rectangular tubing extension by a nickel wire coil at its other end. This coil also incorporates a magnetic slug and an Inconel spring pressing against a strip of platinum paste painted along the bottom of the extension arm. External contact to the photocathode is made by extending the paste over a platinum tape sealed through the glass wall of the tubing.

The processing chamber has the usual antimony and caesium side-arms associated with the preparation of an ordinary photocell. The anode is provided by a probe situated in the antimony side-arm which can be extended into the chamber, and when in this position contact is again made through a second platinum tape seal in the side arm. With this method of obtaining electrical contact, the path length along the walls between the photocathode and anode is greatly increased eliminating D.C. leakage during the processing.

2. Processing of photocathode.

After sealing onto the pump the intensifier and the processing chamber were baked at 320°C until the pressure fell below 10^{-6} torr. On cooling the system was verified to be free from leaks and then the thin swan neck of the caesium capsule was broken with a magnetic slug. The caesium was distilled further up the side arm and the capsule and slug sealed off. Next the antimony was evaporated onto the photocathode plate to an optical transmission for white light of 80% as this was found to give the most sensitive photocathodes.⁹⁷

A length of heater tape was wrapped round the processing chamber and the temperature raised in this compartment only to 160°C . The caesium was then slowly distilled into the chamber from its side arm by an auxiliary heating coil. While this was done the photosensitivity of the surface was monitored. After the sensitivity had reached a maximum, caesiation was continued until the sensitivity declined to 80% of the maximum value. The caesium heater was switched off and the temperature of the chamber lowered to 140°C . The excess caesium was then allowed to bake off until the sensitivity rose to a new maximum about twice that of the previous one. At this point the photocathode "shovel" with the photocathode plate was withdrawn into the extension arm.

This enabled the photocathode to be cooled very rapidly ensuring no subsequent loss in sensitivity.

When the chamber had completely cooled down to room temperature, the photocathode plate was turned in the side arm through 180°C to its original position and then slid down the rectangular tubing into the intensifier body, with the photocathode surface now facing the front window. There it was gently tapped clear of the retaining clips of the shovel and dropped onto the window. Next the rectangular tubing was sealed with a conventional gas-oxygen hand torch across the section between the pumping stem and the intensifier tube. The gases liberated were allowed to pump away and the tube was finally sealed off the pump at the subsidiary pumping stem.

3. Results.

To test the validity of this method a series of simple photocells were first made. Sb-Cs photocathodes with sensitivities up to $35\ \mu\text{A/lumen}$ were successfully obtained. The method devised to protect the photocathode surface was found to be completely satisfactory, no detectable change in sensitivity being observed before or after the seal off.

Image intensifiers with photocathodes subsequently made with this method, operated satisfactorily with inter-dynode

voltages up to 800 V whereas in the previous tubes with cathodes made internally field emission became considerable with voltages greater than 550 V.

Finally it should be pointed out that this method can be taken a step further by applying a technique similar to that used by Lallemand.¹³⁻¹⁶ The photocathode can be prefabricated in a sealed evacuated envelope which can subsequently be fractured in a side arm of the intensifier tube. The photocathode can then be "posted" into the tube through the rectangular tubing and the tube sealed off in the same way as is done at present.

CHAPTER VI. Performance of Channelled Image Intensifiers.

1. Criteria for assessment of the performance of the tube.

The performance of the tube can be judged by measuring the following fundamental parameters: the quantum efficiency of the photocathode, the electron gain of the dynode structure, the energy conversion efficiency of the phosphor and the resolving power inherent in the channel diameter.

In practice, however, it was found more useful to measure the integral photosensitivity of the photocathode in $\mu\text{A/L}$, and the electron and light gain of the tube. The light gain is defined as the ratio of the total light output to input light of the same spectral composition as that emitted by the phosphor. With this method the gain due to the photocathode-phosphor combination could also be determined from the electron and light gain measurements.

2. Mounting and connections of the tube.

The tube was mounted in a Perspex cradle fixed on to a clamp of a small optical bench. At the base of the Perspex cradle a vernier screw arrangement was incorporated allowing accurate movement of the tube in a horizontal direction. The screw controlled movement was used for checking cross-talk between channels (Chapter IV.3) and

for supplying the reciprocating movement necessary for "dynamic viewing" (Chapter II.4.ii).

Voltage was supplied to the dynodes through a potential divider, arranged as shown in Fig. 25. The dynodes were connected by flying leads to the appropriate tapping points on the resistance chain via 4 mm plugs and sockets. The potentiometers incorporated in the chain enabled the voltage between two dynodes to be varied while keeping the voltage between the remaining dynodes fixed. Provision was also made for measuring the electrode current and voltage by having a jack-socket and an extra 4mm socket in series with each tapping point.

The E.H.T. voltage was supplied from a 15 kV power pack. In some cases where the optimum operating conditions of an intensifier were being investigated a separate power pack was used to provide the accelerating voltage between the last dynode and the screen. In this case the last dynode was earthed and a negative E.H.T. was supplied through the potential divider to the electrode structure. The screen was then connected directly through a limiting resistor to the positive E.H.T. of the second power pack.

$$R_1 = R_2 = R_3 = \dots R_{36} = 1M\Omega$$

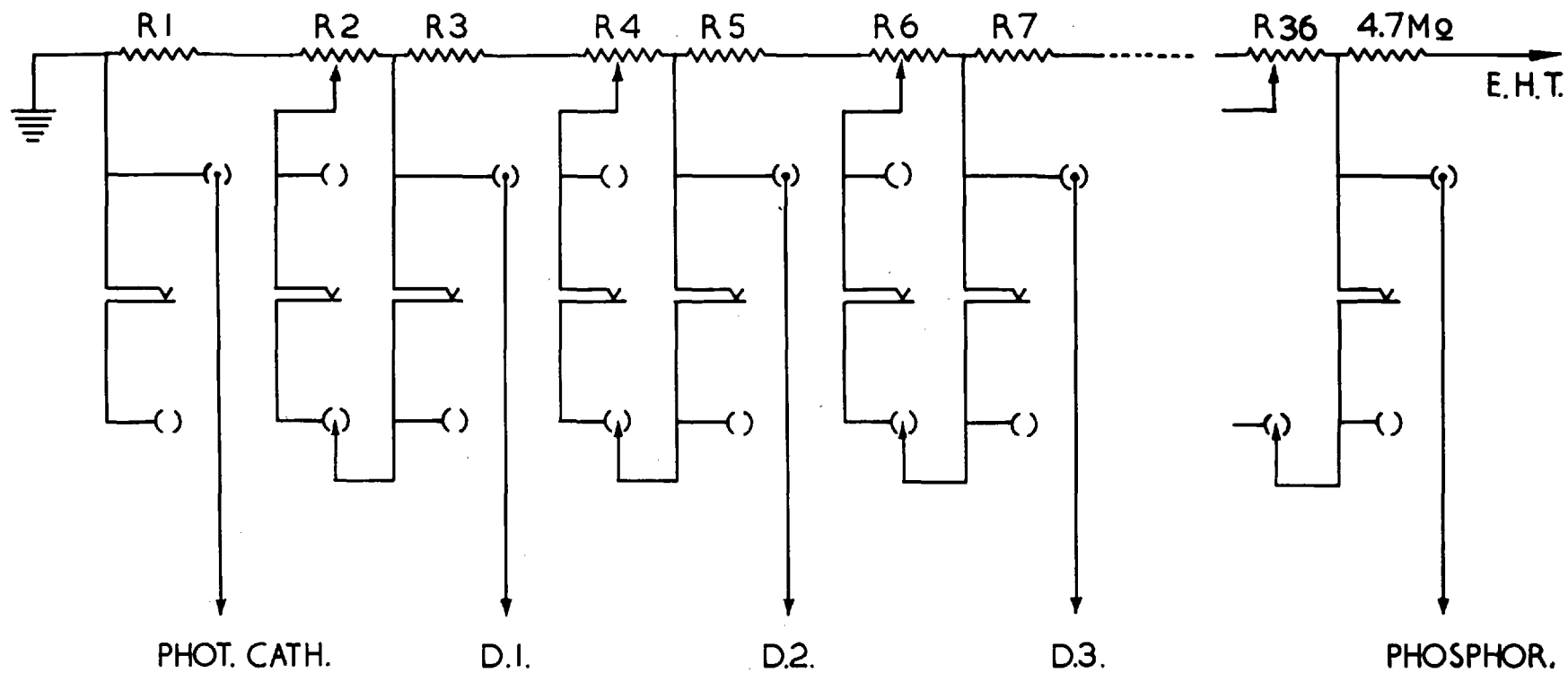


FIG. 25.

3. Measurement of Electron Gain.

The electron gain of a multi-stage tube is very large. To measure it directly without overrunning the tube would require the use of a vibrating-reed electrometer and the measurement of currents over a range of $10^6:1$. It was therefore found more convenient to measure the electron gain in steps. The gain was first measured accurately with a very low overall voltage across the tube. Keeping the voltage steady the light input was next reduced by a factor of about 5, and then the potential in turn increased until the electron gain had increased by a similar factor. The process was then repeated as many times as was necessary.

By arranging the initial electron gain measurement to be equal to five, all the current readings were taken on a single range of the galvanometer, thus reducing instrument errors. In addition this method ensured that throughout the measurements of the electron gain, no excessively high currents were drawn from the last dynode stages.

A slightly different procedure was used for the measurement of the gain of individual stages. In this case, the dynodes were divided in groups of three, and initially only the first two groups were connected to the potential divider. The electron gain of the first group was measured and then the light input was reduced. The third group was next

connected to the potential divider and the gain of the second measured. This was repeated until the gain of all the stages had been determined. The group of dynodes connected in front of the one measured ensured that the electric fields in the early group were similar to those experienced during actual operating conditions.

4. Measurement of light gain.

A similar method to that used for measuring the electron gain was employed in this instance also. A blue filter giving close approximation of the emission spectrum of the phosphor was placed between the tungsten light source and the photocathode. The input light, focused to a small diameter spot on the photocathode, was measured by a photovoltaic cell and galvanometer placed at the front of the tube. The same cell was then used to measure the light output from the phosphor. In the tubes using KCl and MgO as a secondary emitter, the phosphor screen was 2 - 3 cm from the end window and it was impossible to measure the light output directly by pressing the photocell against the screen. Therefore two $f/1.9$ lenses of $3\frac{1}{4}$ in. focal length coupled face to face were used to focus the image of the output screen onto the photocell. The two lenses operating at full aperture and one to one magnification gave a measured blue light transmission of 2.6%.

As with the electron gain, the light gain was measured in steps, the light input being reduced and the applied voltages being increased in succession.

5. Measurement of resolution.

Owing to the limited resolution inherent with the channelled image tubes, no special measuring techniques were required. The static resolution was estimated visually, but in the case of the dynamic resolution the screw controlled movement could not give sufficiently rapid motion to the tube for satisfactory visual observation and a photographic method giving a longer integrating period was adopted. With photography it was also possible to confirm that the improvement in resolution was not subjective.

6. Experimental results.

(i) Gain measurements.

The first tube to give a reasonable electron gain was a four-stage one with MgO as a secondary emitter. The design of this tube was of the earliest type, where no precaution was taken to prevent caesium from penetrating into the electrode structure. As a result only 500 V could be applied to the phosphor stage before severe field emission occurred. The presence of the caesium also limited the

interdynode voltage to 450 V, but on the other hand helped to increase the yield of the multiplying stages. With 450 V/stage an electron gain of over 30 was obtained. The gain of the individual stages in order were 1.35, 2.65, 3.1 and 2.9, giving a mean stage gain of 2.4. Although the photocathode had a sensitivity of 25 $\mu\text{A/lumen}$, no light gain was obtained due to the low accelerating voltage in the phosphor stage. The gain of the first stage was also considerably less than the remaining, being partly due, as explained in Chapter IV.3, to a theoretical loss of some 33% during the electron transfer from the cathode to the first dynode, owing to the packing array losses and wall thickness of the channels.

In tubes of the subsequent series, the first dynode was made thinner than the rest and the caesium was confined to the processing chamber only. In these tubes, however, the phosphor screen was still fixed to the electrode structure and separated a long distance away from the end window (Fig. 18). The most successful of this type was a six-stage tube with KCl as a secondary emitter. The electron gain was 300 at an average of 600 V/stage, and would have been considerably higher but for a severe electrical leak occurring between the fourth and fifth dynode which resulted in a reduction of the electron gain in these two stages. With 500 V/stage, the gain of the individual stages was 2.1, 3.6, 3.6, 2.2 (the

fourth and fifth dynodes together) and 2.0, giving an overall gain of 120. The leakage between the fourth and fifth dynodes was too great to allow their gain to be measured separately but even their combined gain was very low.

The next tube investigated had ten stages with KCl still used as a secondary emitter. The design of the tube was similar to that shown in Fig. 19, with the phosphor screen mounted independently from the end window (p. 93) but with the photocathode processed in the tube. The photocathode had a sensitivity of $18 \mu\text{A/lumen}$ and immediately after sealing off an electron gain of 8,500 was measured at approximately 370 V/stage. The light gain with this interstage voltage, and with 5 kV on the phosphor screen stage, was 1.4×10^5 . Unfortunately the aluminium backing of the phosphor was too thin and optical feed-back occurred through it to the photocathode. The angle of the dynode stack caused the feed-back image to be considerably out of register with the original, so that the image deteriorated rapidly as the gain increased above 5×10^4 . Small amounts of caesium present in the electrode structure limited the maximum interstage voltage to 530 V. Keeping a low screen voltage to prevent optical feed-back, the electron gain at this interstage voltage was 2×10^4 , corresponding to an average stage gain of 2.7.

At this stage in the manufacture of the tubes, the method of processing the photocathodes externally was introduced and the technique and equipment for the evaporation of the KCl onto the dynodes was improved. The dynodes were now cleaned by ion-bombardment prior to the evaporation of KCl and the thickness of the film more accurately controlled (Chapter IV.6.iii).

All subsequent tubes incorporating the above refinements were of the design described on p. 98 (Fig. 20). The first in this series was a five-stage tube with 1 mm diameter channels. The dynodes were separated by 0.006' and the phosphor accelerating gap was 10 mm. The sensitivity of the photocathode was rather low - $8.0 \mu\text{A/lumen}$ - but in all other respects the performance of the tube was very satisfactory. A potential of 900 V could now be applied between the dynodes without breakdown occurring, and over 12 kV could be applied between the last dynode and the phosphor screen. The variation of electron gain with overall dynode voltage is shown in Fig. 26. The maximum electron gain was 660 giving an average yield of 3.6 per stage at an interstage voltage of 900 V. The individual gain of each dynode at 400 V/stage was measured and found to be, in order, 2.0, 3.3, 3.7, 3.2 and 2.6. For 900 V/stage, therefore the gain of individual dynodes, assuming that the ratio of the gain of the individual

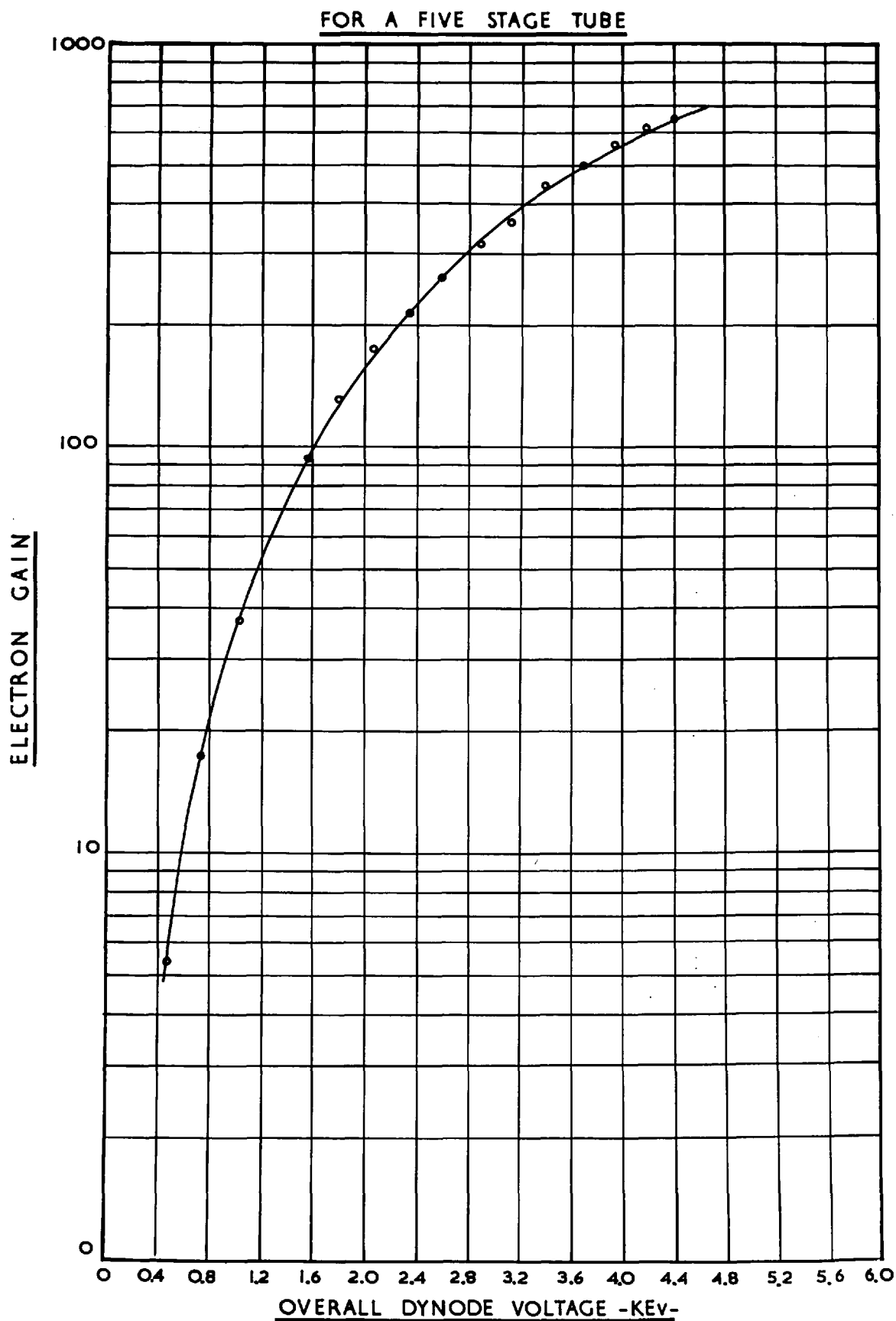


FIG. 26.

stages remains the same, would then be 2.6, 4.2, 4.4, 4.0 and 3.3. It can be seen from these figures that the gain in the first stage has improved considerably by using a dynode half as thick as the rest, and is well in accord with the theoretical loss of about 33% experienced in the coupling of the photocathode plate with the first dynode. The remaining stages gave a mean gain of 4.0, a figure well in excess of the arbitrarily established target of three per stage.

The results obtained from this tube encouraged the building of one of fourteen stages to obtain a higher electron and light gain. Since the chamber for evaporating the dynodes could only accommodate 12 at a time, the KCl was evaporated on two separate batches of 7 dynodes each. During the second evaporation, the first batch was stored in a vacuum dessicator inside the glove box. On sealing off the pump, the photocathode sensitivity was found to be $19 \mu\text{A/lumen}$ and a light gain of over 10^6 obtained with 7.5 kV on the dynode structure and 4 kV on the phosphor screen. Unfortunately a sudden flash-over in the tube resulted in a loss in contact with the phosphor screen before detailed measurements of the light gain versus overall voltage could be taken. It was still possible, however, to measure the electron gain of the dynode structure by using the fourteenth dynode as a collector. The electron gain of the remaining thirteen

stages is given in Fig. 27. A maximum of 8×10^5 was recorded at an interstage voltage of 600 V giving a mean yield of 3.0 per stage.

In parallel with the work done on tubes with KCl as a secondary emitter, intensifiers using an Sb-Cs surface as a secondary emitter were also investigated. In these tubes the first dynode was used as the photocathode, as this was found to improve considerably the contrast of the image over that given by the plane photocathode (Chapter IV.3). Early tubes suffered severely from field emission and breakdown, but with improvement in tube design (p.101) and processing techniques (Chapter IV.6.ii) these were considerably reduced. Both the photoemissive and the secondary emitting yields obtained in all cases were very low. The best tube in the series, a five-stage tube with 1 mm diameter channels, gave an overall electron gain of 18, i.e. an average yield of 1.8 per stage, at an interstage voltage of 250 V. The background at this voltage, however, was very good, and an accelerating voltage of 5 keV could be applied between the last dynode and the screen without field emission becoming noticeable.

(ii) Resolution - static and dynamic.

Measurements on the resolution of tubes with 1 mm diameter channels have already been given by Flinn.⁵⁰ In this

VARIATION OF ELECTRON GAIN WITH OVERALL DYNODE VOLTAGE FOR A 13 STAGE TUBE

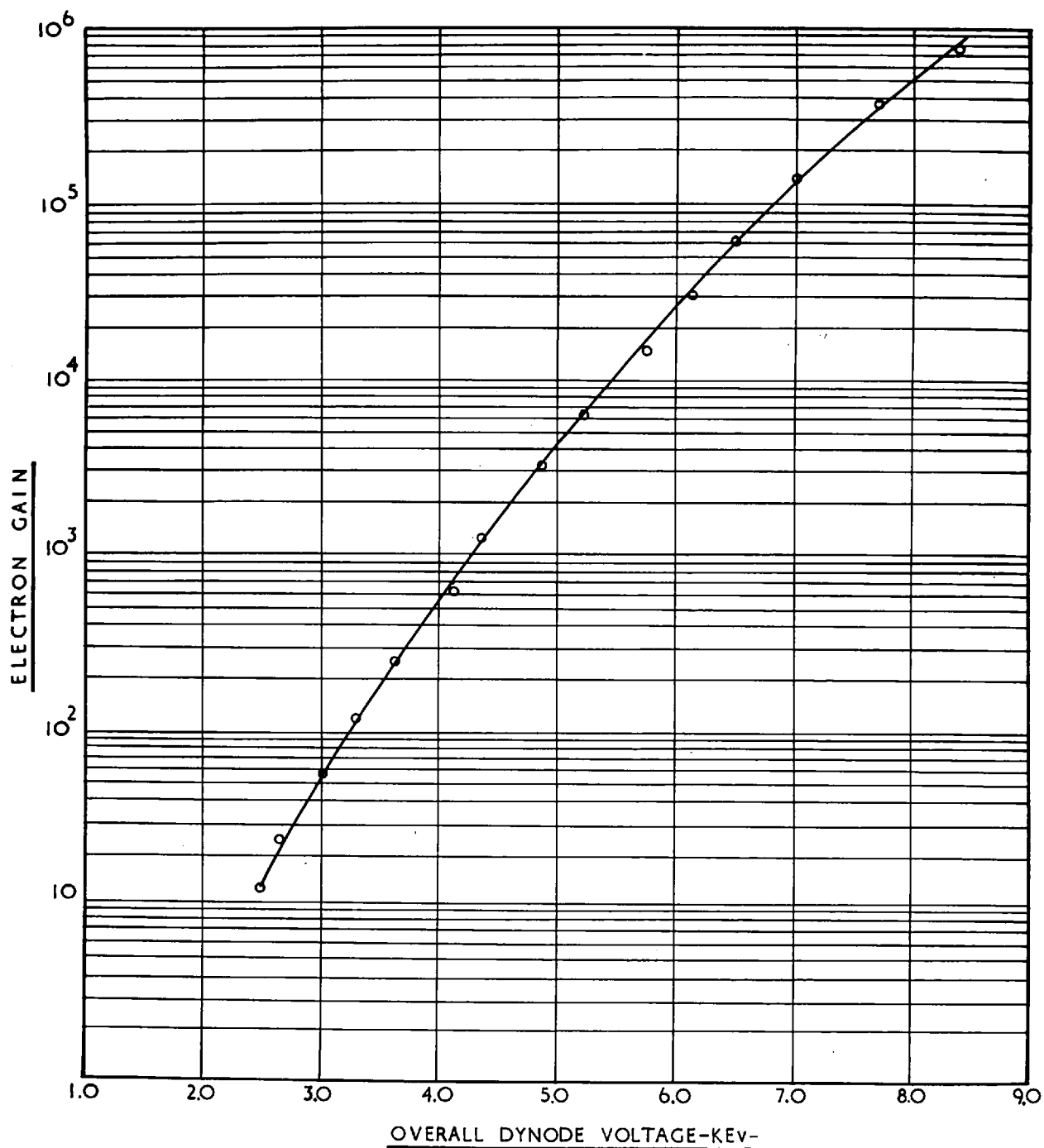


FIG. 27.

section, therefore, the results obtained will be confined only to tubes with 0.5 mm diameter channels.

For this purpose, a five-stage 0.5 mm diameter channel tube was constructed. The image area of the dynodes was 18.0 mm square giving a picture consisting of about 1300 elements. The tube had a posted photocathode, the sensitivity of which was rather low - $8 \mu\text{A/lumen}$ - so that a light gain of only 300 at 600 V/stage was obtained.

Several different test patterns were used to determine various aspects of the resolution. Some test patterns had parallel black and white bars of equal width (Foucault patterns) while others had the bars graduated in width across the pattern in order to determine the minimum resolvable line width. Finally for measuring the resolution at random orientations fan patterns were used.

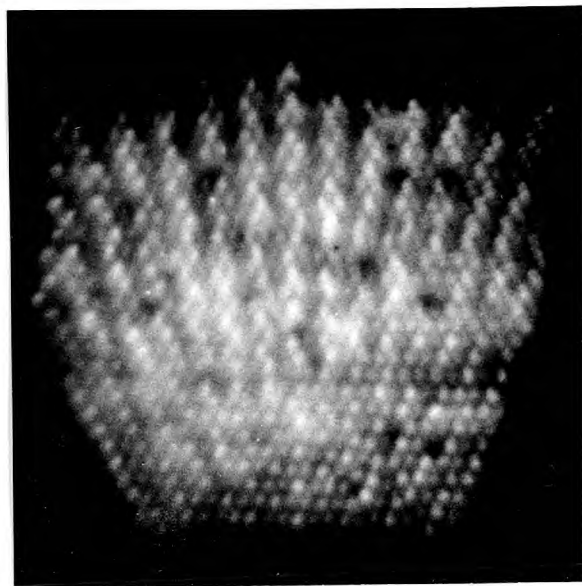
In all cases the results obtained were in good agreement with those expected from a structure of this kind (Chapter II.4). The maximum possible resolution (1.1 lp/mm) was obtained when the lines of the test pattern were exactly aligned with those of the dynode array. Near the limiting case the systematic arrangement of the picture elements gave rise to several spurious effects. If, for instance, the pattern was moved by half a channel width, the lines totally disappeared since the electrons from a bright bar were then

equally divided between two adjacent rows of apertures. Rotating the pattern through a slight angle gave rise to zig-zag effects, while for patterns slightly worse than the limiting case "beating" effects with the dynode structure sometimes occurred (Fig. 29e), greatly reducing the resolution.

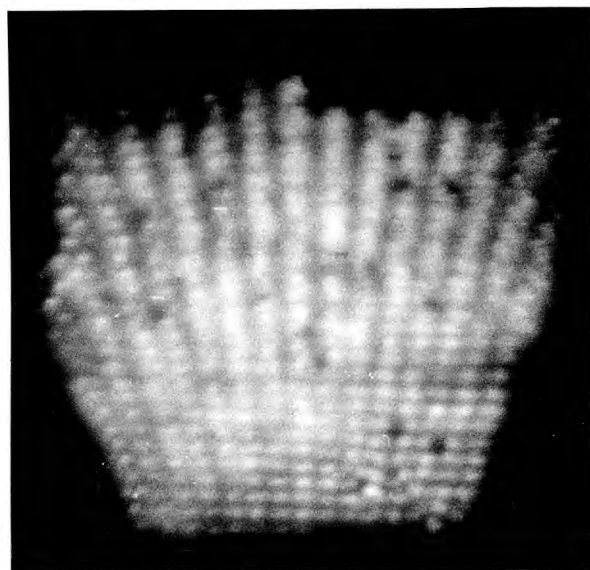
A notable improvement in the resolution can be obtained, however, by reciprocating the tube in the plane of the image with an amplitude of a few channel diameters (Chapter II.4.ii).

Figs. 28,29 show pairs of test fans taken under static and dynamic conditions. The tube was reciprocated in a horizontal direction only, with a period short compared to the exposure time. For the fan in Fig. 28a the resolution at the coarse end corresponds to 0.65 lp/mm, while at the fine end it is 1.5 lp/mm. It is seen that in the static case, the fan can be resolved with difficulty up to 0.8 lp/mm, while for the dynamic case (Fig. 28b) the complete fan pattern is resolved. In Fig. 28c the fan is too fine to be resolved with the tube static, while for dynamic viewing the fan is clearly resolved down to 1.7 lp/mm (Fig. 28d).

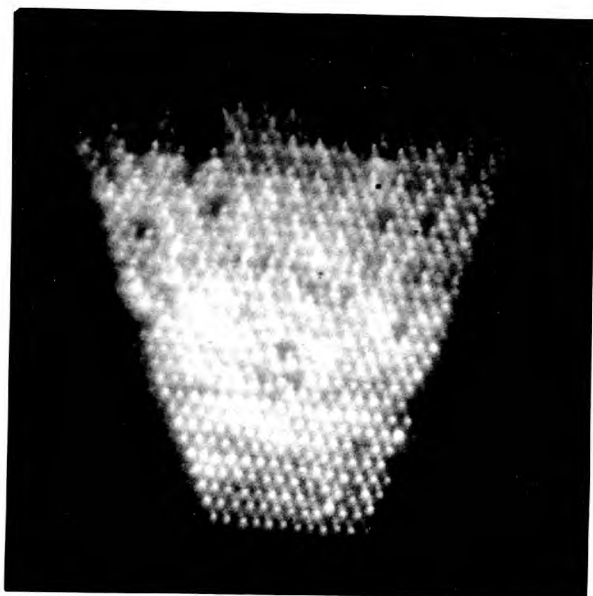
The movement of the tube also reduces the obtrusiveness of the dynode structure so that the complete image is more easily observed. Another great advantage obtained by "dynamic" viewing is in the elimination of the "beating"



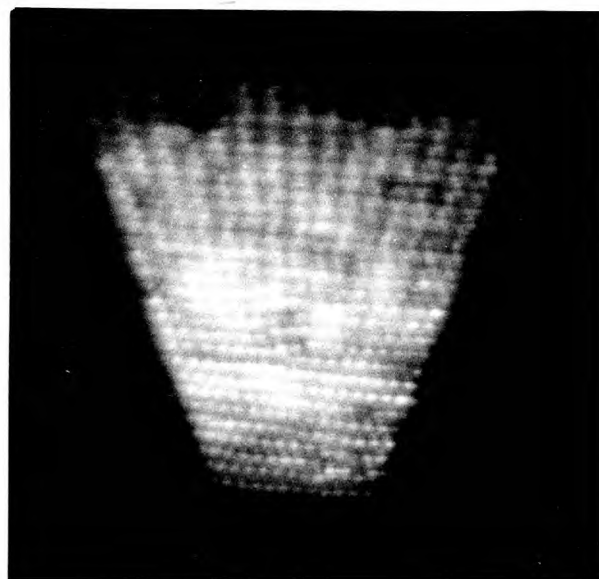
a.



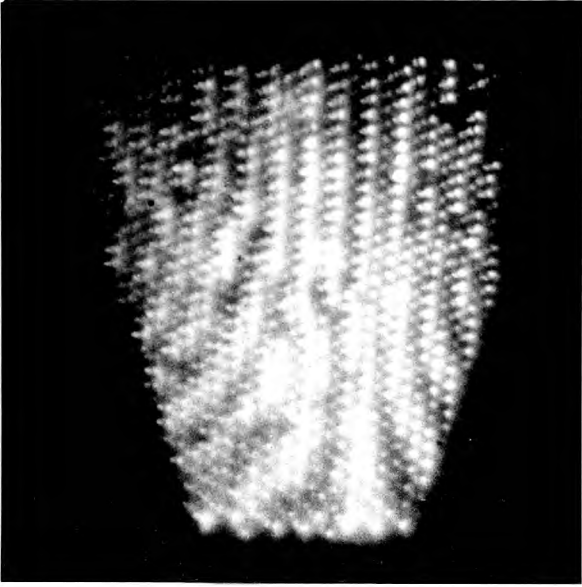
b.



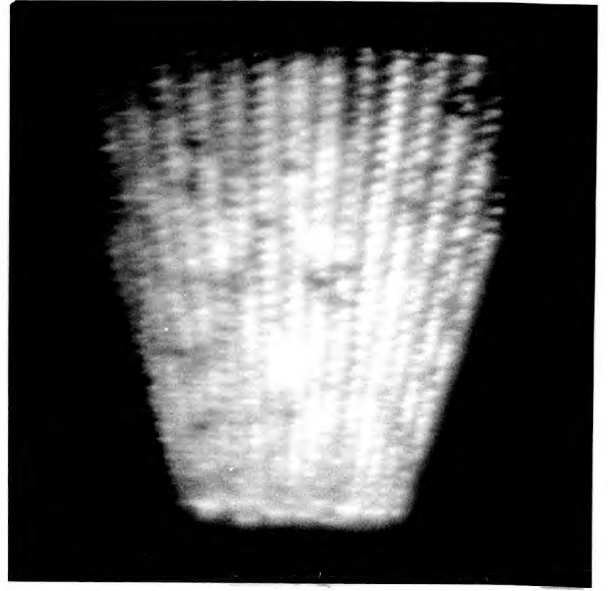
c.



d.



e.



f.

FIG. 29.

effects (Fig. 29 e,f).

In summary, therefore, dynamic viewing offers several important improvements. The linear resolution for a randomly orientated fan pattern is improved by a factor of 2.1 from 0.8 lp/mm in the static case to 1.7 lp/mm in the dynamic. This is in close agreement with the figure quoted by Kapany et al.⁵⁹ in their work on fibre optics. A similar gain in resolution along the other axis, obtained by reciprocating the tube in a perpendicular direction to the first motion, would correspond to a gain of over four in the linear resolution in any direction and is equivalent to an increase of over four in the image area.

With the above limiting resolution of 1.7 lp/mm, a 400 line television picture would then correspond to an image area of 12 cm square, a size readily achieved with the present techniques of dynode manufacture.

(iii) Contrast.

The contrast ratio in the image of most tubes was reasonably good, of the order of 75%, although falling below the theoretical expectation of 100%. In Chapter IV.3 it was shown that nearly all the loss in contrast was due to the coupling of the photocathode with the first dynode. There are three possible causes, first the finite emission velocity

of the photoelectrons, second the reflection of light from the front face of the first dynode striking the photocathode a second time away from the original point, and finally the possibility of some of the photoelectrons travelling straight through the channels of the first thin dynode and entering the adjacent channel vertically below in the second dynode.

With tubes where the photocathode is formed on the cell walls of the first dynode, the above defects are eliminated.

(iv) Background.

The presence of caesium in the dynode structure is very detrimental to the background of a tube. Even for very small amounts present, considerable field emission from the dynodes occurs beyond interstage voltages of 500 V. For tubes with the photocathode processed externally the background is acceptable up to 700 V/stage. Finally there is no reason to suppose that the dark emission from the cathode is not of the same order as that experienced in conventional photomultipliers.

CHAPTER VII. Stability of Characteristics of Image Intensifiers.

1. Shelf life of photocathode.

Since the channelled image intensifier consists of large masses of metal, mica and ceramic, it was important to examine the shelf life of the photocathodes. In the early tubes the photocathodes had a relatively short half life (of the order of a few months) but with improvement in techniques for preparing the components for vacuum the shelf half life was extended to over one year. In the later intensifiers the dynodes were outgassed by vacuum stoving instead of eddy current heating. The mica washers were carefully rinsed in acetone and methyl alcohol, and baked in air for several hours at 600°C, the soft iron slugs and photocathodes shelf were vacuum stoved to 1000°C and electropolished prior to assembly. The assembled intensifiers were baked at 320°C on the pump for 12 - 14 hours, while at seal off the pressure was better than 5×10^{-7} torr.

A typical "posted" photocathode (Chapter V) would conform to the following pattern: during the first 24 hours following seal off the photocathode sensitivity would increase by about 10% of its original value. The sensitivity would then stay at this value for a period of several weeks and then very gradually start to decrease again.

2. Operational life of photocathode and secondary emitter.

The preliminary investigations carried out on the fatigue of the secondary emission of KCl (Chapter III.3.i) showed that the electron gain could be expected to decrease by as much as 55% at an integrated incident charge density of 12 millicoulombs cm^{-2} . In the actual intensifier tubes, however, the current densities are kept very low; the output density is generally between 50 and 100 times less than that used in the preliminary experiments so that for a multi-stage tube the decay in the early dynodes is negligible with only a slight deterioration occurring in the later dynodes. A far more serious disadvantage is in the decay of the photocathode sensitivity during the operation of the tube. This loss of sensitivity is characteristic of all types of tubes using KCl as a secondary emitter^{44,45,47} and is attributed to the poisoning of the photocathode by the dissociation products of the secondary emitter during the electron bombardment.

A five-stage tube was built to investigate the life characteristics of the photocathode and the electron gain. The tube was of the design shown in Fig. 19 with the photocathode processed in the tube envelope. It was decided slightly to over-caesiate the photocathode in the hope that the excess caesium might act as a getter, protecting the photocathode surface beneath it. Unfortunately the over-caesiation was

carried too far and the sensitivity of the photocathode on sealing off was only 7 $\mu\text{A}/\text{lumen}$. Since any changes in the tube characteristics associated with the current densities used on the screen for visual observation take place very slowly, it was found necessary, in order to hasten the effects, to use current densities two orders of magnitude higher. During the measurements an intense beam of light, 5 mm in diameter, was focused on to the photocathode, the sensitivity and electron gain being monitored continuously. With 200 V/stage and 4 kV on the phosphor screen, the results obtained are given in Fig. 30. It is seen that there is a rapid decay in the sensitivity, the photocathode having a half life of 50 mins only. The photocathode current during the measurements varied from 6×10^{-8} amp to 5×10^{-9} amp. The decay in the photocathode sensitivity was found to be restricted to the illuminated area of the photocathode. Similar results were obtained (Fig. 31) on a different uncontaminated surface of the photocathode with 400 V/stage and 7 kV between the last dynode and the phosphor screen. With an initial bombarding current of 1×10^{-7} amps the half life of the photocathode was found to be 27 mins. On plotting the relative sensitivity against the total integrated charge leaving the photocathode (Fig. 32), the sensitivity is seen to drop to 50% of its initial value at an integrated charge of 8×10^{-5} coulombs.

RELATIVE VARIATION OF PHOTOCATHODE SENSITIVITY WITH
TIME OF OPERATION OF TUBE

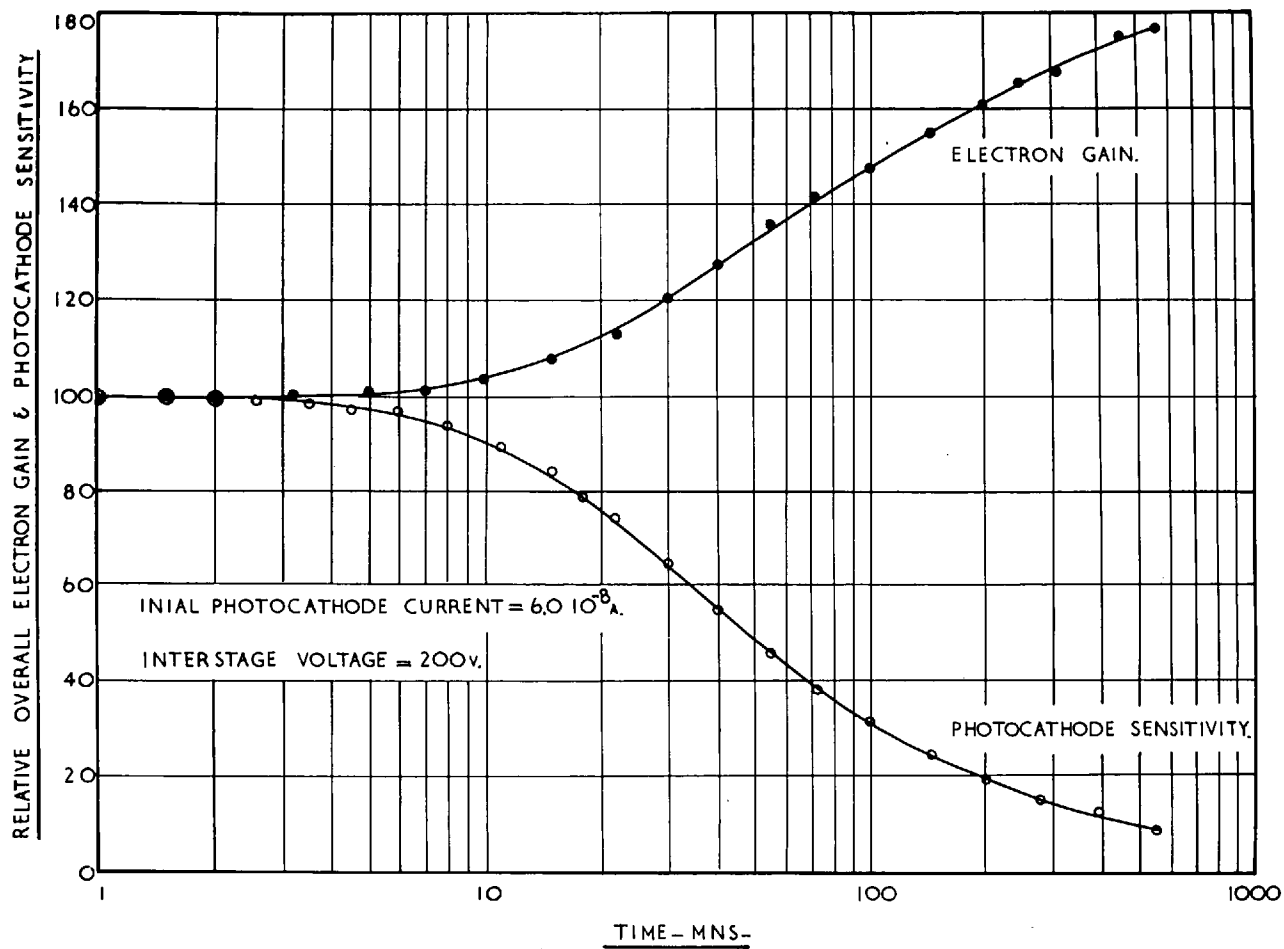


FIG. 30.

Measurements made by Todkill⁴⁵ on image intensifiers with transmitted secondary electron multiplication, at current densities in the range 7×10^{-9} to 2×10^{-7} amp.cm⁻² for an illuminated area on the photocathode of 1 cm², gave results that were consistent with a half life of 3.5×10^{-3} coulombs cm⁻². There is no reason to assume that the processes contributing to the loss of sensitivity are different in the two cases, the factor of 40 in the total integrated charge at half the photocathode life can be accounted for by the fact that whereas the secondary emitting surface for the channel tube is separated by only a few thousands of an inch from the photocathode, for the transmitted tube the dissociation products from the KCl have to diffuse back through and around the supporting aluminium oxide films before they can reach the photocathode. A further point substantiating this argument is that for the transmitted secondary emission (T.S.E.) tubes the loss in sensitivity is uniform across the whole area of the photocathode, whereas for the channelled tube the loss in sensitivity is strongly restricted to the illuminated areas of the photocathode. At first this was thought to be due to positive ions liberated by the secondary emitter travelling back and bombarding the photocathode. Careful measurement along the photocathode area (Chapter VIII.1.ii.a) however, showed that this was not the case, the decay in

RELATIVE VARIATION OF PHOTOCATHODE SENSITIVITY WITH
TIME OF OPERATION OF TUBE

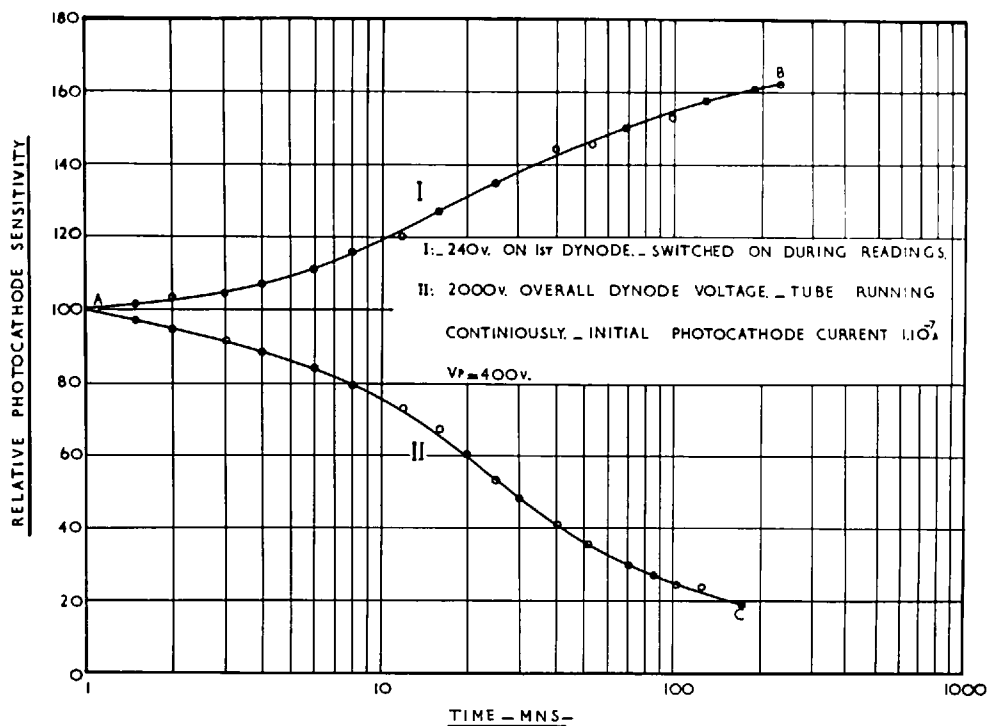
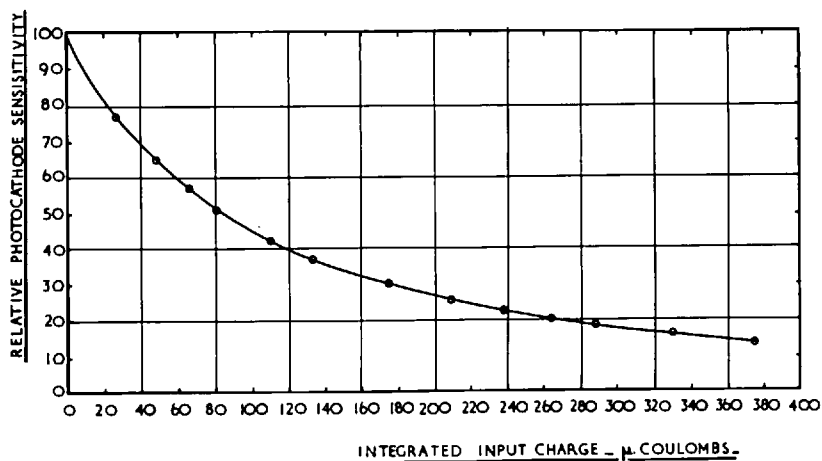


FIG. 31.

RELATIVE VARIATION OF PHOTOCATHODE SENSITIVITY WITH
INTEGRATED INPUT CHARGE



PHOTOCATHODE PROCESSED IN TUBE. - $V_p = 400V.$

FIG. 32.

sensitivity being due to neutral particles emitted from the emitter with an approximate Lambertian distribution.

In order to investigate the effect of heating of the photocathode by the intense light source originally used, another set of experiments was carried out on a fresh surface of the photocathode. On this occasion the first dynode was only connected to the potential divider and the voltage (240 V) switched on only when readings of the photosensitivity were taken. The results are shown in Fig. 31. The sensitivity is seen to increase with time of exposure, indicating that some of the excess caesium was being vaporized off the photocathode, thus improving the sensitivity. The readings were continued until the point B on the curve was reached, whereupon the remaining dynodes and screen were connected to the potential divider and the tube now allowed to run continuously with an interstage voltage of 400 V. Considering the sensitivity at B as the original sensitivity, the curve AC was obtained similar to that of Fig. 30. The overall dynode voltage in the second test was 2 kV with 7 kV on the phosphor screen.

The variation of the electron gain with time of operation of the tube is given in Fig. 30. Contrary to expectation, the gain was found to increase with time. This increase can be accounted for by assuming that some of the excess caesium

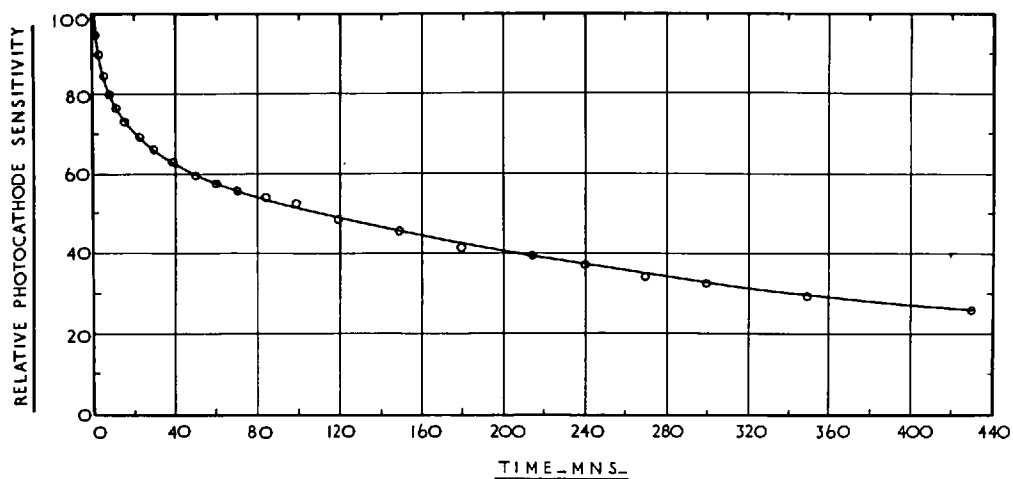
liberated from the heated, over-caesiated photocathode is adsorbed by the KCl surface, thus improving its secondary emission coefficient. It is seen from Fig. 30 that the overall light gain of the tube remains approximately constant. It must be remembered, however, that the loss in sensitivity of the photocathode lowers the quantum efficiency of the input stage of the tube.

At this stage in the work on the channelled intensifier, the method of processing the photocathode externally (Chapter V) was developed. It was soon observed that subsequent intensifiers employing this type of photocathode appeared to have more stable photocathodes than those in the intensifiers with the photocathode processed in the tube. A further series of tests was therefore undertaken to determine the stability of the characteristics of tube with "posted" photocathodes. A twelve-stage tube was used for these tests with design similar to that described on p. 98. The initial sensitivity of the photocathode was $20 \mu\text{amps lumen}^{-1}$. In order to eliminate the heating effect of the photocathode by the light source an infra-red absorbing filter was placed between the photocathode and the light source. Since the previous tube examined with the internally processed photocathode had only five stages, in order to make the appropriate comparison in the first series of tests only the first five stages of the

twelve-stage tube were connected to the potential divider. With 400 V/stage and an initial photocathode current of 1×10^{-6} amps, the variation of decay of the relative photocathode sensitivity obtained with time of operation of the tube is given in Fig. 33a. It is seen that the photocathode sensitivity decreases to 50% of its initial value after 110 mins. The variation of the relative photocathode sensitivity with total integrated charge is also given in Fig. 33b. The half life of the photocathode is reached in this case after an integrated charge of 4.1×10^3 coulombs giving an apparent improvement in the stability of the "posted" photocathode of a factor 50 over the photocathode processed in the tube. Such an improvement was also obtained in the triode tubes during the more detailed investigation of the action of the bombardment of the secondary emitter on photocathode sensitivity (Chapter VII.1.ii). The improvement is probably due to the slight variation in the processing procedure used for the external photocathodes (p. 166). Throughout the above series of measurements no detectable decrease was found to have occurred in the overall electron gain of the five dynodes.

In the second series of tests, all the twelve dynodes were connected to the potential divider. Keeping the same interstage voltage of 400 V and with an accelerating voltage

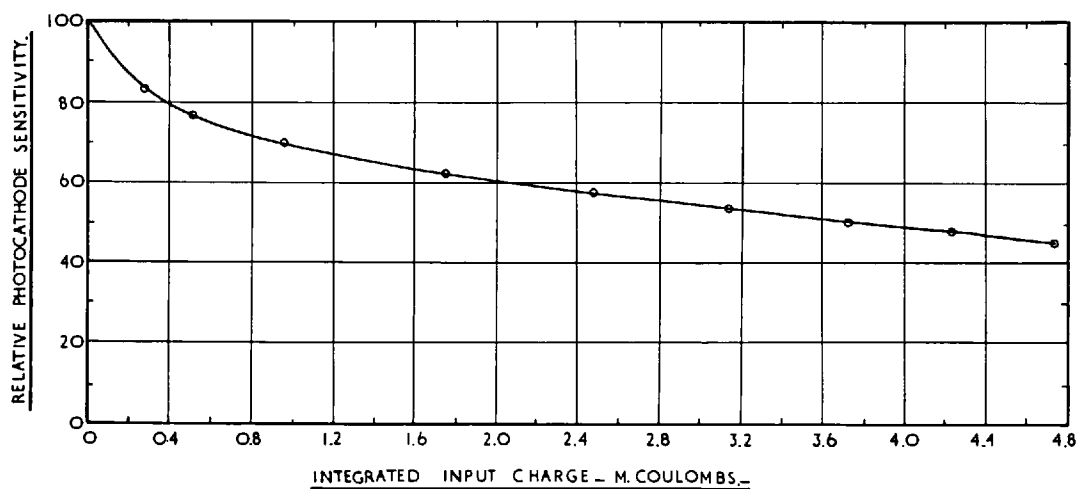
RELATIVE VARIATION OF PHOTOCATHODE SENSITIVITY WITH
TIME OF OPERATION OF TUBE



INITIAL PHOTOCATHODE CURRENT $1.0 \cdot 10^{-6}$ A. — INTERSTAGE VOLTAGE = 400v.

FIG. 33a.

RELATIVE VARIATION OF PHOTOCATHODE SENSITIVITY WITH
INTEGRATED INPUT CHARGE



PHOTOCATHODE PROCESSED EXTERNALLY. — $V_p = 400$ v.

FIG. 33b.

of 7 kV between the last dynode and the phosphor screen, similar measurements were taken on the decay of photocathode sensitivity with time of operation of the tube. In this case the current drawn from the last dynode was two orders of magnitude higher than that drawn from the fifth dynode in the previous experiment. Contrary to expectation, the rate of decay of the photocathode sensitivity was found to have increased by only 20% to the rate of decay obtained when the first five stages were only operated. It appears, therefore, that the decay in the sensitivity of the photocathode is primarily due to the electron bombardment of the first few dynodes, the later ones contributing only a small fraction to the total decay. This is particularly encouraging since in the multi-stage intensifiers the current in the first few dynodes for normal visual observation is extremely small.

In conclusion, therefore, it is seen that the useful life of the channelled intensifier is limited, not by the fatigue of the secondary emitting surfaces, but by the decay of the photocathode sensitivity caused by the dissociation products of electron bombardment of the emitter. To increase the operating life of the tubes, a spare photocathode was incorporated in the tubes (Chapter IV.3) thus effectively doubling their life.

CHAPTER VIII. Investigation of the Bombardment of the
Secondary Emitter on Photocathode Sensitivity.

1. Experimental work.

(i) Introduction and method of measurement.

In the previous chapter the decay in photocathode sensitivity with time of operation of the image intensifier was examined. In order to investigate this phenomenon more fully it was decided to simplify the structure of the electrodes in the tube by using a plane metal plate, coated with the secondary emitter, placed parallel to the photocathode and spaced a short distance (4 mm) away. A tungsten mesh of low shadow ratio was also incorporated between the photocathode plate and the metal plate to determine the nature of the charge, if any, of the dissociation products liberated by the secondary emitter under electron bombardment. The detailed construction of these tubes (triodes) was given in Chapter III.2.ii, when they were used to measure the secondary emission coefficient of the target plate surface.

Measurements on the decay of the photocathode sensitivity were carried out in the following manner: with the photocathode at earth potential a positive voltage of several hundred volts (generally 500 V) was applied to the target plate. Keeping this voltage constant, the potential of the

mesh was varied positively or negatively with respect to the target plate. During the intervals when the grid was positive with respect to the target plate, it suppressed any positive ions liberated under the bombardment of the secondary emitter, while in the intervals when the grid was negative it only helped to localize the electric field gradient between the photocathode and the target plate.

Since any changes in the photocathode sensitivity, associated with the current densities used in the actual intensifiers, take place very slowly, it was decided to use current densities two orders of magnitude higher. Light from a slightly modified 35 mm slide projector was focused on to the photocathode to give a spot of 4 mm diameter. The light source was kept constant throughout the measurements and to minimize heating of the photocathode by the intense light beam used, an infra-red absorbing filter was placed between the source and the photocathode.

(ii). Experimental results.

(a) Potassium chloride - KCl.

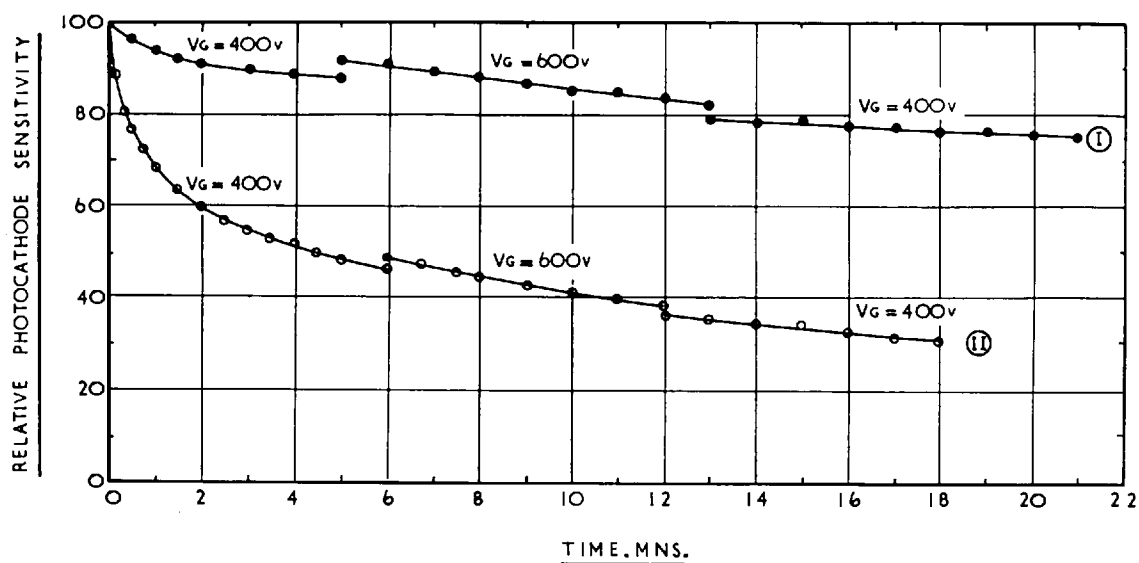
It was necessary to establish first of all whether the deterioration in the photocathode sensitivity was primarily due to the dissociation products liberated from the secondary emitter and not due to gases liberated from the metal sub-

strate under electron bombardment. The KCl was therefore evaporated onto half the target plate area only, the remaining half of the stainless steel plate being left bare or alternatively coated with a film of previously evaporated aluminium. The evaporation of the KCl and aluminium was carried out in the same demountable apparatus (Chapter IV.6.iii) as that used for the dynodes of the intensifier. The tube was finally assembled in a dry argon atmosphere maintained inside a glove box.

Four triodes having KCl as the secondary emitting surface were built and tested. The first two, TR-I and TR-II, had the photocathode processed in the same tube envelope, while tubes TR-III and IV had the photocathode processed in a side chamber and introduced into the main body through a rectangular slit (Chapter V).

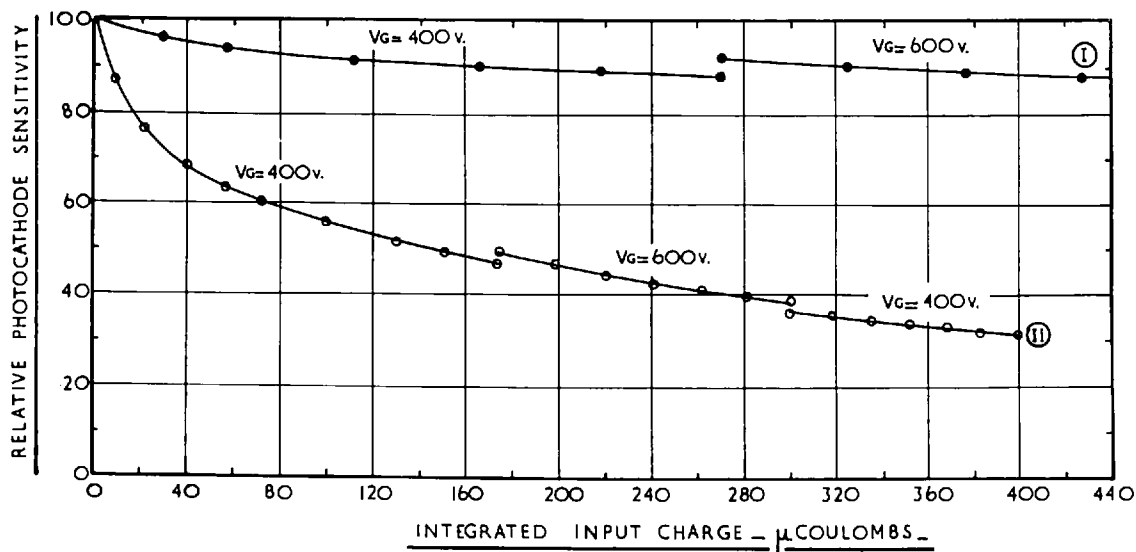
Identical measurements were carried out on the sensitivity of the illuminated area of the photocathode immediately opposite the KCl and metal surfaces bombarded by the photoelectrons. The variation of the relative photocathode sensitivity with time for tube TR-II opposite the KCl and the aluminium surface is given in Fig. 34. In this instance the target plate voltage was kept at 500 V and the grid voltage alternated between 400 V and 600 V, i.e. 100 V negative and positive with respect to the target plate. The initial bombarding

BOMBARDMENT OF KCL. & AL. TARGETS.



I: _AL TARGET II: _KCL TARGET $V_P = 500v$
 INITIAL PHOTOCATHODE CURRENTS: _KCL = $0.72 \cdot 10^{-6} A$ _AL = $1.0 \cdot 10^{-6} A$ _

FIG. 34.



I: _AL TARGET II: _KCL TARGET $V_P = 500v$

FIG. 35.

currents were 0.72μ amps for the KCl surface and 1.0μ amps for the aluminium. A more accurate representation of the difference in magnitude of the decay is given in Fig. 35, where the variation of relative photocathode sensitivity is plotted against the total input charge to the target plate. It is seen that over the KCl surface the photocathode sensitivity drops by half its initial value after an integrated incident charge of 140μ coulombs, while the drop in sensitivity over the metal surface starts levelling off to 85% of its initial value after an integrated charge of 500μ coulombs. It should be noted that each measurement is carried out on fresh areas of the photocathode surface; half the photocathode area being protected from contamination by lying flat against a thin metal foil (Chapter II.2.ii).

A similar set of results but with different target plate and grid voltages is given in Fig. 36 and 37. In this case the sequence of the grid voltage was also reversed so that initially the grid was lying positive at 200 V with respect to the target plate. It is seen that in both cases so far the grid voltage has no effect on the initial or subsequent rate of decay, the slight change in the photocathode current at switch-over being due to non-saturation of the photocathode current with extracting voltage, probably due to the internal resistance of the photocathode. The deterioration in photo-

BOMBARDMENT OF KCL. & AL. TARGETS

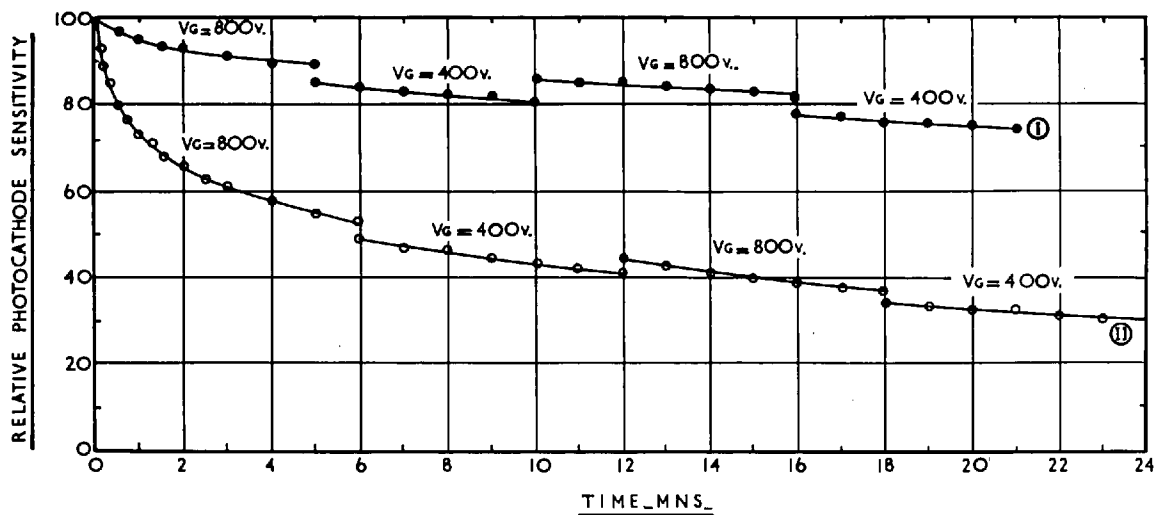
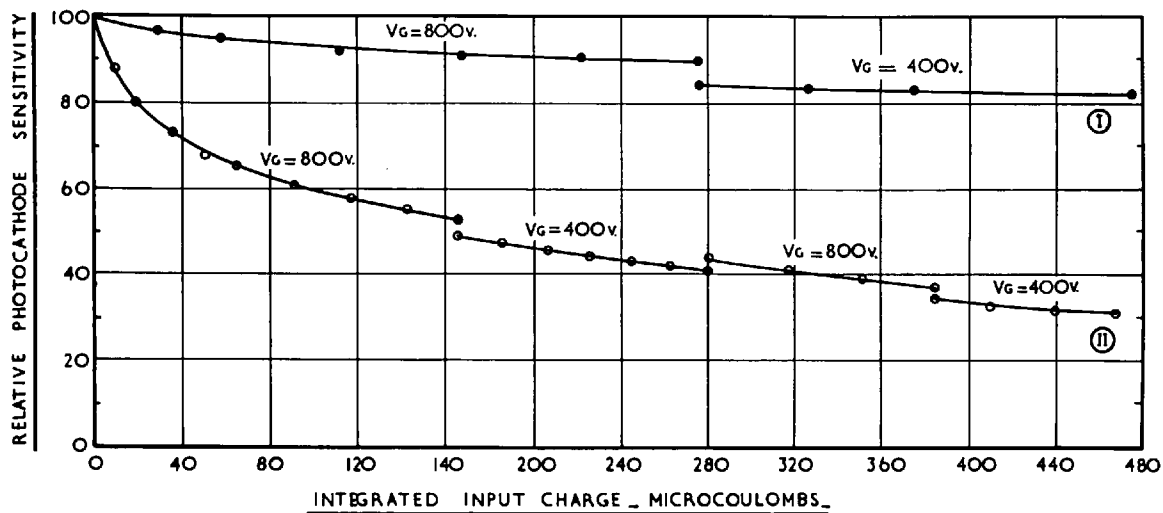


FIG. 36.



I:— AL. TARGET.

INITIAL PHOTOCATHODE CURRENT $1.0 \text{ } 10^{-6}\text{A}$.

II:— KCL TARGET.

INITIAL PHOTOCATHODE CURRENT $0.72 \text{ } 10^{-6}\text{A}$.

$V_P = 600\text{V}$.

FIG. 37.

cathode sensitivity also appears to be independent of target plate voltage.

Since the grid voltage has no effect on the rate of decay the deterioration in photocathode sensitivity cannot be due to positive ion bombardment of the photocathode since it would have been suppressed when the grid was positive relative to the target plate. It is therefore concluded that the loss in photocathode sensitivity is due to neutral particles emitted from the KCl surface and that these particles are very likely neutral chlorine atoms (Chapter VIII.2).

The deterioration of the photocathode sensitivity for both the intensifier tubes and the 'triodes' has always been closely associated with the illuminated area of the photocathode. To determine the exact variation of decay along the photocathode surface a small spot of light 1 mm in diameter was focused on the photocathode and its initial sensitivity measured by moving the tube accurately in a horizontal direction by means of a screw arrangement incorporated at the base of the tube clamp (Chapter VI.2). At this stage a very weak input light source was used. The photocathode current was measured by a vibrating reed electrometer and was of the order of 10^{-10} amps. With such small bombarding current the deterioration in the photocathode sensitivity during the actual time of the measurement of the

sensitivity was negligible. The tube was then moved so that the spot of light was situated at the centre of the photocathode and the light input increased a hundredfold, always being very careful in keeping it a constant ratio to the weak light source. The photocathode current, now 10^{-8} amps, was allowed to bombard the KCl surface ($V_p = 500$ V) for several minutes, then the light input was reduced to its original low value and the photocathode sensitivity sampled along the horizontal axis; the spot was next moved to the centre and the light input increased again. This process was repeated several times until the sensitivity at the origin had deteriorated to 65% of its initial value.

The results obtained showing the variation of the decay from the centre along the photocathode are given in Fig. 38. Taking into account the separation of the photocathode and target plate, it can be seen that the distribution of the decay is roughly Lambertian so that evidently the chlorine atoms are also emitted with a distribution approximating to a Cosine Law. In the case of the image intensifiers, the loss in sensitivity, which is confined more closely to the illuminated areas of the photocathode and which at first was interpreted as being due to positive ion bombardment, can be accounted for in terms of the very close proximity (0.006") of the photocathode and the first dynode.

DISTRIBUTION OF DECAY OF PHOTOCATHODE SENSITIVITY
ALONG THE PHOTOCATHODE FROM A SMALL ILLUMINATED SURFACE

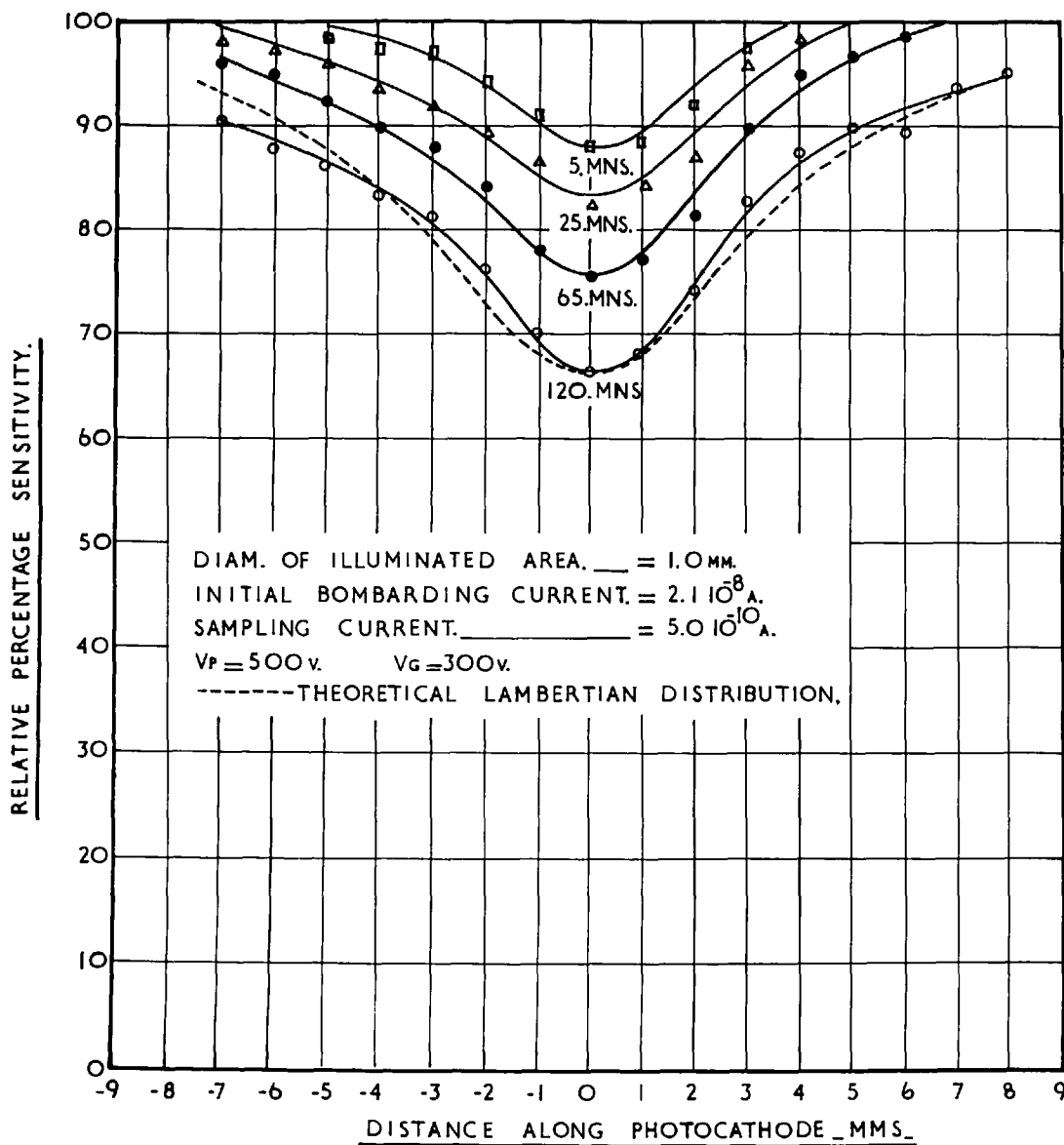


FIG. 38.

The apparent improvement in the life of the photocathode when processed externally, initially observed during the operational life-tests on the channelled intensifiers (Chapter VII.2), was also observed in the case of the triodes. The tubes TR-III and IV, which had "posted" photocathodes, showed a marked improvement in the stability of the photocathode sensitivity over tubes TR-I and TR-II, which had conventional photocathodes. The results obtained with tube TR-IV are given in Figs. 39 to 42. It is seen that the photocathode sensitivity drops to 50% of its initial value after a bombardment of 20 mins at a target voltage of 700 V or 40 mins at a target voltage of 500 V. The corresponding bombarding charges are 0.87 and 1.7 m.coulombs at 700 V and 500 V respectively, comparing very favourably with the figure of 140 microcoulombs (p.158) at target voltage of 500 V for tubes with conventional photocathodes.

Conclusive results on the reality of the improvement of the stability of the photocathode cannot be accurately drawn since measurements are taken on a relatively small number of tubes. In Fig. 43, however, the results obtained on the half-life of photocathode sensitivity with integrated incident charge are summarized for both triodes and image intensifiers. It is seen that there is a close correlation between both types of tubes with an average improvement on

BOMBARDMENT OF KCL. & STEEL TARGETS

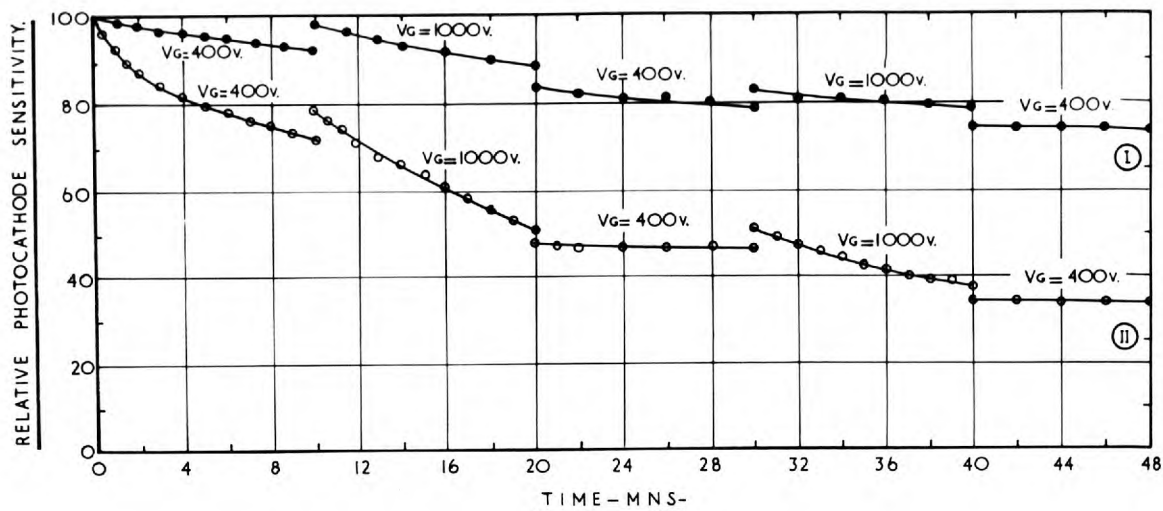
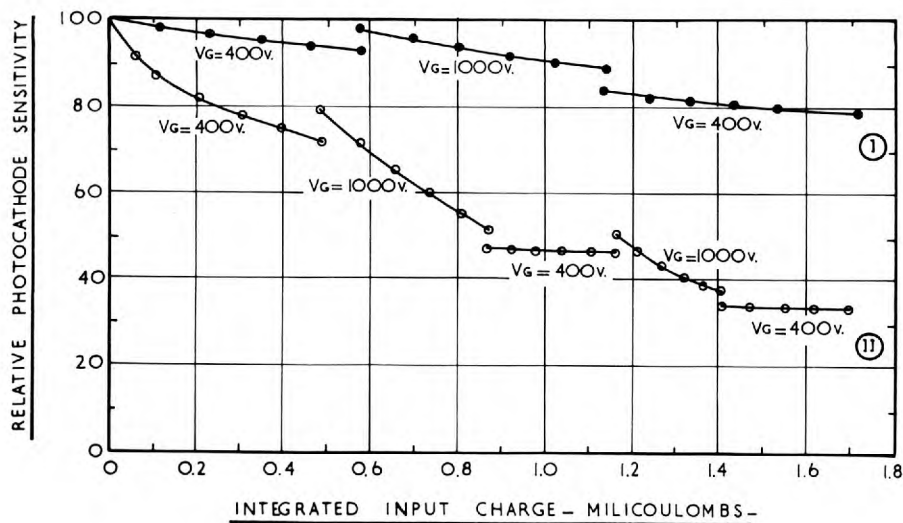


FIG. 39.



I: — STAINLESS STEEL TARGET.

II: — KCL. TARGET.

INITIAL PHOTOCATHODE CURRENTS. = 1.0×10^{-6} A.

$V_P = 700$ V.

FIG. 40.

BOMBARDMENT OF KCL AT DIFFERENT PRIMARY ENERGIES

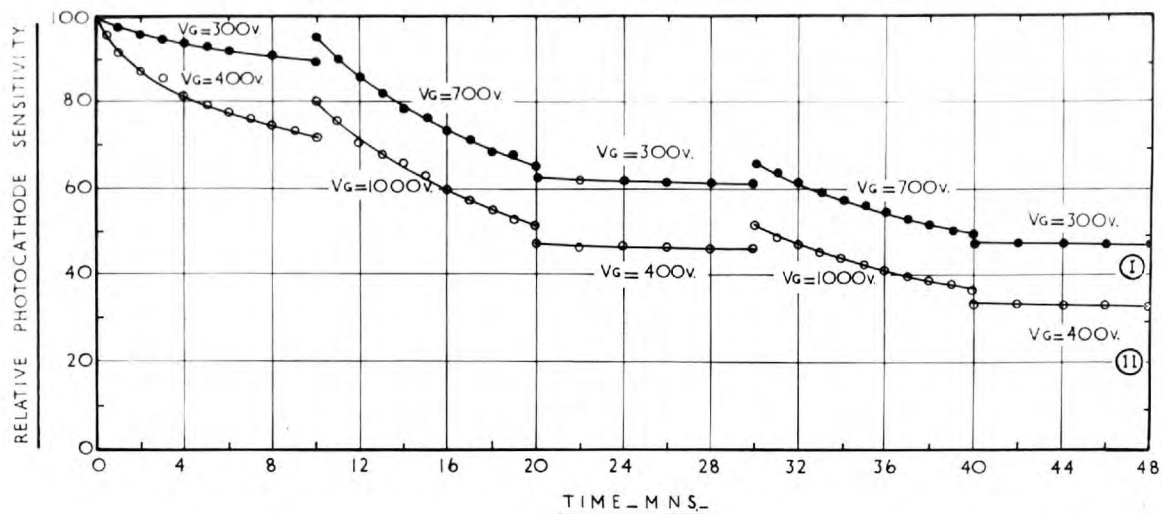
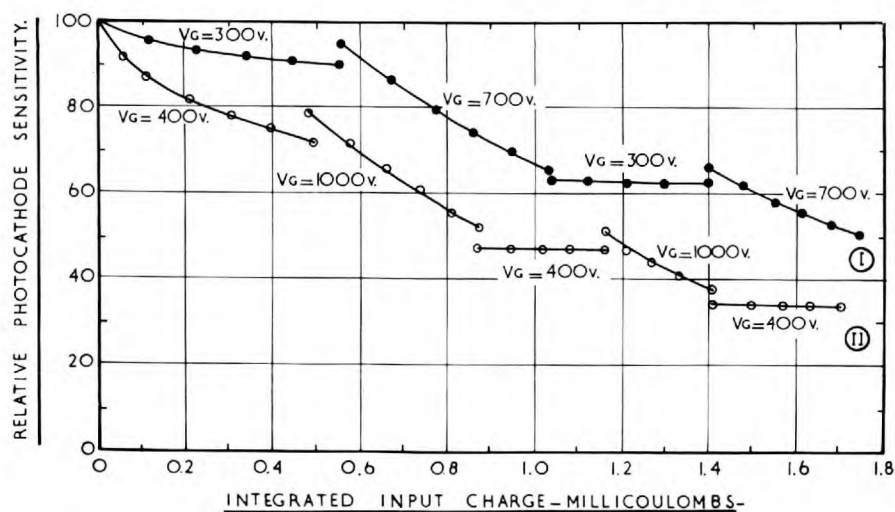


FIG. 41.



I: $V_p = 500$ v.

II: $V_p = 700$ v.

INITIAL PHOTOCATHODE CURRENT = 1.0×10^{-6} A.

$\frac{V_A}{V_g}$ CONST. = 0.7

FIG. 42.

the "posted" photocathodes by a factor 40 over these processed conventionally. A possible explanation of this increase may be due to the method of processing the "posted" photocathode in its external chamber. In the normal method the photocathode is confined to the processing chamber throughout the processing schedule and as a result its surface is in constant equilibrium with the caesium vapour. It was pointed out, however (Chapter V.2), that in the case of the "posted" photocathode a slight variation was adopted in that when the maximum sensitivity was reached the photocathode plate was withdrawn into the extension arm. In this case the equilibrium between the photocathode surface and the surrounding caesium vapour in the chamber is upset and some of the caesium from the hot photocathode tends to evaporate from the surface and condense on the surrounding walls of the extension arm. At the same time, however, a constant source of caesium vapour, at roughly 10^{-2} mm Hg pressure, enters the extension arm from the processing chamber which is cooling far less rapidly than the photocathode. Most of this caesium condenses on the walls of the extension arm and is easily observed, but some also condenses on the photocathode surface. Since the sensitivity of nearly all photocathodes prepared by this method increased by about 10% of their original value during the first 24

Image Intensifiers

Photocathode processed internally			Photocathode processed externally		
Tube No.	Photocathode half life	Bombarding voltage	Tube No.	Photocathode half life	Bombarding voltage
	8.0×10^{-5} coulombs	400 V		4.1×10^{-3} coulombs	400 V
<u>Triodes</u>					
Photocathode processed internally			Photocathode processed externally		
Tube No.	Photocathode half life	Bombarding voltage	Tube No.	Photocathode half life	Bombarding voltage
TR-I	9.3×10^{-5} coulombs	500 V	TR-III	5.3×10^{-3} coulombs	500 V
TR-II	1.4×10^{-4} coulombs	500 V	TR-IV	1.7×10^{-3} coulombs	500 V

FIG. 43

hours following seal-off (Chapter VII.1), a common indication of an over-caesiated photocathode, it appears that the quantity of caesium condensed on the photocathode while in the extension arm was slightly in excess of that evaporated from the surface so that the resultant photocathode was slightly over-caesiated on seal-off. It is probable then that the increased stability, experienced with these photocathodes is due to the few atomic layers of caesium present on the surface of the photocathode which react with some of the chlorine atoms emitted by the KCl, before they can harm the actual photocathode surface.

Referring back to the results obtained from triode TR-IV (p.163) the rate of decay of photocathode sensitivity under 500 V and 700 V primary energies was also investigated. The initial bombarding current was 1.0 amps and the ratios of grid voltage (V_g) to target voltage (V_a) were kept the same in both cases and alternated from $\frac{V_a}{V_g} = 1.7$ to $\frac{V_a}{V_g} = 0.7$. In Fig. 41 the relative photocathode decay is plotted with time of bombardment. It is seen that after the initial decay the rate of a photocathode deterioration is the same in both cases. The half life of the photocathode was reached after 20 mins and after 40 mins for 500 V and 700 V primary energies respectively. The equivalent results for the variation of photocathode decay with integrated incident charge are

given in Fig. 42. In this case the half-life of the photocathode is reached after a charge of 0.9 m.coulombs for 700 V and 1.7 m.coulombs for 500 V primary energy.

Contrary to the results obtained with tube TR-II, the rate of photocathode decay is largely dependent on the voltage of the grid relative to the target plate. With the grid held at an intermediate voltage between the photocathode and the target plate, an initial decrease in the photocathode sensitivity takes place. The deterioration of the photocathode soon levels off however and the photocathode sensitivity drops to a steady value dependent on the bomarding energy.

When, however, the grid potential is made positive with respect to the target plate, the rate of decay of the photocathode sensitivity is suddenly increased very markedly (Figs. 39 - 42). Further the deterioration of the photocathode during this cycle bears no relationship to the deterioration, if any, of the photocathode during the interval when the grid is negative with respect to the target plate.

This phenomenon was exhibited by two out of four of the triode tubes made using KCl as a secondary emitter and one out of two of the "Triode" tubes using BaF_2 . It bears no relationship to the method of preparation of the photocathode since tube TR-I using a conventional photocathode gave a similar effect. The phenomenon also appears to be

related to the KCl area only since during the measurement on the photocathode sensitivity above the stainless steel area (Fig. 39) the decay in this case was found to be independent of the grid voltage.

It is difficult to account for this change in the rate of deterioration of the photocathode but it is probably related in some way to the secondary emission process since it is only during this cycle that the grid can collect the secondary electrons from the emitter.

(b) Barium Fluoride - BaF_2 .

BaF_2 was also investigated as a secondary emitter in the hope that the stronger bond between the barium and the fluorine^{*} would render this material less liable to dissociation under electron bombardment.

Two triode tubes were constructed identical to the ones discussed in the previous section. The results on both tubes are given in Figs. 44 - 47. For tube TR BA I the photocathode appeared to be fairly stable, the sensitivity decreasing to 65% of its initial value after a time of bombardment at 500 V of 50 mins and integrated incident charge of 2.3 m.coulomb. In this instance the decay was

^{*} The lattice energy of KCl crystal is 166 k.cal/mole or 7.1 eV/molecule⁹⁸ at 291°K while that for the BaF_2 at the same temperature is 564 k.cal/mole or 24.5 eV/molecule.⁹⁹

BOMBARDMENT OF BaF_2

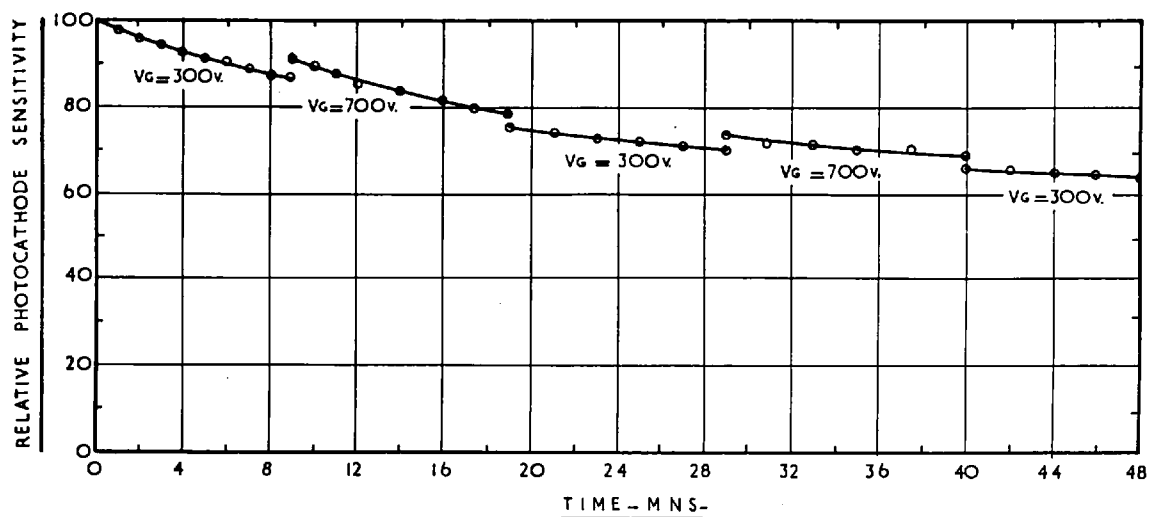
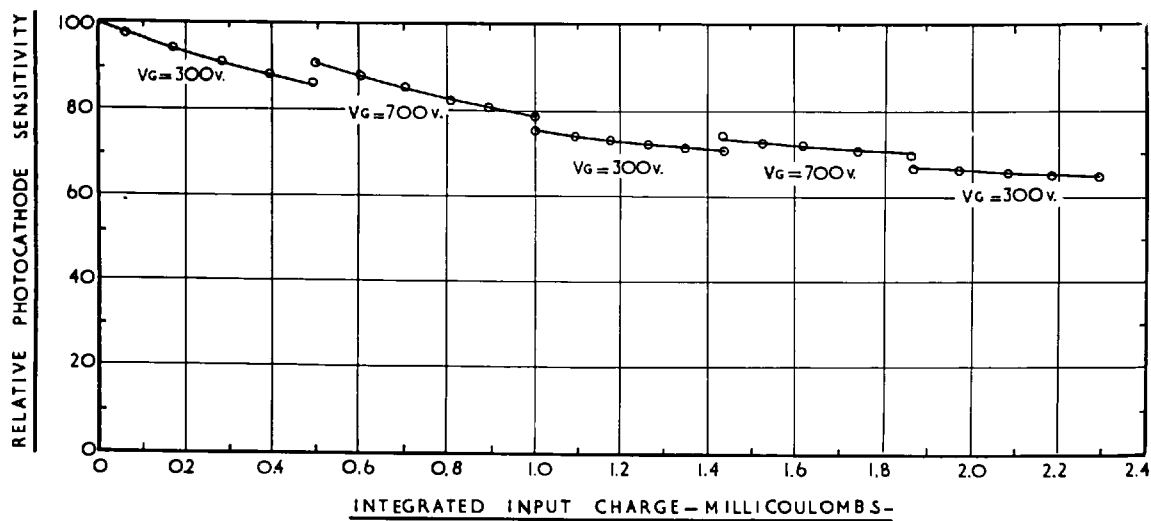


FIG. 44.



$V_F = 500\text{v.}$ INITIAL PHOTOCATHODE CURRENT $= 1.0 \times 10^{-6}\text{A.}$

FIG. 45.

BOMBARDMENT OF BaF_2

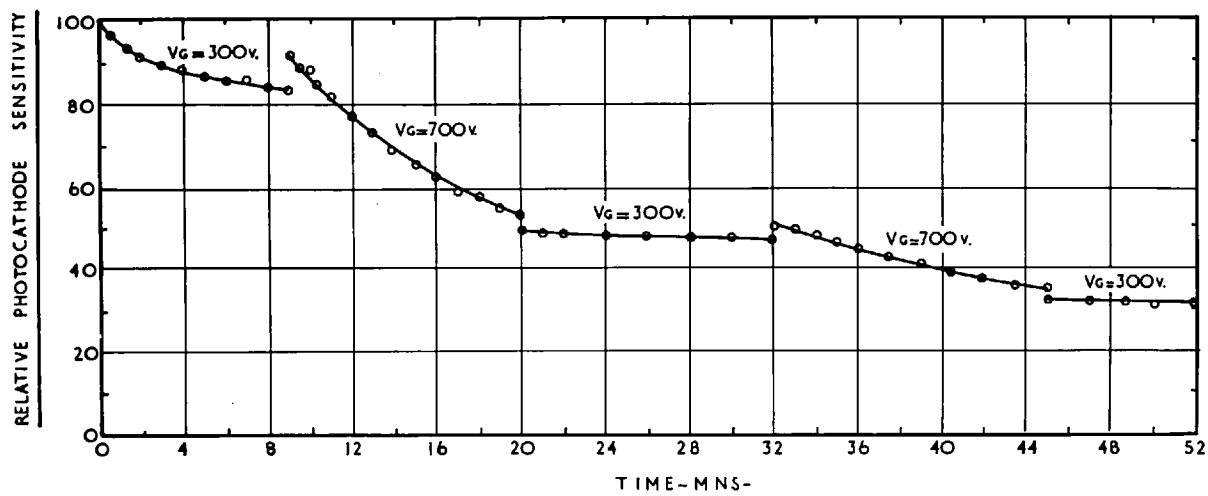
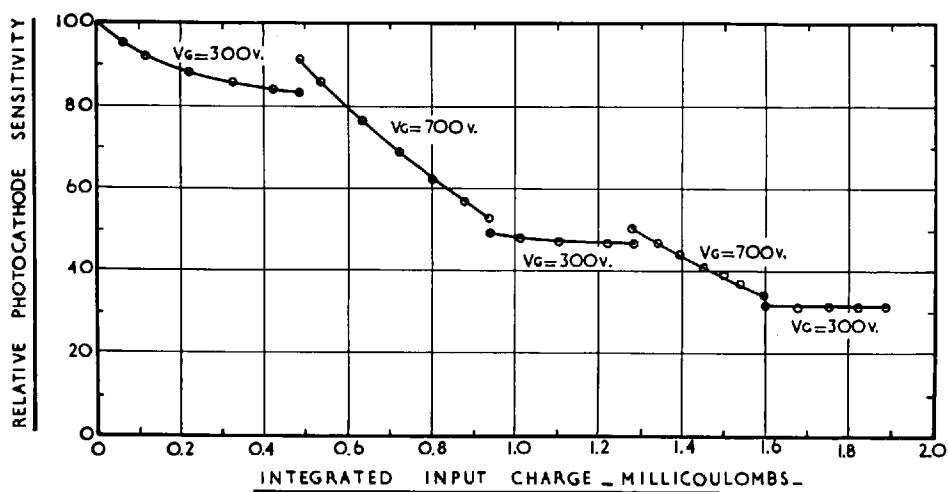


FIG. 46.



$V_p = 500v.$ INITIAL PHOTOCATHODE CURRENT. = $1.0 \cdot 10^{-6} A.$

FIG. 47.

found to be independent of grid voltage (Figs. 44 - 45).

In the second tube (TR Ba II) the decay in photocathode sensitivity was very much more rapid and in this case the deterioration of the photocathode was worse during the interval when the grid was positive with respect to the target plate. For this tube a half life, at 500 V incident energy was reached after a bombarding time of 20 mins and an integrated incident charge of 1.0 m.coulomb (Figs. 46 - 47).

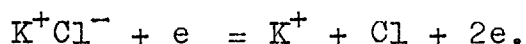
Since measurements on the secondary emission coefficient of the BaF_2 surface (Chapter II.3.iii) gave a disappointingly low yields and the stability of the photocathode was no better than that when KCl was used instead, it was decided that no advantage would be obtained by using BaF_2 as a secondary emitter for the intensifier tube and the use of this substance was suspended.

2. Proposed theory to account for rate of deterioration of photocathode sensitivity.

In the previous section various experimental results were given, relating to the rate of decay of the photocathode sensitivity with time of electron bombardment and integrated incident charge on KCl and BaF_2 surfaces. Experimental evidence was obtained which indicated that the photocathode decay was due to neutral particles liberated from the

secondary emitting surfaces in an approximately Lambertian distribution. In this section the nature of these neutral particles is considered and a theory proposed, (a) to account for the rate of deterioration of the photocathode sensitivity with time of bombardment of the secondary emitter, and (b) to obtain an order of magnitude of the probability of emission of the particles from the surface per incident electron.

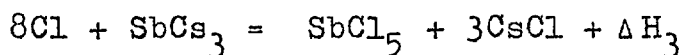
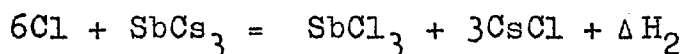
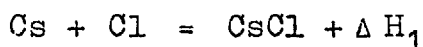
During the electron bombardment of the secondary emitting surface the secondary electrons emitted are those with the highest energy in the crystal, i.e. those occupying the highest energy or the valency band. In the case of KCl these are the 3p electrons. The following reaction is thus responsible for the secondary emitting process.



The positive charge left behind in the crystal lattice is neutralized by an electron delivered from the metal base and the Cl atom is restored to its original negative ionic state. Alternatively it is possible for the Cl atoms to escape from the crystal lattice. In this case the neutrality of the crystal is restored by an electron replacing the hole left behind by the escaping chlorine. The electron now belongs to the six surrounding potassium ions. This process is known as the formation of "colour centres" (Chapter II.3.1) and is also responsible for the subsequent decrease of the

secondary emission yield in this region due to the conduction electrons of the pure metal atoms now present.⁶⁵

The theory that the neutral particles responsible for the photocathode decay are chlorine atoms is further supported by the fact that a violent reaction at the photocathode surface occurs reducing its sensitivity, such as might be expected from the following possible reactions of chlorine with caesium and antimony caesium.



where ΔH is the heat of formation of the reaction and

$\Delta H_1 = + 106.5 \text{ k.cal/mole}$, $\Delta H_2 = + 410.9 \text{ k.cal/mole}$,

$\Delta H_3 = + 426.8 \text{ k.cal/mole}$.

The following assumptions for the decay process of the photocathode can then be made and, to prevent repetition, the KCl surface will only be considered since the same arguments also apply to the BaF_2 surface.

1. The neutral particles observed experimentally are chlorine atoms emitted from the KCl surface in an approximately Lambertian distribution.
2. When a chlorine atom strikes the photocathode, it reacts chemically with the photoemissive surface in the immediate vicinity resulting in a total loss in sensitivity over an

area of the order of the cross-sectional area of the chlorine atom.

3. A chlorine atom arriving on the photocathode on an area already occupied by a previous chlorine atom does not contribute any further to the deterioration of the photocathode surface, i.e. there is no migration of chlorine atoms on the photocathode surface.
4. The fraction of the photocathode current captured directly by the mesh in the triode, together with any subsequent secondary emission process taking place there, is neglected.

If we consider the experimental conditions during which the measurements on the photocathode decay were taken, and if Φ denotes the constant photon flux incident on the photocathode surface, η is the quantum sensitivity of the photocathode and n the total number of electrons leaving the illuminated area A_0 of the photocathode at an interval of time $t = 0$ to $t = t$. Then the rate at which the photoelectrons leave the surface is given by

$$\frac{dn}{dt} = \eta\Phi \quad \dots\dots\dots 7.1$$

and the photocathode current (i) is

$$i = e \frac{dn}{dt}$$

where e is the electronic charge.

$$\therefore i = e \eta \Phi \quad \dots\dots\dots 7.2$$

If p atoms of Cl are emitted per incident electron on the KCl surface, the number of Cl atoms arriving at the illuminated area A_0 of the photocathode surface is then P where

$$P = pf(A_0, d) \quad \dots\dots\dots 7.3$$

and d is the separation of the photocathode plate and the target plate.

Neglecting the presence of the grid, the rate of the bombardment of the KCl surface by the photoelectrons is $\frac{dn}{dt}$.

If now a total of v chlorine atoms are liberated by the electron bombardment at the same time interval $t = 0$ to $t = t$, the rate of arrival of the chlorine atoms at the illuminated area A_0 of the photocathode is

$$\frac{dv}{dt} = P \frac{dn}{dt} \quad \dots\dots\dots 7.4$$

Substituting for $\frac{dn}{dt}$ from equation 7.1,

$$\frac{dv}{dt} = P\eta\Phi \quad \dots\dots\dots 7.5$$

Since every chlorine atom arriving at the photocathode is responsible for a total loss in sensitivity of the photocathode over an area equivalent to its cross-section area, then at a small interval of time from $t = t$ to $t = (t + \delta t)$,

if δv atoms of chlorine arrive at the photocathode, the fraction of the total illuminated area of the photocathode covered is $\frac{P\delta v a}{A_0}$, where a is the cross-sectional area of a chlorine atom.

If the uncontaminated sensitive area of the photocathode at this time is A and since we have assumed that no migration of the chlorine atoms takes place at the surface, then the additional sensitive area covered in time δt is

$$\delta A = -\frac{P\delta v a}{A_0} A$$

the negative sign indicating the decrease in the uncontaminated area.

But since the sensitivity of the photocathode is proportional to the area not yet covered, the ratio of the change in sensitivity (δS) to the sensitivity S at this time in time δt is

$$\frac{\delta S}{S} = -\frac{P\delta v a}{A_0}$$

But $S \propto \eta$

$$\therefore \delta \eta = -\frac{P\delta v a \eta}{A_0}$$

and considering the rate of decrease of the quantum sensitivity in time δt ,

$$-\frac{\delta \eta}{\delta t} = \frac{P a \eta}{A_0} \frac{\delta v}{\delta t}$$

In the limit as δt tends towards zero,

$$-\frac{d\eta}{dt} = \frac{Pa\eta}{A_o} \frac{dv}{dt} \dots\dots\dots 7.6$$

Substituting for $\frac{dv}{dt}$ from equation 7.5,

$$-\frac{d\eta}{dt} = \frac{aP\Phi^2}{A_o} \eta^2 \dots\dots\dots 7.7$$

Solving the differential equation 7.7, we get

$$\frac{1}{\eta} = \frac{aP\Phi^2}{A_o} t + C_1$$

where C_1 is a constant.

Substituting for η from equation 7.2,

$$\frac{e\Phi}{i} = \frac{aP\Phi^2}{A_o} t + C_1$$

$$\therefore \frac{1}{i} = \frac{aP}{A_o e} t + C_2$$

where C_2 is another constant.

When $t = 0$, $i = i_o$,

$$\therefore C_2 = \frac{1}{i_o}$$

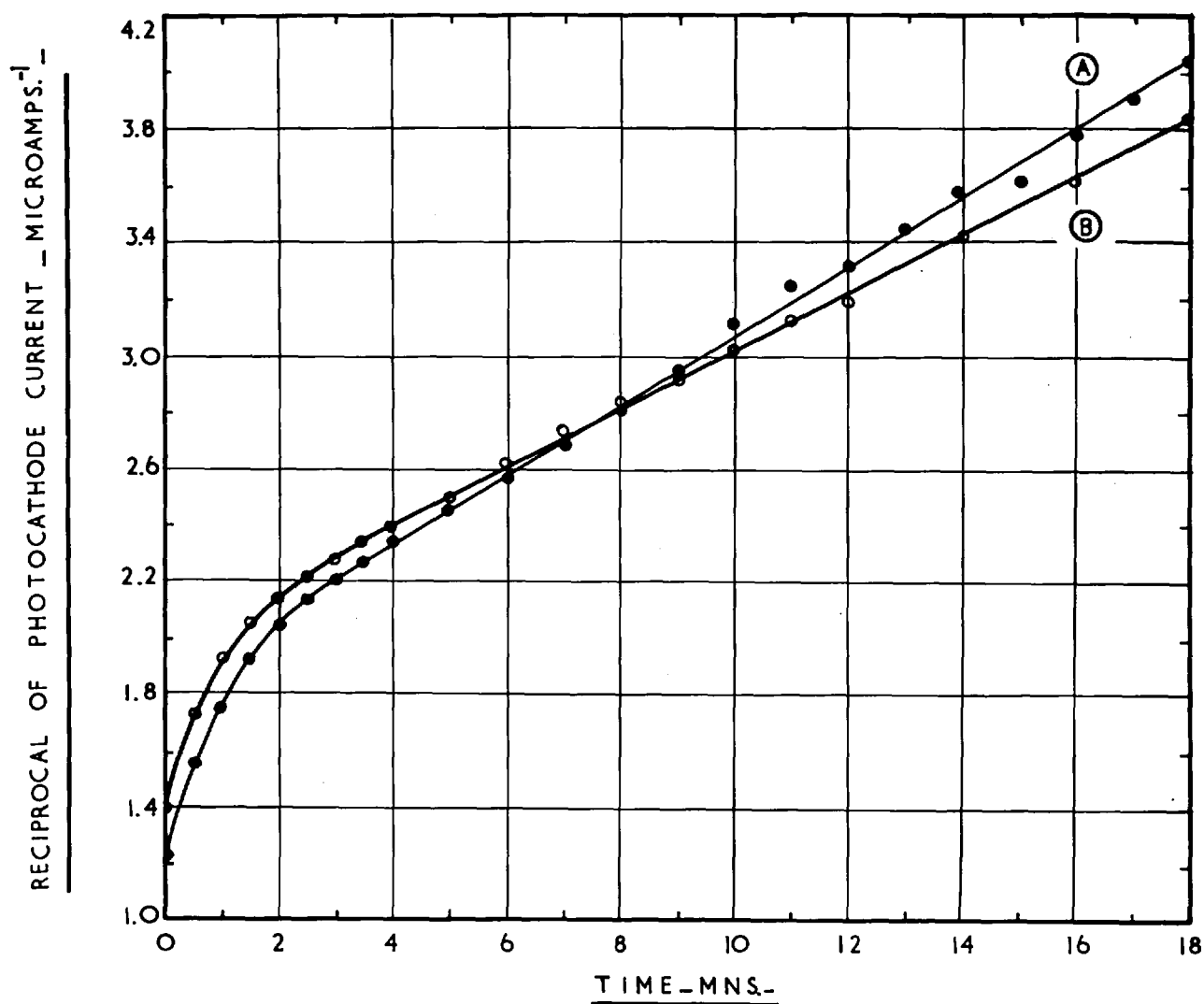
$$\therefore \frac{1}{i} - \frac{1}{i_o} = \frac{aP}{A_o e} t \dots\dots\dots 7.8$$

If the assumptions made for this theory are correct, a plot of the reciprocal of the photocathode current against time of bombardment of the secondary emitter would yield a

straight line. Further, from the slope of this line, a value of P can be obtained where P , it must be remembered, is the probability of arrival of a chlorine atom on the illuminated surface of the photocathode per incident electron on the KCl surface. It should also be noted that the equation in the above form applies to 'triode' tubes only since we have considered plane parallel electrodes.

By plotting in the above manner the experimental results obtained from all the 'triode' tubes discussed so far, the graphs obtained are given in Figs. 48 to 50. For tube TR-II (Fig. 48) the decay of the photocathode sensitivity with time of bombardment of the KCl (Fig. 34 and 36) was extrapolated to a continuous curve since the photocathode sensitivity in this case was found to be independent of the grid voltage. It is seen from Fig. 48 that the initial decay in sensitivity is too rapid to be accounted for in terms of the proposed theory, but that after a bombardment of 4 mins the points fall fairly accurately in a straight line. The slopes of the two lines for $V_p = 500$ V and $V_p = 600$ V are 2.03×10^3 and $1.7 \times 10^3 \text{ amp}^{-1} \text{ sec}^{-1}$ respectively. If we now consider the equivalent radius of the chlorine atom as being equal to the distance (1.8 \AA) at which the Van Der Waal forces begin to interact, the cross-sectional area a is then $1.0 \times 10^{-15} \text{ cm}^2$. Substituting also for the appropriate values of the illuminated

VARIATION OF RECIPROCAL OF PHOTOCATHODE
CURRENT WITH TIME.



TUBE KCL-TR.II.

A:- $V_p = 500\text{V}$.B:- $V_p = 600\text{V}$.

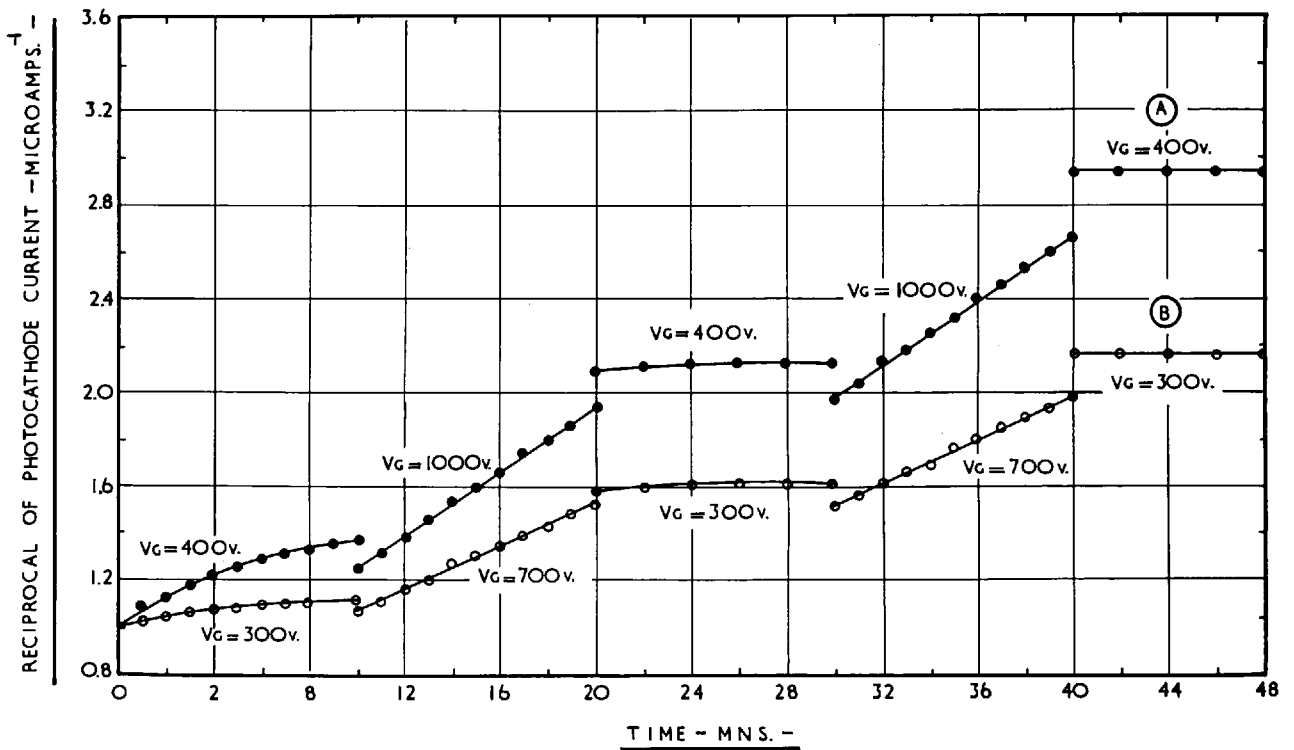
FIG. 48.

area A_0 of the photocathode in the two cases and for the electronic charge e where $e = 1.6 \times 10^{-19}$ coulombs, we obtain $\bar{P}^2 = 4.1 \times 10^{-2}$ for $V_p = 500$ V and $\bar{P}^2 = 4.3 \times 10^{-2}$ for $V_p = 600$ V.

In the case of tube TR-IV, where the rate of photocathode decay was largely dependent on the grid voltage (Fig. 41) the theory applies only during the intervals when the voltage of the grid was positive with respect to that of the target plate (Fig. 49). The initial decay in this instance also is found to be more rapid than that predicted by the theory. The values of \bar{P}^2 obtained for the positive cycles of the grid are 9.5×10^{-3} and 1.3×10^{-2} for $V_p = 500$ V and $V_p = 700$ V respectively.

The results obtained from the triode tubes using BaF_2 as a secondary emitter (Fig. 50) are very similar to the two sets already discussed. There again when the rate of photocathode decay is independent of grid voltage (Tube TR BI) the theory applies over a range of time of bombardment from 4 - 50 mins, while in tube TR BII a straight line is obtained during the intervals at which the grid was positive only. The values obtained for \bar{P}^2 at 500 V primary energy are 9.8×10^{-3} for tube TR BI and 4.7×10^{-2} for tube TR BII.

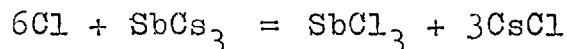
VARIATION OF THE RECIPROCAL OF THE PHOTOCATHODE
CURRENT WITH TIME.



TUBE KCL TR. IV.

A: $V_P = 700v$.B: $V_P = 500v$.FIG. 49.

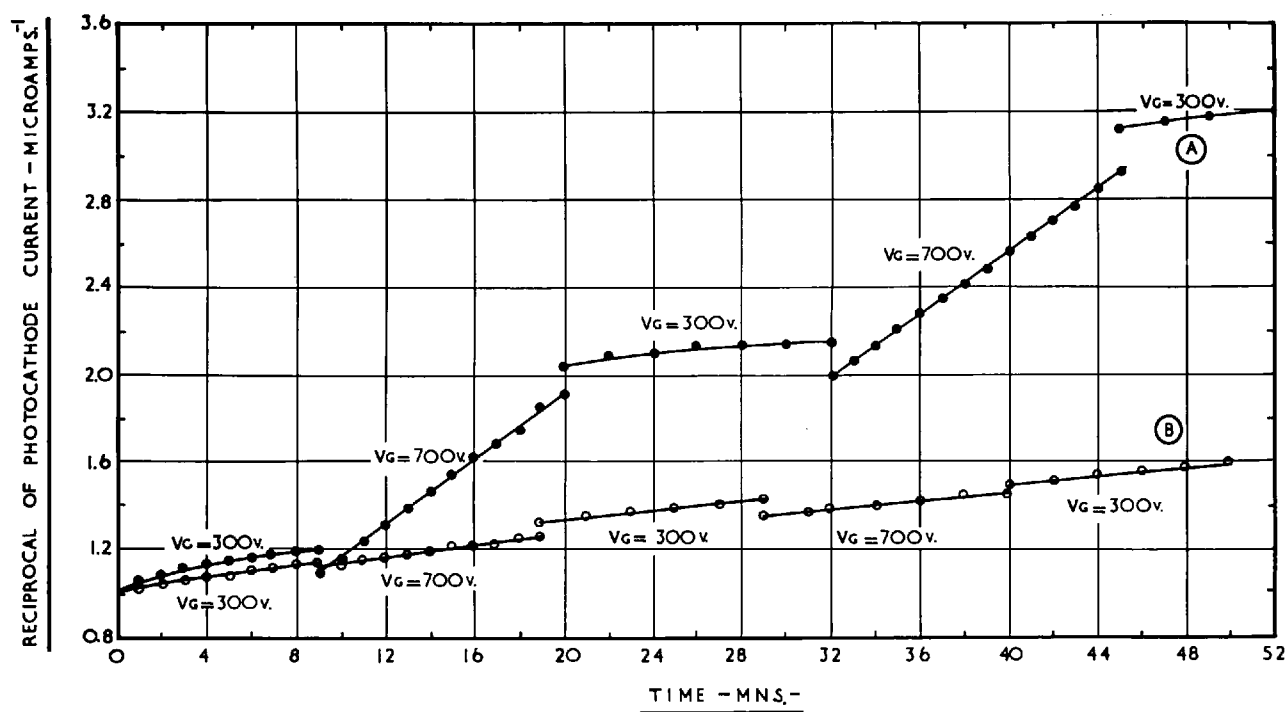
The initial rapid decay in the deterioration of the photocathode is probably due to the violent reaction between the Cl or F with the antimony caesium surface. For example in the reaction:



the energy of formation of CsCl is $106.5 \text{ k.cal.mole}^{-1}$ or $4.6 \text{ eV molecule}^{-1}$ and, for SbCl_3 , $91.4 \text{ k.cal.mole}^{-1}$ or $4.0 \text{ eV molecule}^{-1}$. It may then be that when a chlorine atom strikes the photocathode surface the heat of the reaction affects some of the more sensitive areas of the photocathode in the vicinity. As a progressively greater area on the photocathode surface is covered by the chlorine atoms, the numbers of the more photosensitive sites rapidly diminish and the decay in sensitivity soon becomes restricted to the cross-sectional area of the chlorine atoms.

It is difficult to prove directly any of the assumptions made so far by determining chemically the quantity of chlorine transferred from the KCl surface to the photocathode, since the quantities involved are extremely small. It should be possible, however, to use radio-active tracer techniques giving a very high degree of precision in the measurements. The facilities available in the laboratory unfortunately did not permit such an experiment to be readily carried out. It is suggested, therefore, that in order to obtain a more

VARIATION OF THE RECIPROCAL OF THE PHOTOCATHODE
CURRENT WITH TIME



$V_p = 500$ v.

A: TUBE BaF_2 TR. II.

B: TUBE BaF_2 TR. I

FIG. 50.

fundamental knowledge of the processes affecting the decay of photocathode, triodes should be built with KCl containing traces of radio-active chlorine. During the operation of these tubes a part of this radio-active chlorine should be deposited on the photocathode. In this manner, the rate, as well as the total quantity of chlorine transferred, could then be easily measured and correlated directly to the decrease in sensitivity of the photocathode.

CHAPTER IX. Proposed Improvements in the Channelled
Electron Intensifier.

1. General considerations.

The intensifier tubes constructed by the author were primarily intended for the fundamental investigation of the properties and parameters of the channelled image intensifier. It is useful at this stage to consider any improvements that might be necessary on the present design of the tubes to enable them to be put to practical use. Due to the rather restricted facilities available, the area of the dynodes was kept to a minimum. With dynodes 20 mm square and with 0.5 mm diameter channels, the total information content of an image was thus limited to about 1600 picture points, so that it is possible to intensify satisfactorily only very simple images. In order that the intensifier would yield output images equivalent to a 400 line television picture, the area of the dynodes would have to be considerably increased. For dynodes with 0.5 mm diameter channels the resolution obtained for a randomly orientated fan pattern under dynamic viewing is $1.7 \text{ line-pairs mm}^{-1}$ (Chapter VI.6.ii). With such a resolution, a 400 line television picture would correspond to an image area of 12 cm square. Such an area could be readily achieved by extending the constructional techniques used at

present for the dynodes. A sufficient number of 0.5 mm diameter tubing could be stacked and brazed together to give the required area or alternatively several dynodes could be sliced from a "unit" block of smaller area and then rebrazed together side by side. In this case use can be made of the large range of palladium-silver copper alloys available commercially (Chapter IV.1) to enable the second brazing step to be made at a lower temperature than the first, thus maintaining the cell packing intact. With 0.5 mm diameter channels the dynodes would be still sufficiently robust to be stacked in the same manner as used at present and kept insulated from each other by mica spacers. Alternatively an insulating coating such as MgF_2 could be evaporated on the edge of the cell walls so that the dynodes could be assembled in contact with each other forming a rigid electrode structure. Any straying of electrons into neighbouring channels would thus be completely eliminated. It should also be quite possible with this method to reduce the size of the channels to 0.25 mm diameter keeping the same area. The limit in the reduction of the channel diameter would be set in this instance, by the dielectric strength of the insulator, since the separation of the dynodes would decrease proportionately while the interstage voltage would remain unaltered.

The attack of the photocathode surface by chlorine in tubes using KCl as a secondary emitting material could be greatly reduced by evaporating a suitable chlorine absorbing material on to the walls of the channels opposite to those covered by the KCl. By this means it should be possible to make tubes combining the several advantages of the KCl secondary emitting surface with the long life required from a practical device.

The method developed for processing the photocathode in an external chamber and subsequently introducing it to the main intensifier body through a rectangular section glass tubing (Chapter IV) could be taken a step further. The photocathodes could be prefabricated in sealed evacuated envelopes which would subsequently be fractured in a side arm of the intensifier tube and the photocathodes "posted" in the same way as is done at present. In addition to being able to choose beforehand photocathodes with the maximum sensitivity, with this method the amount of caesium vapour released in the working part of the tube would be even less than with the present method, hence greatly improving the background of the tubes. For the large area dynodes envisaged, the photocathode would consist of several rectangular strips placed side by side, all originally "posted" through the same rectangular aperture. Irregularities in the image corresponding

to the edges of the photocathode strips would be largely eliminated by dynamic scanning of the image.

Another very useful improvement would be obtained if a method were developed similar to that proposed by Huttar¹⁰⁰ and Andrea¹⁰¹ whereby a uniform high resistive coating could be applied to the ceramic rods used for stacking and aligning the dynodes. Only three external electrical connections would then be necessary - the photocathode, the last dynode and the phosphor screen - the remaining dynodes in the electrode structure taking up the appropriate potential along the internal voltage divider. Alternatively one or all of the ceramic rods could be replaced by a rod made from a suitable semiconducting material.

Finally with the continuous decrease in the size of the tube envelope, a different method such as helium arc welding of two metal flanges would have to be used for sealing the end window of the intensifier after assembly. The AgCl sealing process used at present would generate too much heat in the restricted volume of the tube, resulting in possible contamination of the secondary emitting surfaces.

2. A colour image intensifier.

A further development envisaged for the channelled tube is the intensification of coloured images.¹⁰² This can be

achieved relatively simply in the channelled intensifier by dividing the total number of channels into three groups, each group intensifying one primary colour. The colour separation could be effected at the photocathode by a tri-colour mask consisting of an array of tiny colour filters. Accurate registration between each filter and the appropriate channel could be obtained by evaporating the three filters through a suitably modified dynode. Similarly the phosphor would consist of an array of discrete dots, each giving output light appropriate to the electrons arriving from the corresponding channel. Accurate registration between the correct channels and the phosphor dots would be ensured by a pair of electrostatic deflection plates incorporated between the last dynode and the phosphor. Dynamic viewing of the image would also probably tend to blend the speckled structure of the image improving the colour rendering. The resolution of such a tube would be worse than a corresponding monochrome intensifier, due to the effective reduction in the total number of channels. On the other hand, however, the colour would increase the information content of the image.

It should be noted that the same principle of colour intensification could be applied to other types of intensifier. In practice, however, in other intensifiers slight

image distortions or very small drifts in the power supplies would make it almost impossible to maintain accurate registration of the corresponding colour picture point between the photocathode and the phosphor screen.

CHAPTER X. Conclusions.

It has been satisfactorily demonstrated that the principle of secondary electron multiplication from small diameter channels can be used in an image intensifier to give very high light gains. Electron gains between three and four per stage have been achieved with a steady progression of the secondary electrons along a channel and with very little or no straying of the electrons into neighbouring channels.

Of the three secondary emitting surfaces investigated -- MgO, SbCs₃, KCl -- the last surface was found to give the most consistent and highest secondary emission yields per stage. The lowest gains, below two, were obtained in the case of the Sb-Cs surface. In other respects, however, the difficulties which were originally thought to limit the use of Sb-Cs as a secondary emitter were successfully surmounted. Tubes were built operating with interstage voltages of over 250 V and with 5 kV between the last dynode and the phosphor screen without any field emission or breakdown occurring. The first dynode of the electrode structure was used as the photocathode and this was found to considerably improve the contrast in the image. If Sb-Cs surfaces could therefore be successfully prepared to yield higher gains per stage, similar to those obtained in conventional photomultipliers, the use of this emitter in the channelled intensifier should be reconsidered.

Electron gains between two and three were obtained with MgO surfaces. The surface was relatively troublesome to prepare and gave inconsistent results. In addition, care had to be taken to ensure that the films were thin enough to allow adequate conduction through them, otherwise field enhanced emission would occur. If this occurred it would upset the electron optics configuration in the dynode channels and also limit the frequency response of the intensifier.

Consistently high gains between three and four per stage were obtained with KCl as the secondary emitting surface. The surface was prepared by evaporating KCl on to the inner channel walls of the dynodes to a thickness of 1000 \AA . The only precaution necessary was to protect the KCl surface from attack by atmospheric moisture. Fourteen-stage tubes were constructed with an overall electron gain of 8×10^5 and light gain of over 10^6 . The resolution obtained, both under static and dynamic conditions, was consistent with that expected from such a channelled structure. For dynodes with 0.5 mm diameter channels the static resolution for a randomly orientated fan pattern was found to be $0.8 \text{ line-pairs mm}^{-1}$ improving to $1.7 \text{ line-pairs mm}^{-1}$ when the image was dynamically viewed.

Little or no fatigue in the secondary emission yield of KCl under prolonged electron bombardment was observed in tubes

using KCl as a secondary emitter. However, decay in the photocathode sensitivity due to evolved chlorine from the KCl under electron bombardment was found to limit the effective life of the tubes.

In conclusion it is considered that the physical principles and the technical problems of this particular approach to the channelled electron image intensifier have been investigated sufficiently fully to justify the claim that a tube with useful performance with regard to gain, resolution and background, could be constructed, given adequate technical facilities.

Summary of collaboration with colleagues.

When the author commenced work on the channelled electron image intensifier, a preliminary investigation on a suitable electrode structure had already been completed by Dr. E.A. Flinn. The early image tubes described in Chapter V were made with the collaboration of Flinn.

The author was wholly responsible for the investigation of a suitable secondary emitting material, the development of the photocathode "posting" technique and the subsequent improvement in the design and performance of the intensifier tubes. The author also investigated the stability of the characteristics of the image tubes and the decay of the photocathode sensitivity with electron bombardment of the secondary emitter.

ACKNOWLEDGEMENTS.

The author is deeply indebted to Professor J.D. McGee, who first conceived the channelled intensifier, for his constant interest and encouragement during this work, and to Dr. W.L. Wilcock for many helpful discussions and suggestions.

Thanks are also due to Dr. E.A. Flinn for his valuable assistance during the early part of the work described here, and to Messrs. M. Whillock and E. Rogers for their assistance in the constructional work and preparation of the dynodes.

The author wishes to acknowledge receipt of a subsistence grant from the Carnegie Institution of Washington during the early part of the work, and latterly from the Department of Scientific and Industrial Research. The project was supported throughout by the National Research Development Corporation

REFERENCES.

1. Rose, A., Advances in Electronics and Electron Physics I, p.131, Academic Press: New York and London (1948).
2. Hiltner, W.A., Trans.I.A.U. IX, 687 (1955).
3. Baum, W.A., Trans.I.A.U. IX, 611 (1955).
4. Felgett, P.B., "The Present and Future of the Telescope of Moderate Size", p.51, University of Pennsylvania Press (1956).
5. Sommer, A.H., Rev.Sci.Instrum. 26, 725 (1957).
6. Mandel, L., J.Sci.Instrum. 32, 405 (1955).
7. Zacharov, B.O., Thesis, University of London (1960).
8. McGee, J.D., Airey, R.W. and Wheeler, B.F., Advances in Electronics and Electron Physics XVI, Ed. J.D. McGee, W.L. Wilcock and L. Mandel, p.61, Academic Press: New York and London (1962).
9. Kapany, N.S., Optica Acta 7, 201 (1960).
10. Kapany, N.S. and Capellaw, D.F., J.Opt.Soc.Am. 51, 23. (1961).
11. Kapany, N.S., Proceedings of Image Intensifier Symposium (Fort Belvoir, Oct. 1961), p.143.
12. Lallemand, A., Comptes Rendus 203, 243 (1936).
13. Lallemand, A. and Duchesne, M., Comptes Rendus 233, 305 (1951).
14. Lallemand, A. and Duchesne, M., "The Present and Future of the Telescope of Moderate Size", p.25, University of Pennsylvania Press (1956).
15. Lallemand, A., Duchesne, M., Wlérick, G., Augarde, R. and Dupré, M.F., Annales d'Astrophysique 23, 320 (1960).

16. Lallemand, A., Duchesne, M. and Wlérick, G., 'Advances in Electronics and Electron Physics XII, Ed. McGee, J.D. and Wilcock, W.L., p.5, Academic Press: New York and London (1960).
17. Lallemand, A., Advances in Electronics and Electron Physics XVI, Ed. McGee, J.D., Wilcock, W.L. and Mandel, L., p.1, Academic Press: New York and London (1962).
18. McGee, J.D., Private Communication.
19. Hiltner, W.A., "The Present and Future of the Telescope of Moderate Size", p.11, University of Pennsylvania Press (1956).
20. Hiltner, W.A., Image Intensifier Symposium, USAERDL Fort Belvoir, 1958 (Washington D.C.: U.S. Department of Commerce O.T.S. 151813.500), p.53 (1959).
21. Hiltner, W.A., Advances in Electronics and Electron Physics XII, Ed. McGee, J.D. and Wilcock, W.L., p.17, Academic Press: New York and London (1960).
22. Hall, J.S., Ford W.K. and Baum, W.A., Advances in Electronics and Electron Physics XII, Ed. McGee, J.D. and Wilcock, W.L., p.21, Academic Press: New York and London (1960).
23. Hiltner, W.A. and Niklas, W.F., Advances in Electronics and Electron Physics XII, Ed. McGee, J.D., Wilcock, W.L. and Mandel, L., p.37, Academic Press: New York and London (1962).
24. McGee, J.D. and Wheeler, B.E., J.Phot.Sci. 9, 106 (1961).
25. McGee, J.D. and Wheeler, B.E., Advances in Electronics and Electron Physics XVI, Ed. McGee, J.D., Wilcock, W.L. and Mandel, L., p.47, Academic Press: New York and London (1962).
26. Wheeler, B.E., Thesis, University of London (1962).
27. McGee, J.D. and Khogali, A., Private Communication.
28. Philips Gloeilampenfabrieken, 1928.
Brit.Pat. No. 326200 (5/11/28).

29. Echart, F., Ann.Phys. (Leipzig) 14, 98 (1954).
30. Zavoisky, E.T., Butslov, M.M. and Smolkin, G.E.,
Dokl.Acad.Nauk.SSSR 100, 241 (1955).
31. Stoudenheimer, R.G., Advances in Electronics and
Electron Physics XII, Ed. McGee, J.D., Wilcock, W.L.,
p.41 (1960).
32. Davis, G.P., Advances in Electronics and Electron Physics
XII, Ed. McGee, J.D. and Wilcock, W.L., p. 119 (1960).
33. Davis, G.P., Thesis, University of London.
34. Catchpole, C.E., Thesis, University of London (to be
submitted, 1963).
35. Morton, G.A., Trans.I.A.U. 9, 679 (1955).
36. Orvin, L.T., Brit.Pat.'No. 445,156' (1934).
37. Sternglass, E.J., U.S. Patent No. 2,905,804.
38. Sternglass, E.J., Phys.Rev. 100, 1238 (1955).
39. Wilcock, W.L., Emberson, D.L. and Weekley, B.,
Trans.I.R.E. NS-7, 126 (1960).
40. Emberson, D.L., Thesis, University of London (1961).
41. Emberson, D.L., Private Communication.
42. Wachtel, M.M., Doughty, D.D. and Anderson, A.E.,
Advances in Electronics and Electron Physics XII,
Ed. McGee, J.D. and Wilcock, W.L., p.59, Academic
Press: New York and London (1960).
43. Wachtel, M.M., Doughty, D.D., Anderson, A.E. and
Sternglass, E.J., Rev.Sci.Instrum. 31, 576 (1960).
44. Groo, H.R., III, Proceedings of Image Intensifier
Symposium, Fort Belvoir, Virginia, p.55 (1961).
45. Emberson, D.L., Todkill, A. and Wilcock, W.L., Advances
in Electronics and Electron Physics XVI, Ed.
McGee, J.D., Wilcock, W.L. and Mandel, L., p.127,
Academic Press: New York and London (1962).

46. Davison, M., Private Communication.
47. Anderson, A.E., Proc.I.R.E., Scintillation Counter Symposium, Washington, p.133 (1959).
48. McGee, J.D., Brit.Pat.No. 790,416 (5/6/1953).
49. McGee, J.D., Flinn, E.A. and Evans, H.D., Advances in Electronics and Electron Physics XII, Ed. McGee, J.D. and Wilcock, W.L., p.87, Academic Press: New York and London (1960).
50. Flinn, E.A., Thesis, University of London (1963).
51. Burns, J. and Neumann, M.J., Advances in Electronics and Electron Physics XII, Ed. McGee, J.D. and Wilcock, W.L., p.97, Academic Press: New York and London (1960).
52. Burns, J. and Neuman, M.J., Trans.I.R.E. NS-7, 142 (1960).
53. Burns, J., Final Report LAS-TR-P150-13, University of Chicago, Illinois (1961).
54. Goodrich, G.W. and Wiley, W.C., Rev.Sci.Instrum. 32, 847 (1961).
55. Goodrich, G.W. and Wiley, W.C., Rev.Sci.Instrum. 33, 761 (1962).
56. Wiley, W.C. and Hendee, G.F., Trans.I.R.E. NS-9, 103 (1962).
57. Zworykin, V.K. and Morton, G.A., "Television", p.351, 2nd Edition, Chapman & Hall: London (1954).
58. Brill, A., Klaseus, H.A., Philips Res.Rep. 7, 401 (1952).
59. Kapany, N.S., Eyer, J.A. and Keim, R.E., J.Opt.Soc.Am. 47, 432 (1957).
60. Bruining, H., Physica 5, 913 (1938).
61. Gomoyunova, M.V., Fiz.Tverdogo Tela 1, 328 (1959).
62. Holliday, J.E. and Sternglass, E.J., J.App.Phys. 28, 1189 (1957).

63. Sternglass, E.J. and Wachtel, M.M., Phys.Rev. 99, 646 (a), (1955).
64. Hilsh, R., Z.Phys. 77, 427 (1937).
65. Bruining, H., Physics and Applications of Secondary Electron Emission, Pergamon Press, p.39 (1954).
66. Tonk, F., Jb.drahtl Telegr. 20, 82 (1922).
67. van der Pol Jr., B., Physica Haag 3, 108 (1923).
68. Hyatt, J.M., and Smith, A.H., Phys.Rev. 32, 929 (1928).
69. De Lussanet, C.J., Hock frequenz techn. 41, 195 (1933).
70. Myers, D.M., Proc.Phys.Soc. 49, 264 (1937).
71. Trieloar, L.R.G., Wireless Eng. 15, 535 (1938).
72. Jonker, J.H., Telleger, B.D.H., Philips Res.Rep. 7, 13 (1945).
73. Hirashima, M., Wireless Eng. 29, 246 (1952).
74. Nakhodin N.G. and Romanovsky, V.A., Izv.Akad.Nauk. SSSR Ser.fiz. 22, 454 (1958).
75. Petzel, B., Ann.Phys. 6, 55 (1960).
76. Gomoyunova, M.V., Fiz.Tverdago Telo 1, 315 (1959).
77. Bruining, H. and De Boer, Secondary Emission, Part IV, Physica Haag 6, 623.
78. Knoll, M., Z.Physic 22, 137 (1944).
79. Dumond, H. and Saget, P., Jl. de Physique et le Rad. 20, 232 (1959).
80. Johnson, J.B. and McKay, K.G., Phys.Rev. 91, 582 (1953).
81. Whetten, N.R. and Laponsky, A.B., Phys.Rev. 107, 1521 (1957).
82. Borrisson, V.L. and Lepenshinskaya, Izv.Akad.Nauk. SSSR, Ser.fiz. 22, 518 (1958).

83. Whetten, N.R. and Laponsky, A.B., J1.Appl.Phys. 30, 432 (1959).
84. Arntz, F.O. and Van Vliet, K.M., J1.Appl.Phys. 33, 1563 (1962).
85. Zworykin, V.K., Reudy, J.E. and Pike, E.K., J1.Appl.Phys. 12, 696 (1941).
86. Rappoport, P., J1.Appl.Phys. 25, 288 (1954).
87. Wargo, P., Haxby, B.V. and Shepherd, W.G., J1.Appl.Phys. 27, 1311 (1956).
88. Hirashima, M. and Diyasimo, S., J1.Appl.Phys.Soc.Jap. 12, 770 (1957).
89. Sommer, A.H., J1.Appl.Phys. 29, 598 (1958).
90. Daglish, H.V., Private Communication.
91. Appelt, J. and Hackenberg, P., Ann.Phys. 6, 67 (1960).
92. Perry, E.R., Engineering Materials and Design, March 1959.
93. Rhys, D.W. and Betteridge, W., Metal Industry, July 1962.
94. McGee, J.D. Private Communication.
95. Balkwill, J.T. and Folkes, J.T., Brit. Patent Application No. 9796/56 (1956).
96. Folkes, J.R., Advances in Electronics and Electron Physics XVI, Ed. McGee, J.D., Wilcock, W.L. and Mandel, L., p.325. Academic Press: New York and London (1962).
97. Rome, M., J.App.Phys. 26, 166 (1955).
98. Landolt and Bornstein, "Zahlenwerke und Funktionen", 6th Edition, 1st Series 4, 450.
99. Landolt and Bornstein, "Zahlenwerke und Funktionen", 6th Edition, 1st Series 4, 542.

100. Huttar, D.E., U.S. Patent No. 2,837,487 (1958).
101. D'Andrea, J.B., U.S. Patent No. 2,924,540 (1960).
102. Theodorou, D. and Flinn, E.A., Brit.Pat.Application
No. 13702/63 (5/4/63).